71-22,665

BARTEL, Eugene William, 1945-
INVESTIGATION OF RECOVERY TIMES IN THE ELECTRICAL DISCHARGE MACHINING PROCESS AND THE CONSEQUENCES OF THE INFLUENCE OF THE RECOVERY TIME ON THE TIME BETWEEN DISCHARGES.

Carnegie-Mellon University, Ph.D., 1971
Engineering, electrical

University Microfilms, A XEROX Company, Ann Arbor, Michigan

THIS DISSERTATION HAS BEEN MICROFILMED EXACTLY AS RECEIVED

INVESTIGATION OF RECOVERY TIMES IN THE ELECTRICAL DISCHARGE MACHINING PROCESS AND THE CONSEQUENCES OF THE INFLUENCE OF THE RECOVERY TIME ON THE TIME BETWEEN DISCHARGES

by

Eugene W. Bartel

Carnegie-Mellon University

CARNEGIE INSTITUTE OF TECHNOLOGY

THESIS

SUBMITTED IN PARTIAL FULFILLMENT OF THE REQUIREMENTS

FOR THE DEGREE OF Doctor of Philosophy

TITLE Investigation of Recovery Times in the Electrical Discharge Machining Process and the Consequences of the Influence of the Recovery Time on the Time Between Discharges.

PRESENTED BY Eugene William Bartel

ACCEPTED BY THE DEPARTMENT OF Electrical Engineering

Terry C. Hoelzenbein — MAJOR PROFESSOR — Mar 29, 1971 — DATE

A. G. Jordan — DEPARTMENT HEAD — MAR 30 1971 — DATE

APPROVED BY THE COMMITTEE ON GRADUATE DEGREES

C. Brosseau — CHAIRMAN — 4/1/71 — DATE

ABSTRACT

An investigation of the time interval following an electrical discharge and its relationship to the electrical discharge machining (EDM) process is presented. The recovery time following a discharge is defined and a set of reference recovery times is experimentally determined with which other recovery time data is compared. The reference recovery times are obtained by using copper on steel and graphite on steel electrode combinations. The copper and the graphite are used as both the anode and as the cathode for each particular electrode combination. The effect of contamination on the reference recovery data is included. Possible explanations of the shape of the reference recovery time curve are also given.

Different types of graphite materials are used to obtain recovery time graphs for comparison with the reference data and possible reasons for the differences that occur are given. The steel electrode is replaced with other metallic materials to determine their affect on the recovery times when compared to the reference recovery time. The effect that the EDM dielectric fluid has on the recovery times is investigated and discussed.

The damaging gap conditions termed 'coking', which is the growth of carbon type stalactite and stalagmite formation on the opposing electrode surface, and 'burring',which is the apparent occurrence of consecutive discharges in the same spot, are investigated and their relationship to the recovery time information is discussed. The effect of the gap polarity, electrode materials, and EDM fluid on these detrimental conditions is investigated and discussed. Possible mechanisms for the coking phenomena are mentioned. A favorable comparison of the recovery time data and actual EDM machine results is made and a comparison with experienced minimum 'off' time graphic results is also made.

ACKNOWLEDGEMENT

The author wishes to express his appreciation to Dr. T.O. Hockenberry for his advise and counsel during the course of this investigation. The author is also grateful for the discussions and guidance received from Rowland C. Rudolf III, Dr. Walter T. Haswell, III, Dr. Glenn J. Grachis, and Michael N. Diamond. The author also is deeply indebted for the moral support received from his parents, his wife, and his best friend, John Pine.

The main block of support for this work was received from Siltronics, Incorporated.

TABLE OF CONTENTS

			Page
Abstract			i
Acknowledgement			ii
Table of Contents			iii
List of Figures and Illustrations			v
List of Tables			xii
INTRODUCTION			1
Chapter I		EXPERIMENTAL CONSIDERATIONS	6
	A.	Experimental Technique	6
	B.	Apparatus	13
	C.	Electrical Parameters	20
	D.	Materials Employed in the Investigation	20
Chapter II		RECOVERY TIME MEASUREMENTS USING TYPICAL EDM PARAMETERS	26
	A.	Results for the Reference Electrode and Workpiece Materials	26
		1. Reverse Polarity, Clean Gap, Reference Set Recovery Data	27
		2. Normal Polarity, Clean Gap, Reference Set Recovery Data	32
		3. Reverse and Normal Polarity Contaminated Gap, Reference Set Recovery Data	41
		4. Discussion of the Recovery Time Results and Some General Conclusions in Light of Some Prior Findings	49
	B.	Influence of Different Types of Graphite Electrode Material on the Recovery Time Results	53
	C.	Influence of Different Workpiece Materials on Recovery Time Results	67

TABLE OF CONTENTS (continued)

		Page
	D. Influence of Different Types of EDM Fluids on Recovery Time Results	77
	E. Discussion and Conclusions Regarding the Recovery Time Results	88
Chapter III	COMPARISON OF RECOVERY TIME MEASUREMENTS WITH CERTAIN DELETERIOUS EDM MACHINING RESULTS	98
	A. Carbon Growth on the Tool Electrode and Workpiece Surfaces	98
	B. Formation of a Burr on the Workpiece Surface	118
Chapter IV	GENERAL CONCLUSIONS ABOUT THE INFLUENCE OF THE RECOVERY INTERVAL ON THE EDM PROCESS AND SUGGESTIONS FOR FUTURE STUDY	128
	A. Conclusions Relating to the EDM Machining Process and the Recovery Time Data	128
	B. Suggestions for Future Work	132
APPENDIX A -	Circuit Details for the Experimental Apparatus Used	134
APPENDIX B -	Extraneous Test Data Regarding Different EDM Fluids	144
List of References		159

LIST OF FIGURES AND ILLUSTRATIONS

		Page
1.1	Fully Recovered Checking Pulse Waveform at Various Expanded Scales	7
1.2	"Checking Pulse" Waveform for the Time Interval 0 - 1.25 Microseconds After the Termination of the Power Discharge	9
1.3	"Checking Pulse" Waveform for the Time Interval 1.25 - 3.0 Microseconds After the Termination of the Power Discharge.	10
1.4	"Checking Pulse" Waveform for the Time Interval 3.0 - 10.2 Microseconds After the Termination of the Power Discharge	11
1.5	Block Diagram of Experimental Apparatus	14
1.6	Photographs of Experimental Apparatus	15
1.7	Gap Voltage and Gap Current Waveforms for the Equivalent Load Resistance R_1= 1.25 ohm (Lower Trace), R_2= $R_1/2$ = .625 ohm (Middle Trace), and R_3= $R_1/4$ = .3125 ohm (Upper Trace)	17
1.8	Simplified Machining Gap Circuitry Showing the Power Pulse Stage, The Gap Shorting Circuit, and the Checking Pulse Circuit.	19
1.9	The Thermal Properties of Graphite	22
2.1	The Reference Recovery Times for Copper in Reverse Polarity with a Clean Gap and Texaco Code 499 EDM Fluid	30
2.2	The Reference Recovery Times for Elarc 90 in Reverse Polarity with a Clean Gap and Texaco Code 499 EDM Fluid	31
2.3	The reference Recovery Times for Copper in Normal Polarity with a Clean Gap and Texaco Code 499 EDM Fluid	39
2.4	Photograph of Copper Cathode and the Opposing #416 Wrought Stainless Steel Anode with a Pillar of Steel Protruding From Its Surface	33

LIST OF FIGURES AND ILLUSTRATIONS (continued)

		Page
2.5	Photograph of the Surface of the #416 Wrought Stainless Steel Produced by Normal and Reverse Polarity Machining	36
2.6	The Reference Recovery Times for Elarc 90 in Normal Polarity with a Clean Gap and Texaco Code 499 EDM Fluid	40
2.7	Erratic Gap Current Waveform Occurring When Elarc 90 and #416 Wrought Stainless Steel Are Used in Normal Polarity	38
2.8	The Reference Recovery Times for Copper in Reverse Polarity with a Highly Contaminated Gap and Texaco Code 499 EDM Fluid	45
2.9	The Reference Recovery Times for Elarc 90 in Reverse Polarity with a Highly Contaminated Gap and Texaco Code 499 EDM Fluid	46
2.10	The Reference Recovery Times for Copper in Normal Polarity with a Highly Contaminated Gap and Texaco Code 499 EDM Fluid	47
2.11	The Reference Recovery Times for Elarc 90 in Normal Polarity with a Highly Contaminated Gap and Texaco Code 499 EDM Fluid	48
2.12	Gap Current Waveforms Obtained with Poco 1 Graphite on #416 Steel	54
2.13	Recovery Times for Poco 1 in Reverse Polarity with a Highly Contaminated Gap and Texaco Code 499 EDM Fluid	59
2.14	Recovery Times for Poco 1 in Normal Polarity with a Highly Contaminated Gap and Texaco Code 499 EDM Fluid	60
2.15	Gap Current Waveforms Obtained with Poco 3 Graphite on #416 Steel	56
2.16	Recovery Times for Poco 3 in Reverse Polarity with a Highly Contaminated Gap and Texaco Code 499 EDM Fluid	61

LIST OF FIGURES AND ILLUSTRATIONS (continued)

		Page
2.17	Recovery Times for Poco 3 in Normal Polarity with a Highly Contaminated Gap and Texaco Code 499 EDM Fluid	62
2.18	Gap Current Waveforms Obtained with 'EC-3' Carbon on #416 Steel	57
2.19	Recovery Times for 'EC-3' in Reverse Polarity with a Highly Contaminated Gap and Texaco Code 499 EDM Fluid	63
2.20	Recovery Times for 'EC-3' in Normal Polarity with a Highly Contaminated Gap and Texaco Code 499 EDM Fluid	64
2.21	Gap Current Waveforms Obtained with #6466 Graphite on #416 Steel	67
2.22	Recovery Times for #6466 Graphite in Reverse Polarity with a Highly Contaminated Gap and Texaco Code 499 EDM Fluid	65
2.23	Recovery Times for #6466 Graphite in Normal Polarity with a Highly Contaminated Gap and Texaco Code 499 EDM Fluid	66
2.24	Gap Current Waveforms Obtained with Elarc 90 on Hardtem B Tool Steel	68
2.25	Recovery Times for Elarc 90 on Hardtem B in Reverse Polarity with a Highly Contaminated Gap and Texaco Code 499 EDM Fluid	71
2.26	Recovery Times for Elarc 90 on Hardtem B in Normal Polarity with a Highly Contaminated Gap and Texaco Code 499 EDM Fluid	72
2.27	Gap Current Waveforms Obtained with Elarc 90 on Armco Iron	70
2.28	Recovery Times for Elarc 90 on Armco Iron in Reverse Polarity with a Highly Contaminated Gap and Texaco Code 499 EDM Fluid	73

LIST OF FIGURES AND ILLUSTRATIONS (continued)

		Page
2.29	Recovery Times for Elarc 90 on Armco Iron in Normal Polarity with a Highly Contaminated Gap and Texaco Code 499 EDM Fluid	74
2.30	Cap Current Waveforms Obtained with Elarc 90 on Gray Cast Iron	77
2.31	Recovery Times for Elarc 90 on Gray Cast Iron in Reverse Polarity with a Highly Contaminated Gap and Texaco Code 499 EDM Fluid	75
2.32	Recovery Times for Elarc 90 on Gray Cast Iron in Normal Polarity with a Highly Contaminated Gap and Texaco Code 499 EDM Fluid	76
2.33	Recovery Times for Elarc 90 on #416 Steel in Reverse Polarity with a Highly Contaminated Gap and Using Silicone 40, Silicone 80, Silicone 100, and Silicone 200 EDM Fluids	82
2.34	Recovery Times for Elarc 90 on #416 Steel in Normal Polarity with a Highly Contaminated Gap and Using Silicone 40, Silicone 80, Silicone 100, and Silicone 200 EDM Fluids	83
2.35	Recovery Times for Elarc 90 on #416 Steel in Reverse Polarity with a Clean Gap and Pure Silicone SF-96 (5) Oil	84
2.36	Recovery Times for Elarc 90 on #416 Steel in Reverse Polarity with a Highly Contaminated Gap and Pure Silicone SF-96 (5) Oil	85
2.37	Recovery Times for Elarc 90 on #416 Steel in Normal Polarity with a Clean Gap and Pure Silicone SF-96 (5) Oil	86
2.38	Recovery Times for Elarc 90 on #416 Steel in Normal Polarity with a Highly Contaminated Gap and Pure Silicone SF-96 (5) Oil	87
3.1	Photographs of Coking Growths	99
3.2	Typical Damage Done When a Coking Condition Occurs During an Actual Machining Test	100-1

LIST OF FIGURES AND ILLUSTRATIONS (continued)

		Page
3.3	Typical Machining Voltage and Current Waveforms Observed when Correct Machining and a Coking Condition Occurs	104
3.4	Photograph of Gap Current and Voltage Waveforms that Convert from a Standard Machining Pulse to a Coking Pulse	105
3.5	Photomicrograph of a Graphite Whisker from "An Unusual Form of Graphite" by Davis, Swanson, and Rigby in Nature, Vol. 171, 1953 pg. 756	107
3.6	Recovery Times for Elarc 90 on Hardtem B Tool Steel in Reverse Polarity with a Coking Condition and Texaco Code 499 EDM Fluid	112
3.7	Recovery Times for Elarc 90 on Hardtem B Tool Steel in Normal Polarity with a Coking Condition and Texaco Code 499 EDM Fluid	113
3.8	Recovery Times for Poco 3 on #416 Steel in Reverse Polarity with a Coking Condition and Texaco Code 499 EDM Fluid	114
3.9	Recovery Times for Poco 3 on #416 Steel in Normal Polarity with a Coking Condition and Texaco Code 499 EDM Fluid	115
3.10	Recovery Times for Elarc 90 on #416 Steel in Reverse Polarity with a Coking Condition and Pure Silicone SF-96 (5) Oil	116
3.11	Recovery Times for Elarc 90 on #416 Steel in Normal Polarity with a Coking Condition and Pure Silicone SF-96 (5) Oil	117
3.12	Photograph of the Workpiece Damage Done when Burring Occurs During a Machining Operation	118
3.13	Test Cavities Produced by Changing the Duty Cycle from Low to Very High Values	120
3.14	Test Cavities Produced by Changing the Duty Cycle from Low to Very High Values with a 5 Minute Seating Time at a Low Duty Cycle	122

LIST OF FIGURES AND ILLUSTRATIONS (continued)

		Page
3.15	Minimum 'Off' Time Indicated by Machining Test Results When Using a Graphite on Steel Electrode Combination in Reverse Polarity	124
3.16	Minimum 'Off' Times Indicated by Machining Test Results When Using a Graphite on Steel Electrode Combination in Normal Polarity	125
3.17	Minimum 'Off' Times Indicated by Machining Test Results When Using a Copper on Steel Electrode Combination in Reverse Polarity	126
3.18	Minimum 'Off' Times Indicated by Machining Test Results When Using a Copper on Steel Electrode Combination in Normal Polarity	127
A-1	Buffering Stage and Flip-Flop Stage Circuitry	135
A-2	Pilot Pulse Breakdown Circuitry	137
A-3	Integrator, Schmitt Trigger, and Buffering Circuitry	139
A-4	The Gap Shorting and Supplemental Circuitry	140
A-5	The Circuitry Used to Indicate that the Power Pulse has terminated	141
A-6	The Gap Recovery Checking Circuitry	142
B-1	Average Bubble Volume, Average Crater Diameter, and Gap Machining Pulse Voltage for Texaco Code 499 EDM Fluid	146
B-2	Average Bubble Volume, Average Crater Diameter, and Gap Machining Pulse Voltage for Amoco MSO EDM Fluid	147
B-3	Average Bubble Volume, Average Crater Diameter and Gap Machining Pulse Voltage for Wolf's Head 510 EDM Fluid	148
B-4	Average Bubble Volume, Average Crater Diameter, and Gap Machining Pulse Voltage for Factopure EDM Fluid	149

LIST OF FIGURES AND ILLUSTRATIONS (continued)

		Page
B-5	Average Bubble Volume, Average Crater Diameter, and Gap Machining Pulse Voltage for Shell EDM Fluid	150
B-6	Average Bubble Volume, Average Crater Diameter, and Gap Machining Pulse Voltage for Mineral Seal Oil	151
B-7	Average Bubble Volume, Average Crater Diameter, and Gap Machining Pulse Voltage for Citgo No. 90109	152
B-8	Average Bubble Volume, Average Crater Diameter, and Gap Machining Pulse Voltage for Silicone EDM 40 Fluid	153
B-9	Average Bubble Volume, Average Crater Diameter, and Gap Machining Pulse Voltage for Silicone EDM 80 Fluid	154
B-10	Average Bubble Volume, Average Crater Diameter, and Gap Machining Pulse Voltage for Silicone EDM 100 Fluid	155
B-11	Average Bubble Volume, Average Crater Diameter, and Gap Machining Pulse Voltage for Silicone EDM 200 Fluid	156
B-12	Average Bubble Volume, Average Crater Diameter, and Gap Machining Pulse Voltage for Pure Silicone SF-96 (5) Oil	157
B-13	Average Bubble Volume, Average Crater Diameter, and Gap Machining Pulse Voltage For Fluro Chemical FC-77 Fluid	158

LIST OF TABLES

		Page
1.1	Properties of Copper	21
1.2	Composition and Properties of Workpiece Materials	23
1.3	The Properties of Kerosene	24
1.4	The Properties of Pure Silicone Fluid	25
2.1	Average Properties of Electro-Carb 'EC-3' Electrode	57
2.2	EDM Fluids Tested and Manufacturer	80
3.1	Typical Composition of Gases Evolved from Various Types of Discharges	109
3.2	Machining Data Corresponding to the Machining Cavities Shown in Figure 3.13	120
3.3	Machining Data Corresponding to the Machining Cavities Shown in Figure 3.14	122

INTRODUCTION

In 1945, B.R. and N.I. Lazarenko [1] found that the erosion of materials accompanying a transient electrical discharge under a dielectric fluid could be used to machine metals. Since that time, there has been an increasing interest in the Electrical Discharge Machining (EDM) process. The initial interest in the EDM process was a result of its ability to machine extremely hard metals (tungsten carbide, tool steels, etc.); more recently the process has been used commercially to produce intricate patterns in softer materials such as aluminum, simply because it can perform the job at a substantial savings in time and labor cost.

The early EDM machines followed the design used by the Lazarenkos [2]. Their design was a simple capacitive charge and discharge circuit, where the capacitor is electrically connected across a machining gap and allowed to charge through a resistor. When the voltage across the capacitor and gap was sufficiently high to cause electrical breakdown of the gap, the capacitor would then discharge through the machining gap. Once the capacitor was discharged, the cycle would start over again. The relaxation type EDM machine, however, was inherently slow to remove materials.

With the advent of the pulsed type power supply, the EDM process began to increase in importance as a modern machining tool. This supply was generally constructed using vacuum tubes to turn the discharges on and off; later the vacuum tube was replaced by the transistor as the switching device. The pulsed machine has several advantages over the capacitive

discharge type, i.e. the current pulse is more or less constant during the discharge, the energy directed towards machining is larger owing to increased average current capabilities, the discharge rates are much higher without substantially decreasing the machining current, and as a result machining rates are much higher with the pulsed supply than with other supplies.

The periodically pulsed type power supply was the most efficient EDM machine available until the advent of the new "Self-Timed" power supplies [3]. The "Self-Timed' supply does not use an independently set frequency generator as the repetitively pulsed supplies do; it uses information gathered from the machining gap to determine when and if a machining pulse should be generated, hence the name "Self-Timed".

Although a current pulse produces the actual machining in the EDM process, the time interval between machining pulses, or the "off time", is just as important to the machining operation. The main purpose of this study is then to gain a better understanding of the time interval between successive discharges and the phenomena associated with it.

The research and experimentation that has accompanied the growth of the EDM industry, has been generally concerned with metal erosion methods [4, 5, 6], electrode materials [7, 8], EDM fluid effects [4, 8, 11], etc., but very little attention has been directed towards the recovery time between the electrical discharges in the EDM process.

Much work has been done concerning the recovery of the arc columns which occur in circuit breakers, contactors, and

relays [9, 10]. In most of the investigations of the recovery interval, the researchers were primarily interested in the voltage recovery. Voltage recovery, or reignition voltage, as defined by previous investigators, is the magnitude of voltage necessary to cause electrical breakdown of the gap spacing, with the reignition occurring after the current stops flowing in the primary discharge. From the breakdown data, a reignition curve is constructed by measuring the reignition voltage at various time intervals after the termination of the primary discharge and plotting the resultant voltage values versus the time after the termination of the main pulse current [10, 12]. "Complete" recovery occurs when the reignition voltage reaches the voltage originally needed to establish the primary discharge. Some experimenters were also concerned with the thermal recovery of the arc or discharge column and its relationship to the total voltage recovery of the discharge [13, 14].

Aside from Pittman, most of the prior arc recovery research was concerned with various ranges of gap distances and pulse durations much larger that the ranges found in the EDM process. For instance, arcs with pulse durations in the range from 5 to 400 milliseconds [15, 16, 17] and gap distances in the range of .76 mm to 7 mm [16, 17] were studied. Some previous research, however, was done with the discharge current magnitude in a range approximately the same as found in EDM [18]. Even though the electrical parameters and experimental conditions used by most previous investigators are not the same as those found in the EDM science, some of the recovery processes described in the prior art may occur in the EDM gap.

The most comprehensive investigation of the voltage recovery of the EDM gap was done by Pittman [19]. Ten years have passed since Pittman's work and much more is now known about the physical events accompanying an EDM discharge. It has been shown that a high pressure gas bubble surrounds the discharge and the solid material resulting from the electrode erosion accumulates at the gas bubble-fluid interface during a single discharge [20]. Consequently, the breakdown voltage recovery is dependent, not only on the original discharge column recovery, but also on the contamination effects at the gas bubble-EDM fluid interface, which are a result of the primary discharge. Essentially then, Pittman was measuring the parallel effects of the discharge column recovery and the contamination breakdown effects when he investigated the breakdown voltage recovery of the EDM gap space. The resistive recovery of the gap space, however, is considered to be more closely associated with the discharge column recovery. The recovery of the original discharge column is directly related to the random nature [21] of the discharge point necessary in efficient EDM machining. If sufficient time is not allowed for the recovery of the original discharge column, the succeeding pulses would, in all probability, occur at the same physical location on the workpiece, an occurrence which eventually leads to severe pitting and destruction of the workpiece. Pittman had, therefore, inadvertantly neglected the random nature necessary in the EDM process when he investigated the breakdown voltage of the gap space.

Considerable emphasis is placed on the resistive recovery in the present work; the resistive recovery is considered to be much more important in EDM than re-ignition voltage because the resistive recovery is more directly related to the achievement of "random" sparking in the repetitive discharge EDM process. Therefore, the purpose of this thesis is:

1.) To investigate the time interval immediately following an EDM discharge in order to gain a better understanding of its role in the EDM machining process.

2.) To determine the effects of various physical parameters such as electrode material, workpiece polarity, current magnitude, pulse duration, and different EDM fluids upon this recovery interval.

3.) To relate the information of 1.) and 2.) above to the EDM process and the phenomena associated with it and thereby aid in the design of machines and enhance the understanding of the processes and factors involved in the Electrical Discharge Machining operation.

CHAPTER I

EXPERIMENTAL CONSIDERATIONS

A. Experimental Techniques

The procedures followed in this study were somewhat similar to those used by the researchers of arc column and spark discharge voltage recovery time that were mentioned previously. The primary difference was related to the interest in the gap resistive recovery rather than its voltage recovery.

The procedure used to investigate the resistive recovery was to generate a single discharge and then, after the termination of the discharge current, to generate a second pulse (checking pulse) at a variable time interval after the first, in order to determine the progress of the gap recovery. Only one checking pulse was generated after each primary discharge in order to minimize the possible influence which the recovery monitoring has on the resistive recovery of the gap. The checking pulses were observed on an oscilloscope and compared to a standard checking pulse produced without a primary discharge. When the wave shapes of the checking pulses, with and without the primary discharge were as similar as could be visibly observed on the oscilloscope, the gap was considered recovered and the time interval between the end of the power discharge and the beginning of the checking pulse, was designated as the recovery time.

Figure 1.1 shows the waveform of a standard checking pulse plotted on three different scales for comparison to waveforms

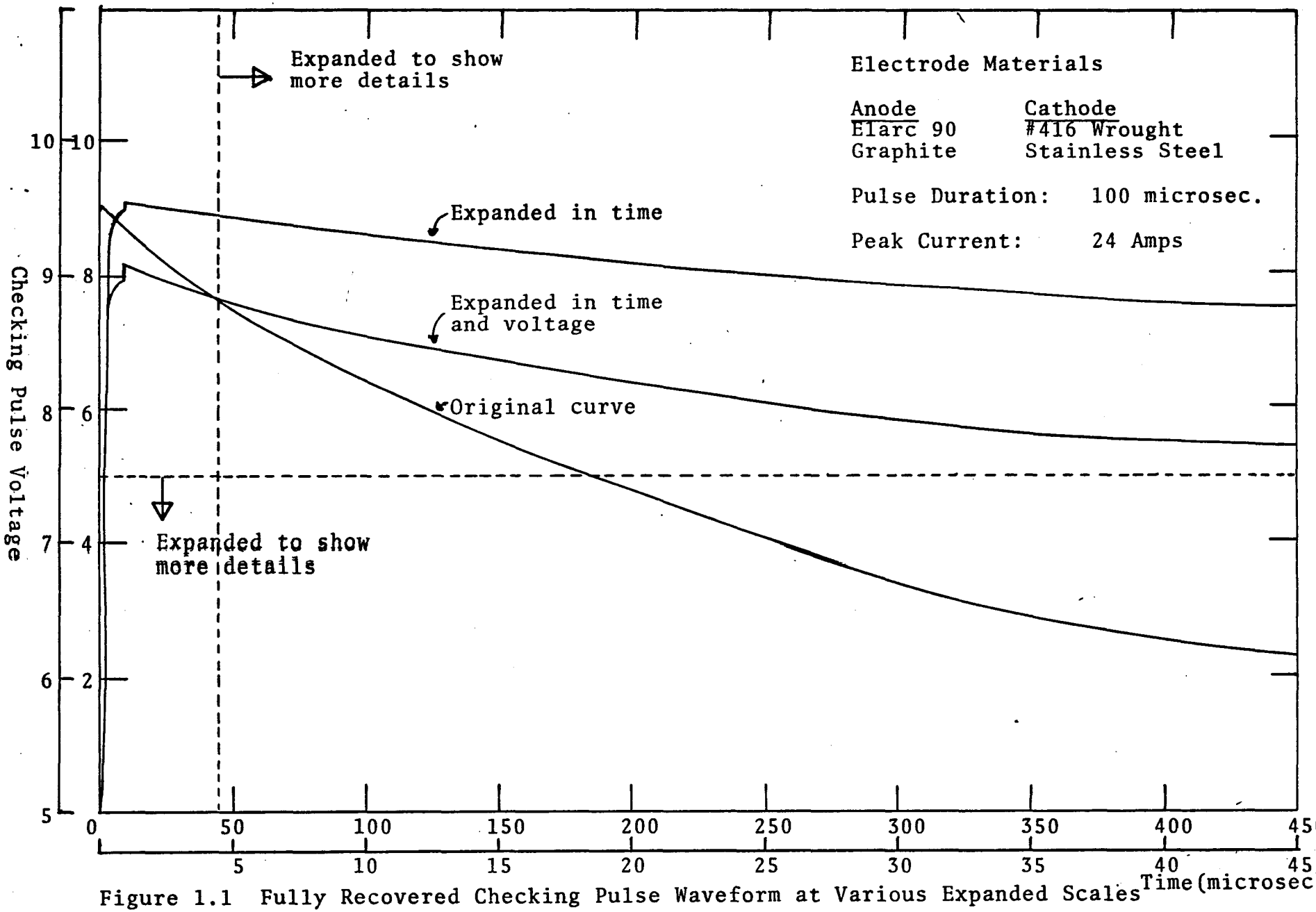

Figure 1.1 Fully Recovered Checking Pulse Waveform at Various Expanded Scales

shown in Figure 1.2, 1.3, and 1.4. Figure 1.2 shows the recovery time interval during which the gap recovery has the largest influence on the checking pulse. There are very noticeable effects on the voltage rise, peak voltage, and decay of the checking pulse. The longer the time interval between the power discharge and the checking pulse, the less the effects are detectable. In Figures 1.3 and 1.4, only the initial peak voltage is different from the standard waveform; this is the expected result owing to the diminishing effect that the primary discharge has on the checking pulse when the checking pulse occurs at relatively long time intervals after the primary discharge.

A recovery sequence similar to that shown in Figures 1.2, 1.3, and 1.4 was observed for different pulse durations, electrode combinations, polarities, peak currents, and for different EDM fluids. In addition, different gap conditions were studied, i.e., a highly contaminated gap and a clean gap. A clean gap is considered by many EDM operators to be the ideal environment for optimum machining, but, as was shown by Grachis [22], a contaminated gap may, in some cases, be the optimum, depending upon the electrode material and polarities used. To insure that the gap was kept clean, no more than 4 discharges were permitted to occur in succession, then the gap electrodes were separated and cleaned with a brush. At pulse durations greater than 300 microseconds, only two or three consecutive pulses were generated between cleanings. In order to eliminate the possibility of influence from changes on the electrode surface caused by prior discharges, the tool electrodes were removed and polished, using emery paper. One such case is

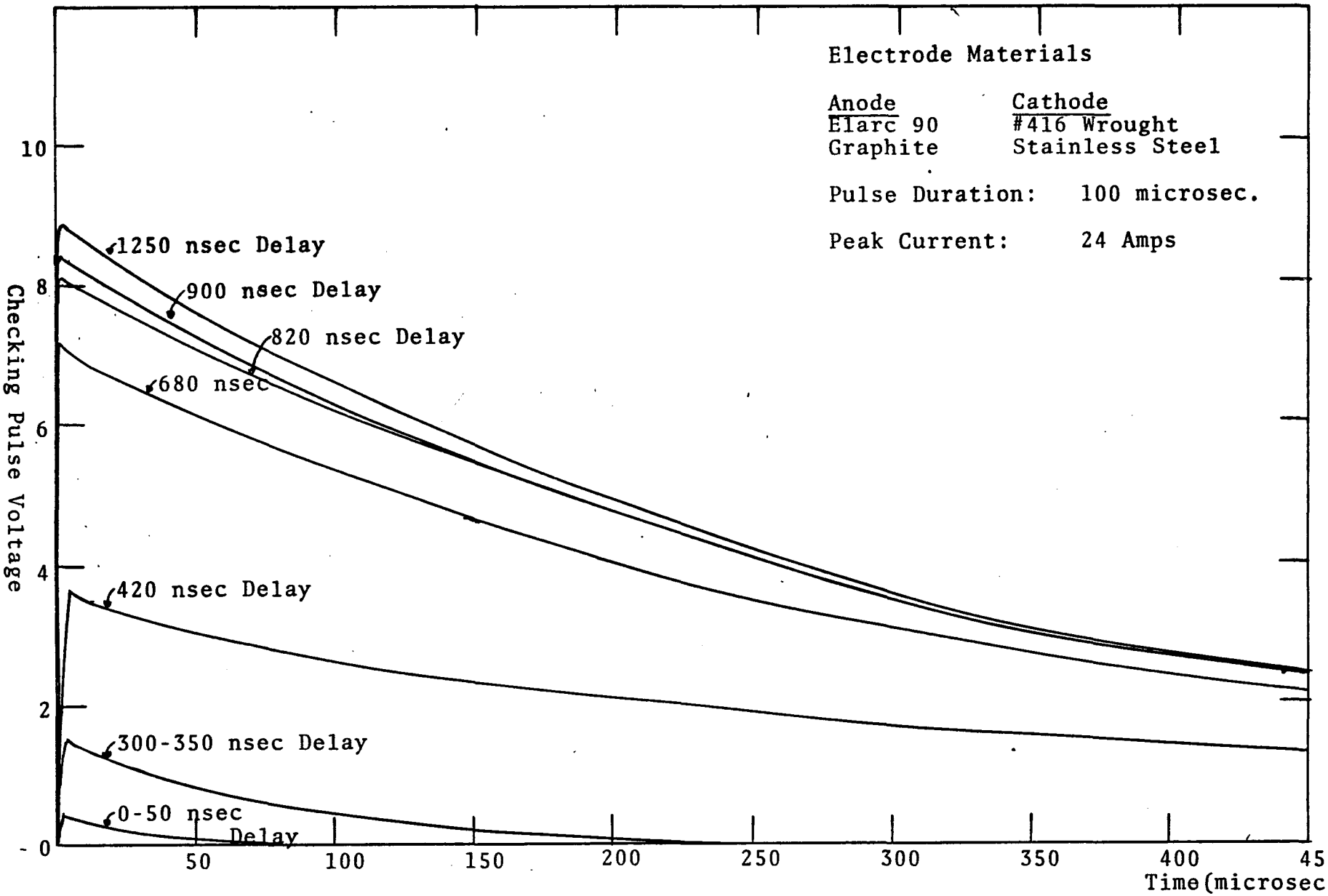

Figure 1.2 Checking Pulse Waveforms for the Time Interval 0-1.25 microseconds After the Termination of the Power Discharge

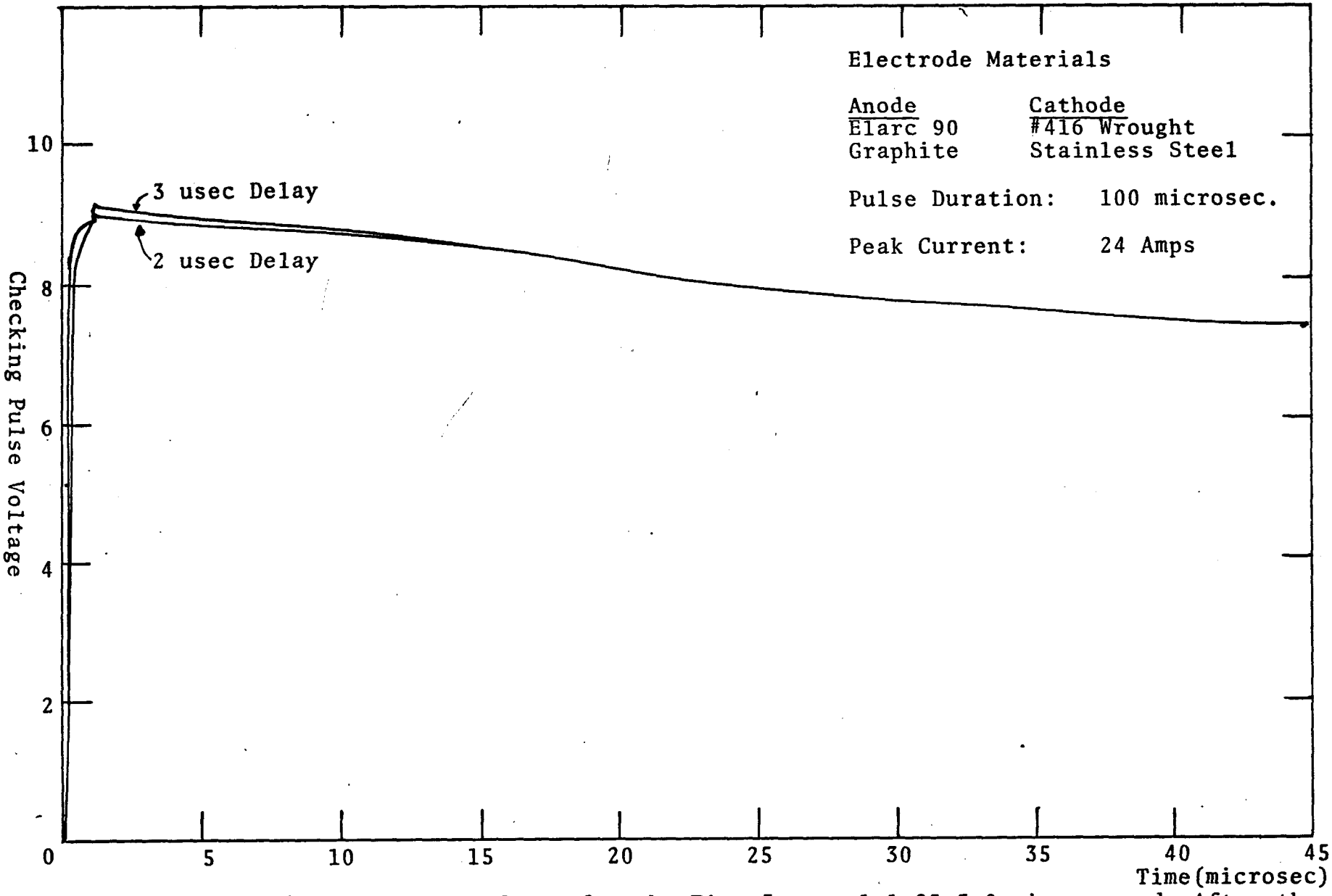

Figure 1.3 Checking Pulse Waveforms for the Time Interval 1.25-3.0 microseconds After the Termination of the Power Discharge

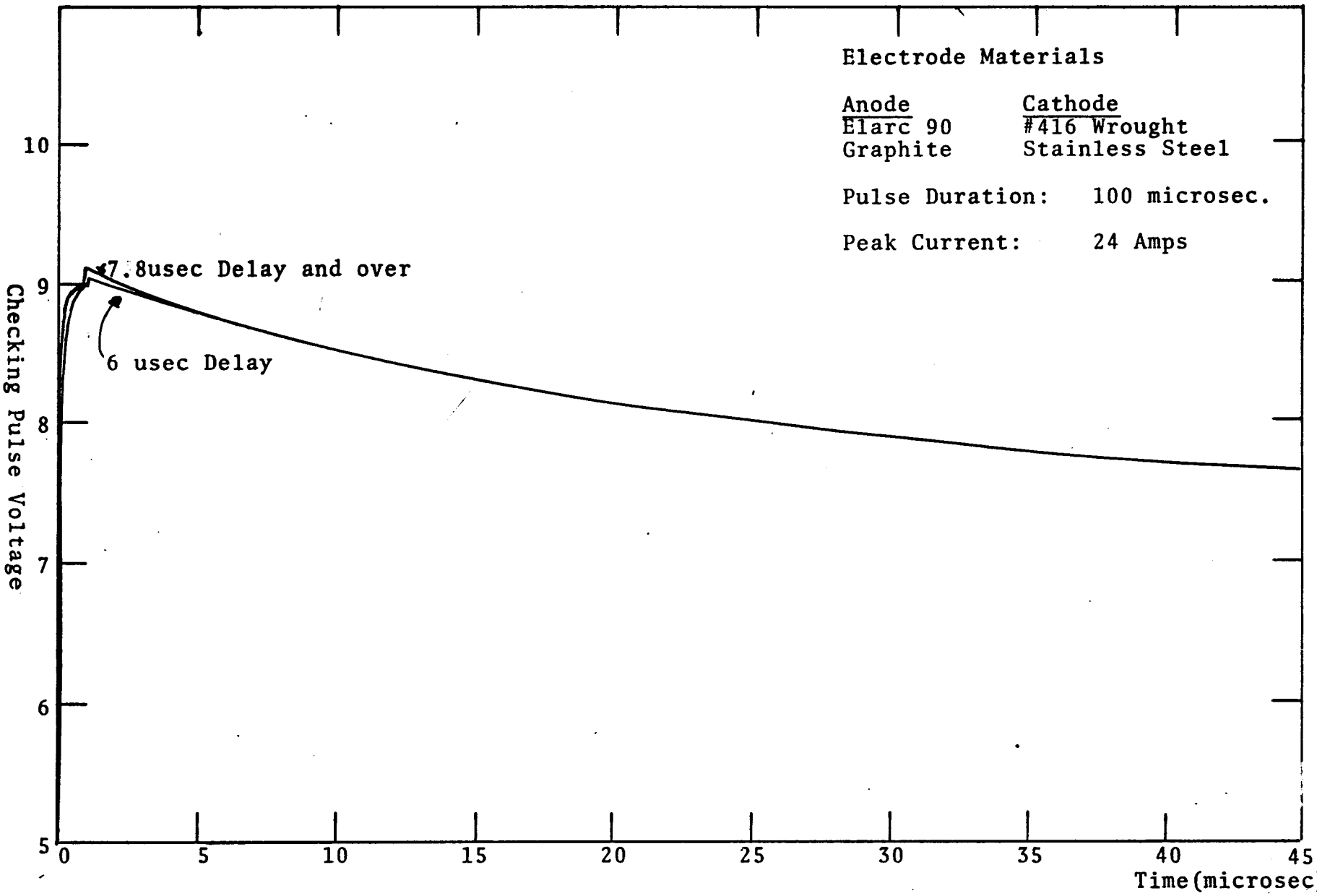

Figure 1.4 Checking Pulse Waveforms for the Time Interval 3.0-10.2 microseconds After the Termination of the Power Discharge

the reverse polarity condition with a graphite electrode where much steel plating occurs on the graphite electrode. Fresh EDM fluid was used for each test to eliminate the possible effects of previously contaminated and chemically cracked fluid.

The highly contaminated gap case was used to approximate, as closely as possible, the conditions that exist in a machining gap during an actual EDM operation. The EDM fluid used was as contaminated as it would ordinarily become from repeated usage and no attempt was made to clean the fluid or the gap space. The gap was permitted to discharge as many times as necessary to establish that the checking pulse indicated recovery of the gap. No attempt was made to clean the electrodes, other than the initial grinding and polishing done before each test set. Any difference in the results in this case, however, cannot be contributed totally to the debris in the gap. The tests were conducted in such a manner that electrode heating could have been a factor, but this would also occur in an actual machining operation, therefore, no attempt was made to alleviate it.

The final gap condition that was considered is the coking condition which is explained in Chapter 3. Once the typical stalagmite and stalactite formations were observed, the tests were conducted much as they were with other electrode materials, except occasionally the gap was checked to make sure the coking case still existed. The coking case is, without a doubt, the worst condition that can exist during an EDM machining operation. In almost all instances where coking occurs, the work-

piece is either completely ruined, or requires extensive repairs before it can be completed; not to mention the damage it can do to expensive tool electrodes. These detrimental results prompted the investigation of the coking case, in an attempt to better understand it and possibly to prevent it from occurring. A more vivid portrait of coking will be presented in Chapter III along with pictorial examples of the damage it can do.

B. Apparatus

The experimental apparatus was constructed in such a manner that the conditions existing at the gap are the same as those existing in a commercial EDM machine. The current waveform of the primary discharge is a rectagular pulse. The sample holder, or machining gap, was the same as that used by Konnerth [23] with slight modification. The sample holder was hand-operated and could be positioned with a gap spacing between .0005 - .005 inch. A block diagram and photographs of the apparatus are shown in Figures 1.5 and 1.6, respectively, and the details of the circuitry are given in Appendix A.

Referring now to the block diagram in Figure 1.6, notice that at the left side of the diagram, there are two blocks labeled 'single pulse' and ' pulse generator'. These blocks indicate that the system can be operated either in the single pulse or repetitively pulsed mode.

The monostable multivibrators shown in the block diagram are essentially identical, except the one following the flip-flop has an output pulse which is continuously variable. This output pulse determines the duration of the discharge at the

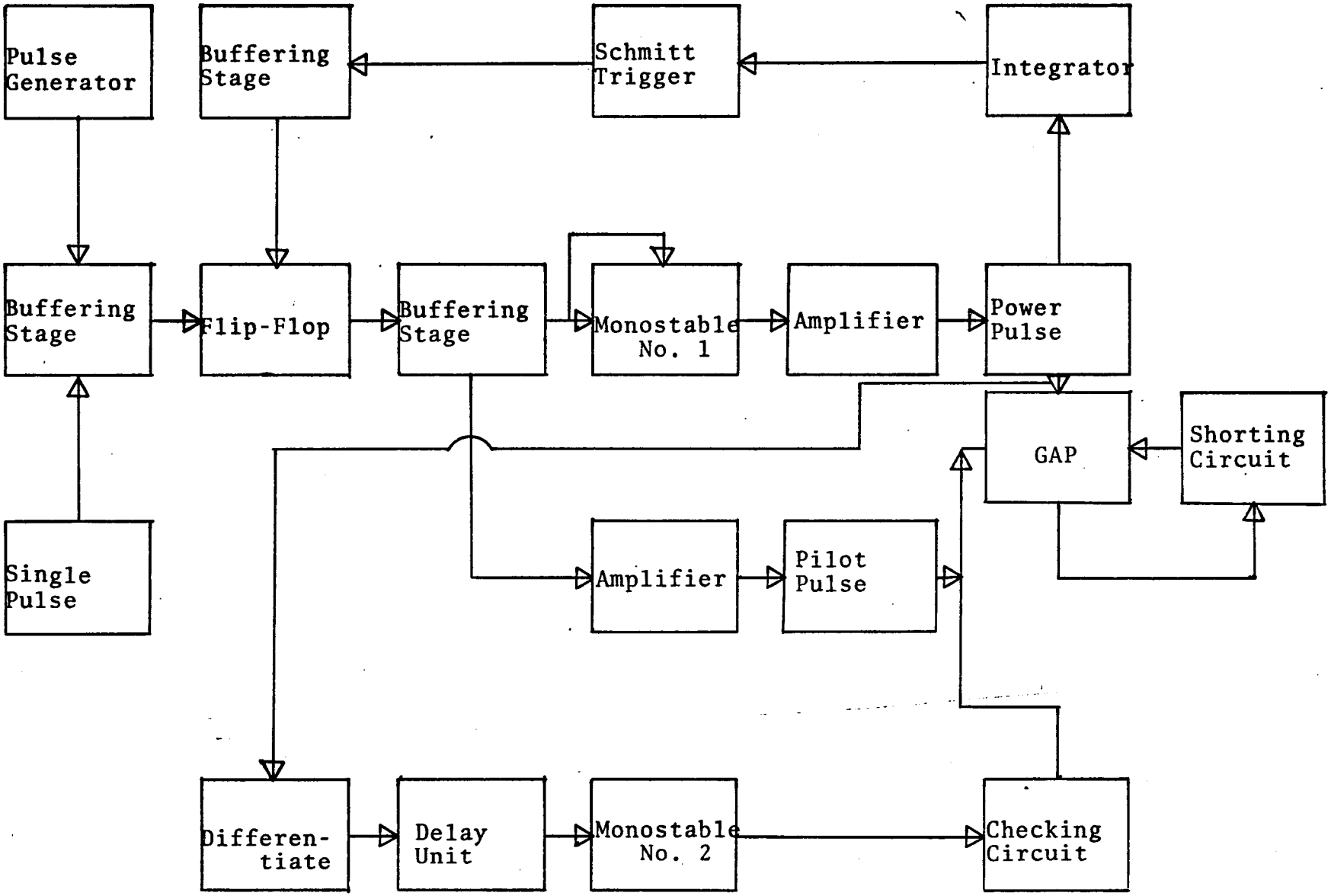

Figure 1.5 Block Diagram of Experimental Apparatus

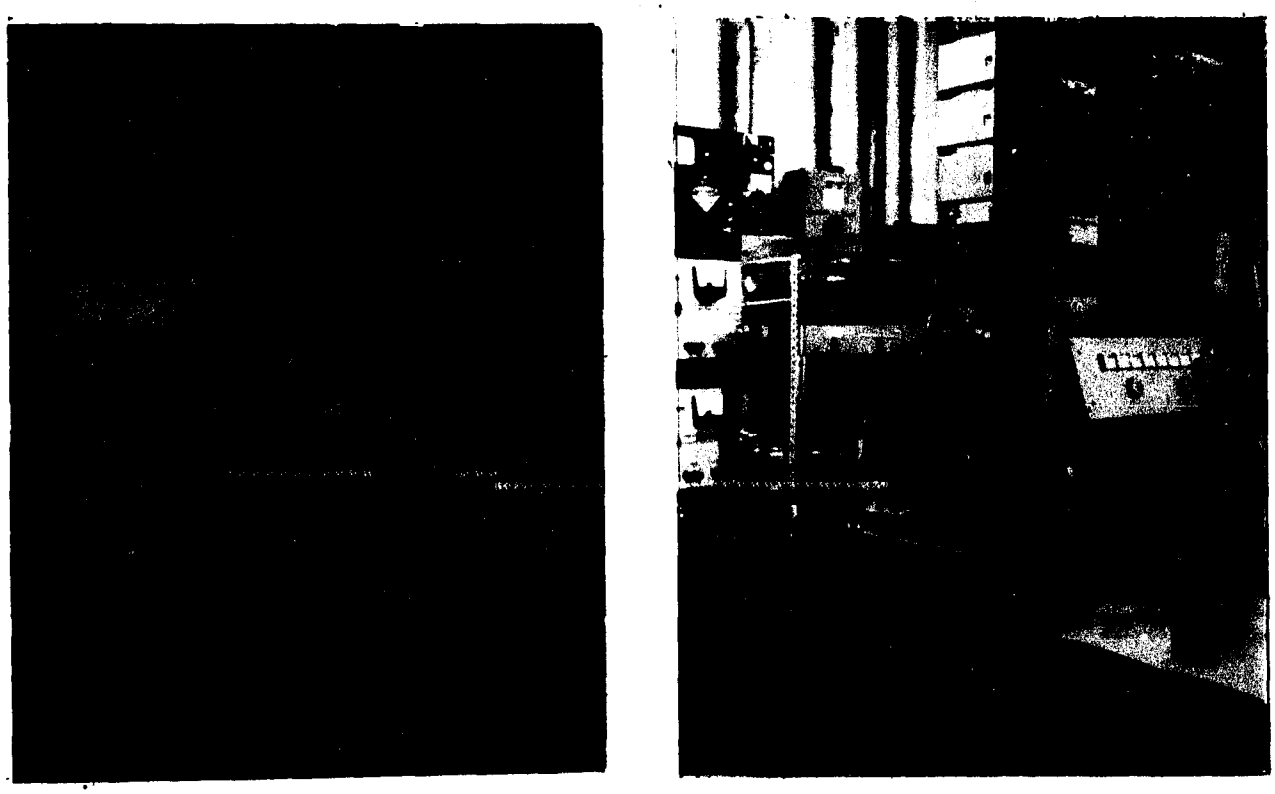

Figure 1.6 Photographs of Experimental Apparatus

gap. The pulse durations range from 10 microseconds to 1500 microseconds. The input labeled 'hold-on' on the variable monostable multivibrator is to insure that the beginning of the output current pulse coincides with the initiation of the monostable timing interval. The 'hold-on' control prevents extreme variations in the duration of the discharge. There was, however, a variation of about $\pm$ 10% of the desired pulse duration caused by the triggering of the Schmitt trigger circuit. The Schmitt trigger circuit is used

to monitor the gap voltage and determine the state of the gap.

The pilot pulse section is used to initiate electrical breakdown of the gap. It receives its input from the flip-flop and as soon as electrical breakdown occurs, the pilot pulse turns off. The pilot pulse section uses a power supply of 200 volts with a current capability of about 1 amp and it has a voltage rise-time of about 500 nanoseconds. The fast rise-time is necessary to avoid the effects of long statistical time delay breakdowns [24], which could possibly influence recovery measurements.

The power output stage consists of eight power transistors, which are paralleled to provide a variable range of current outputs similar to commercial machines. These stages were constructed with the lowest possible inductance to produce a current output pulse that is almost constant in amplitude, however, some inductance always remained in the circuit (about 3 microheneries) and limited the current rise-time. The current output oscillograms, as shown in Figure 1.7 represent different equivalent load resistances in series with the main supply voltage, i.e., $R_L = R_1 = 1.25$ ohm, $R_L = R_2 = R_1/2 = .625$ ohm, and $R_1 = R_3 = R_1/4 = .3125$ ohm. The time variation in the current waveforms was caused by the gap voltage variation during the discharge. As can be seen in Figure 1.7, the current waveforms are different for graphite and copper. This difference is caused by the higher resistivity and larger gap voltage associated with graphite electrodes [25].

For each output transistor, there is about 200 microamps leakage current. It was necessary to eliminate this leakage

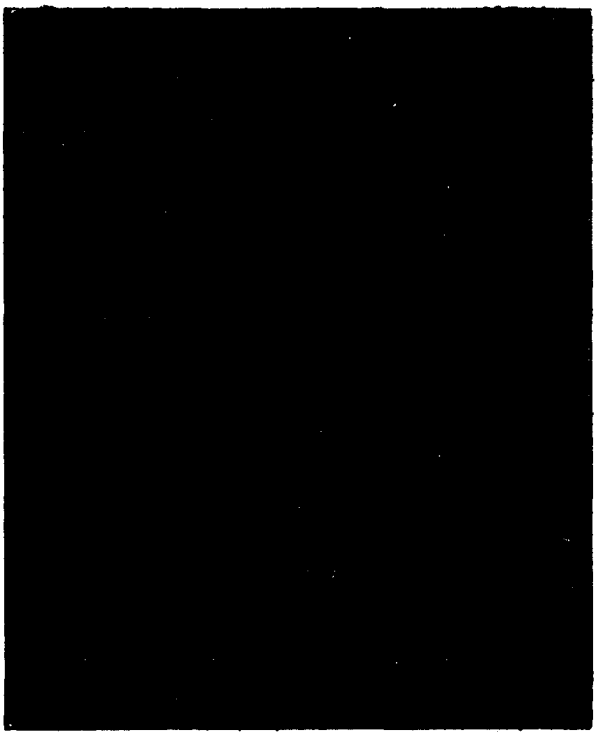

Reverse Polarity Copper on #416 steel

Scale:	Vertical	Horizontal
A)	10 volts/div	20 usec/div
B)	25 amps/div	20 usec/div

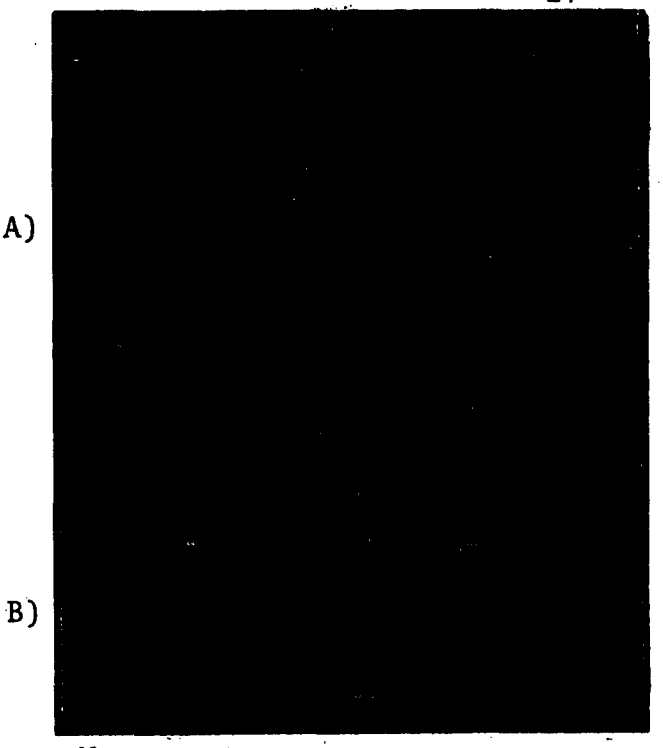

Normal Polarity Copper on #416 steel

Scale:	Vertical	Horizontal
A)	10 volts/div	20 usec/div
B)	25 amps/div	20 usec/div

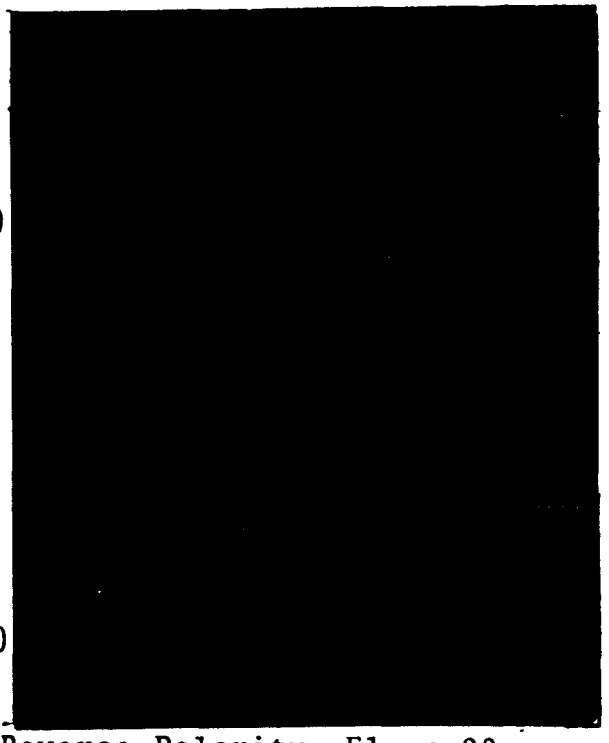

Reverse Polarity Elarc 90 on #416 steel

Scale:	Vertical	Horizontal
A)	10 volts/div	20 usec/div
B)	25 amps/div	20 usec/div

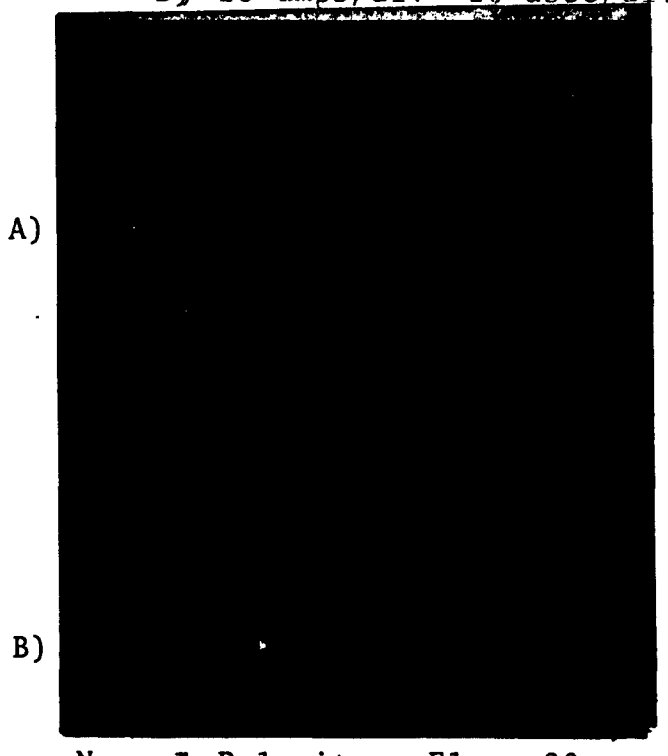

Normal Polarity Elarc 90 on #416 steel

Scale:	Vertical	Horizontal
A)	10 volts/div	20 usec/div
B)	25 amps/div	20 usec/div

Figure 1.7 Gap Voltage and Gap Current Waveforms for the Equivalent Load Resistances R_1=1.25ohm(lower trace), R_2=R_1/2 = .625ohm(middle trace), and R_3=R_1/4=.3125ohm(upper trace)

during the recovery time interval because it interfered with measurements to be made on the gap. The leakage current was eliminated by means of the shorting circuit which caused the leakage current to flow around the gap without interfering with the gap recovery or the checking voltage pulse. A simplified version of the gap circuitry is shown in Figure 1.8.

The checking circuitry was designed to produce the least amount of interference with the natural recovery of the machining gap. The voltage used in the checking circuit (10 volts) was chosen to be smaller that the gap voltage could ever be (about 15 volts). The current output of this circuit (1.3 ma) was also picked to be below the value needed to maintain a discharge [26].

The oscilloscope used throughout the entire project was a Tektronix 555 dual-beam scope. All voltages were sampled, using the Tektronix P6006 times-ten probe to lessen the effects of capacitance. The probe, however, had a specified load resistance of 10 million ohms and with the probe connected across the gap, this resistance appeared in parallel with the gap. The recovery of the gap was, therefore, measured relative to a 10 million ohm resistor. In other words, if the recovering gap were considered to be a time-varying resistance that would increase with time, the scope probe would appear as a constant resistance in parallel with the gap. By using the previously given definition and explanation of recovery time, the fully recovered waveforms of Figure 1.1 would be the result of changing the gap capacitance and discharging it through the scope probe resistance. When the gap was not

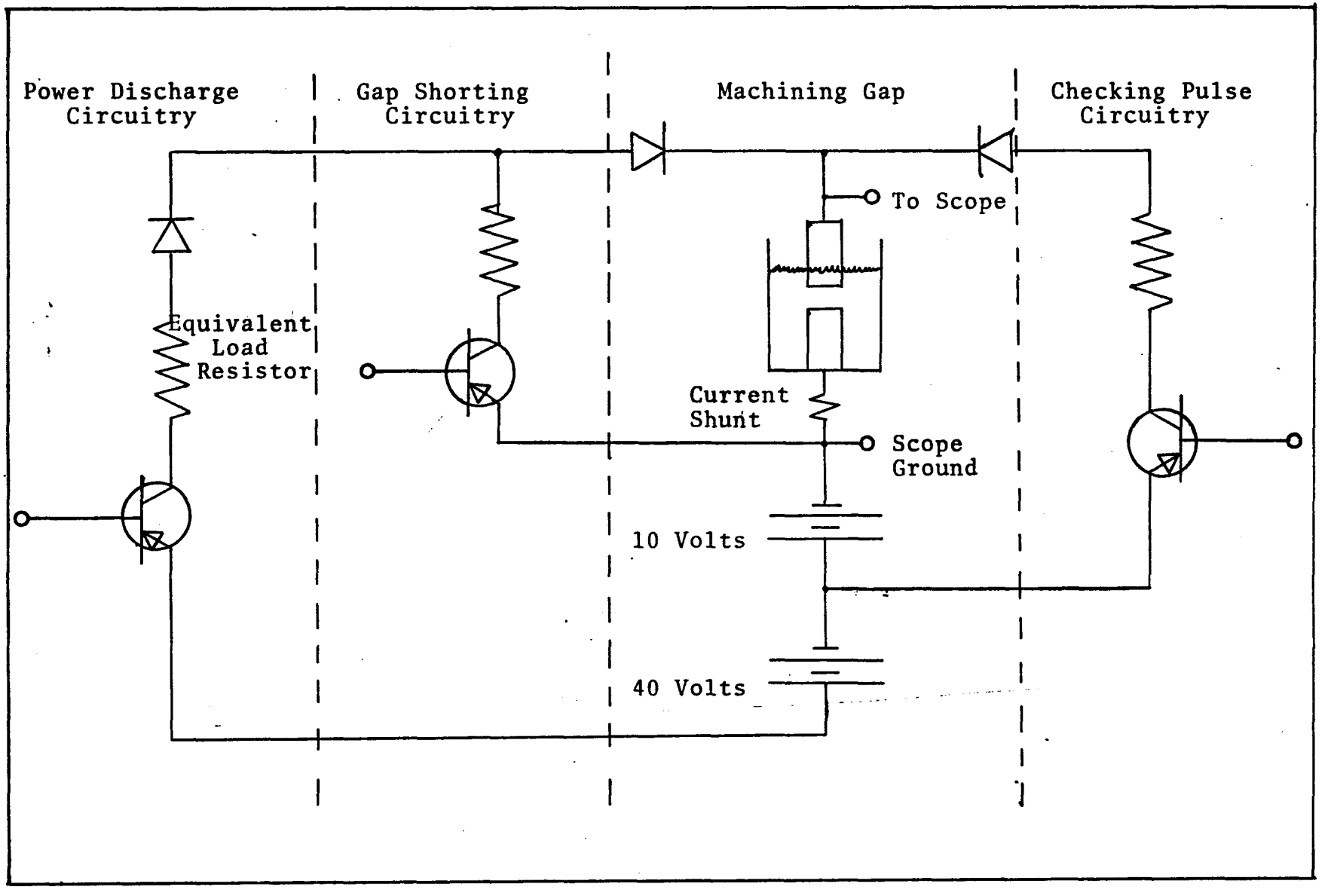

Figure 1.8 Simplified Machining Gap Circuitry Showing the Power Pulse Stage , the Gap Shorting Circuit , and the Checking Pulse Circuit

fully recovered, the capacitance would discharge through the recovering gap and the parallel scope probe. Therefore, when the gap resistance was much greater than the scope probe resistance, the parallel combination of the two were more or less equal to the probe resistance and hence, the fully recovered waveform was observed on the oscilloscope.

In addition to the equipment already described, some supplemental data, shown in Appendix B, concerning various EDM fluids was collected by using the apparatus described and used by Haswell [27] in his Doctorial thesis.

C. Electrical Parameters

The parameters used in this study were chosen to be similar to actual EDM operating conditions associated with a commercial EDM machine. The breakdown voltage used in this study was 200 volts which is within the range of breakdown voltage available on EDM machines (150 - 300 volts). The pulse durations investigated were between 10 to 1500 microseconds, which are again typically available durations. The peak currents used were between 0 to 100 amps. The duty cycle capability of the experimental apparatus was somewhat limited, however, single current pulses were of the main interest as opposed to continuous operation, although the apparatus could function in a continuous mode. The main current supply voltage was 50 volts which was typical of commercial machines (40-50 volts).

D. Materials Employed in the Investigation

The electrode materials used throughout the experiments were standard materials used in many machining operations;

they were, however, not a complete spectrum of all the materials used, but only typical electrodes. The basic tool electrodes used were graphite, carbon, and copper. Some selected properties of the copper electrodes used in this investigation can be seen in Table 1.1. A general representation of the thermal properties of one of the graphites used (Elarc 90) [28] can be seen in Figure 1.9. Various other varieties of graphites and carbons were used and will be mentioned as their experimental results are explained. The workpiece materials were also typical metals used in many EDM operations. The metals considered were:

(1) Hardtem-B Tool-Steel (Heppenstall Co.)

(2) Armco Iron

(3) #416 Wrought Stainless-Steel

(4) Gray Cast Iron

The typical composition and basic thermal properties of these metals are given in Table 1.2.

	Ref. 29	Units
Melting Temperature	1083	°C
Boiling Temperature	2595	°C
Thermal Conductivity (20°C)	.94	Cal/cm °C Sec
Density (20°C)	8.96	gms/cm^3
Specific Heat (20°C)	.092	Cal/gm °C
(1083°C)	.118	Cal/gm °C
Resistivity (20°C)	1.67	ohm-cm x 10^6

Table 1.1 Properties of Copper

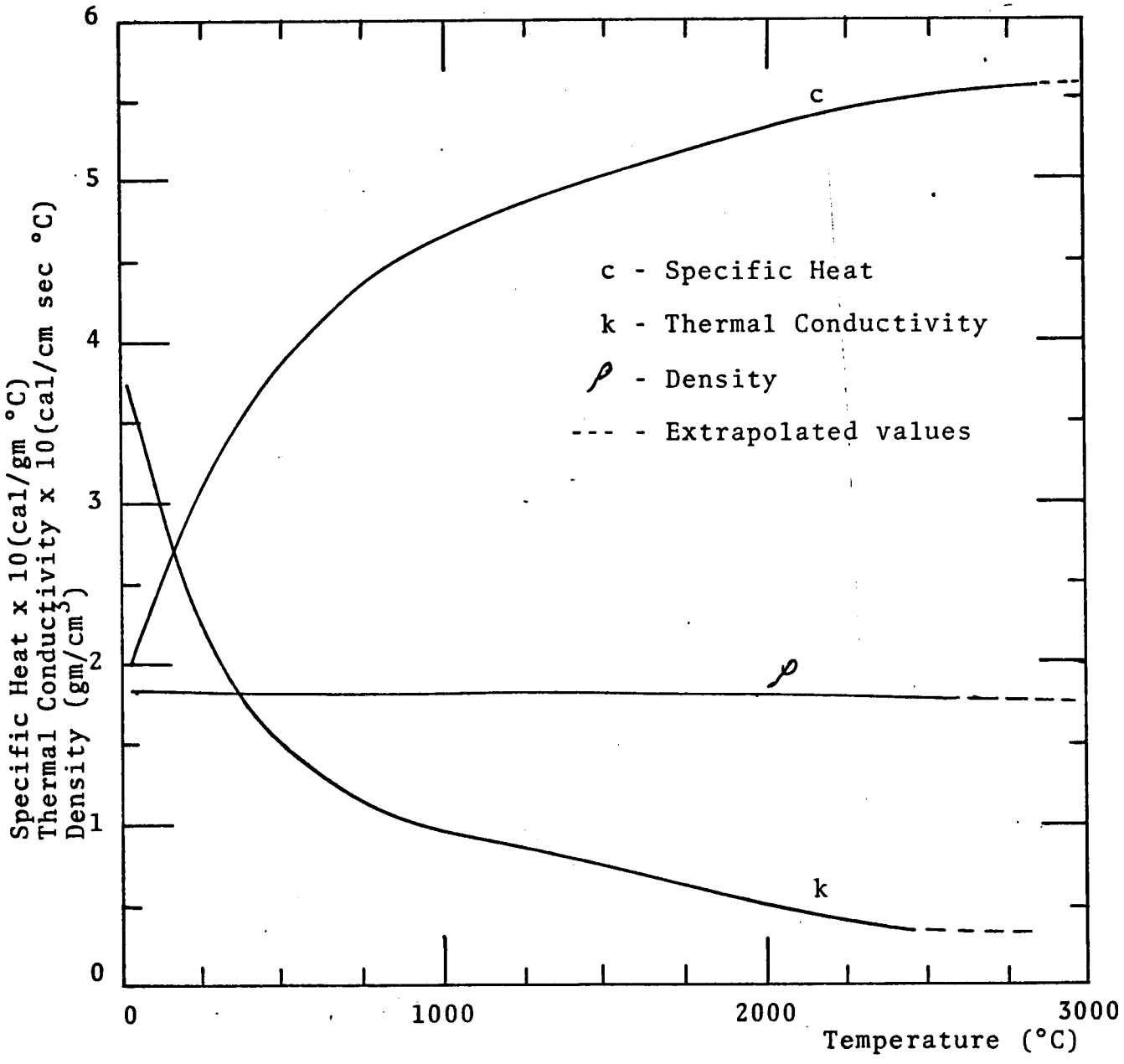

Figure 1.9 The Thermal Properties of Graphite

	Ref. 6,31 Hardtem B	Ref. 30,6,29 Armco Iron	Ref. 29,32 #416 Steel	Ref. 29,33,34 Gray Cast Iron
Elements Wt. percent				
Carbon	.5-.6	.0060	.16max.	2.75-3.00
Manganese	.65-.95	.0050	1.25max	.80-1.00
Silicon	.20-.35	.0040	1.00max	2.00-2.50
Chromium	.85-1.15	.0050	12.0-14.0	.35-.50
Molybdenum	.38-.48	.003	.06	.35-.50
Vanadium	.06-.1	.0020		
Phosphorous	.04max	.0010		.12max
Sulfur	.04max	.004	.06max	.12max
Nickel	.45-.6	.009		
Hydrogen	----	.0005		
Oxygen	----	.03		
Nitrogen	----	.002		
Aluminum		.01		
Copper		.01		
Titanium		.001		
Properties at 20°C				
Melting Temperature (°C)		1536	2700-2750	1147
Boiling Temperature (°C)		3000		
Thermal Conductivity (cal/cm °C sec)	.102	.18 .07(627°C)	.096 .06(100°C)	.11
Density (gms/cm^3)	7.83	7.87	7.70	7.97
Specific Heat (cal/gm °C)	.11	.11	:154	
Resistivity (ohm-cm x 10^{-6})	22.3	9.71	22.7	

Table 1.2 Composition and Properties of Workpiece Materials

			Ref. 35	Units
Gravity: Specific		@ 60°F	.8348	____
	API	@ 60°F	38.00	____
Viscosity (liquid):	Absolute	@ 70°F	4.00	Centipoise
	Kinetic	@ 100°F	6.35	Centistokes
		@ 210°F	2.00	Centistokes
Specific Heat (liquid)		@ 300°F	.576	Btu/lb °F
		@ 400°F	.625	Btu/lb °F
		@ 500°F	.675	Btu/lb °F
		@ 600°F	.724	Btu/lb °F
Thermal Conductivity (liquid)		@ 25°F	.07	Btu/ft hr °F
		@ 250°F	.0485	Btu/ft hr °F
Latent Heat of Vaporization (liquid)		@ 100°F	123	Btu/lb
		@ 200°F	113	Btu/lb
		@ 300°F	102	Btu/lb
		@ 400°F	91	Btu/lb
		@ 500°F	80	Btu/lb
		@ 600°F	69	Btu/lb
Average Molecular Weight			170	AMU

Table 1.3 The Properties of Kerosene

The EDM fluid used for most of the measurements, was a commercial EDM fluid (Texaco Code 499), which is typically kerosene with additives. The typical properties of kerosene are given in Table 1.3. Various other EDM fluids were also used to determine their basic differences and affects on the recovery time of the gap. The other fluids were either hydrocarbon, hydrocarbon-silicone mixtures of pure silicone. Some of the properties of pure silicone fluid are given in Table 1.4. Data was not available concerning the hydrocarbon-silicone mixtures and the other fluids were basically kerosene, but produced by different manufacturers.

	Ref. 36, 37	Units
Viscosity (25°C)	5.0	Centistokes
Specific Gravity (25°C)	.916	
Thermal Conductivity	.067	BTU/hr.ft.°F
Specific Heat (20°C)	.37	Cal/gm °C
(200°C)	.41	
Resistivity (20°C)	4×10^{15}	ohm-cm

Table 1.4 The Properties of Pure Silicone Fluid

CHAPTER II

THE RECOVERY TIME MEASUREMENTS USING TYPICAL EDM PARAMETERS

A. Results for the Reference Electrode and Workpiece Materials

In the repetitive discharge EDM process, the recovery time is important because it represents a time interval during which no work is being done. Consequently, the optimum machining condition usually results from a minimum recovery time condition. If the off time is less than this minimum recovery time, then it is possible for a discharge to occur at the same physical location as the immediately preceding discharge. This condition signals the onset of arcing or coking. It is of utmost importance in EDM for succeeding discharges to occur at different physical locations on the machining surface for the EDM process to function correctly.

In the present investigation, many parameters were changed and the resultant recovery times compared in an attempt to understand and optimize the recovery time. Since many parameters were changed and the results measured, some "reference" data was needed for comparison with the results obtained after conditions were changed. Two sets of electrode-workpiece materials were chosen as reference materials - Copper with #416 Wrought Stainless Steel and Elarc 90 Graphite with #416 Wrought Stainless Steel. There is nothing particularly unique in these combinations of materials. The materials are commonly encountered in the EDM utilization art and, in addition, it was

considered that the results from both a typical metallic (copper) electrode and a graphite electrode should be examined.

As mentioned previously, the recovery time, as measured in this investigation is the time required for the discharge gap to attain a resistance much greater than 10 million ohms. The recovery times measured in this way do not necessarily correspond to the minimum acceptable "off" time. Nevertheless, as will be discussed later, there is some correlation between the recovery times measured in this manner and the minimum acceptable "off" time results obtained from an actual EDM machine.

1.) Reverse Polarity, Clean Gap Reference Set, Recovery Data

The first electrode combination considered was copper and #416 Wrought Stainless Steel using copper as the anode (tool electrode) and steel as the cathode (workpiece). The EDM Fluid used was Texaco Code 499. Figure 2.1 shows the recovery results with the clean gap conditions for three current output settings. (current waveforms were given in Figure 1.7.) The pulse duration was varied from 10 microseconds to 1500 microseconds and the recovery time was recorded. The scattering of the data points can be attributed to the following factors:

(1) Variation in the gap spacing at various pulse duration settings;

(2) Different delay times between the application of the pilot pulse breadkown voltage and the actual breakdown of the gap;

(3) Slight contamination from succeeding discharges even though care was taken to avoid this effect, and

(4) Steel plating of the copper electrode at higher pulse durations.

The first conclusion that could be drawn from Figure 2.1, is that the recovery time becomes longer as the amplitude of the current pulse increases. With a current of approximately 24 amps peak value, $R_L = R_1$, the recovery time is about 7 microseconds and it appears to be relatively constant with varying pulse duration. When the current is increased to 45 amps with $R_L = R_2 = R_1/2$, the recovery time doubles to approximately 14 microseconds and again it appears to remain constant, with increasing pulse duration. When the current is again doubled, to about 85 amps with $R_L = R_3 = R_1/4$, the recovery time again increases. With $R_L = R_3$, the constant recovery time - approximately 22 microseconds - appears to be about 7 microseconds greater than what it is with $R_L = R_2$, but only for the pulse duration range from about 50 to 300 microseconds. Below this pulse duration range, the recovery times are shorter, while with longer durations, the recovery time appears to be increasing slightly with increasing pulse durations. The lower recovery time, at short pulse durations, can be attributed partially to the relatively slow rise of the current caused by circuit inductance (see Figure 1.7). The increasing recovery times found at the longer pulse durations may possibly be caused by the increased heating effects accompanying the higher current and longer duration pulse.[38]

The next electrode combination considered was Elarc 90 graphite on #416 steel with Elarc 90 as the anode, using

Texaco Code 499 EDM Fluid. The recovery data was relatively easy to collect and no major problems were encountered during this test set. The recovery time results for Elarc 90 on #416 steel can be seen in Figures 2.2. Initial observation of this recovery data, again, shows that there is an increase in recovery time with increasing current amplitude, as was found for the case of a copper electrode. Figure 2.2 shows the clean gap case. With the clean gap and pulse durations below 100 microseconds, the data for Elarc 90 is very similar to the data for a copper electrode. One difference between the two sets of data is that the recovery time is slightly longer with the Elarc 90. Above 100 microseconds, the copper and Elarc 90 data sets are very different. All three current settings have recovery times that increase with increasing pulse duration, somewhat different from the results found with copper. The lower thermal conductivity of the graphite, when compared to copper at the arc temperatures involved (6940°K for graphite and 5900°K for copper[39]), and the high vaporization temperature of graphite in comparison to copper, probably act to increase the recovery times. The graphite undoubtedly achieves a higher temperature and remains at a higher temperature longer than the copper, thereby causing the gap to recover more slowly at the higher pulse durations.

The approximately constant recovery times found for pulse durations below 100 microseconds can probably be attributed to minimal involvement of the electrodes in the thermal recovery of the gas temperature in the gap space. The electrode simply does not absorb sufficient energy to cause its thermal decay

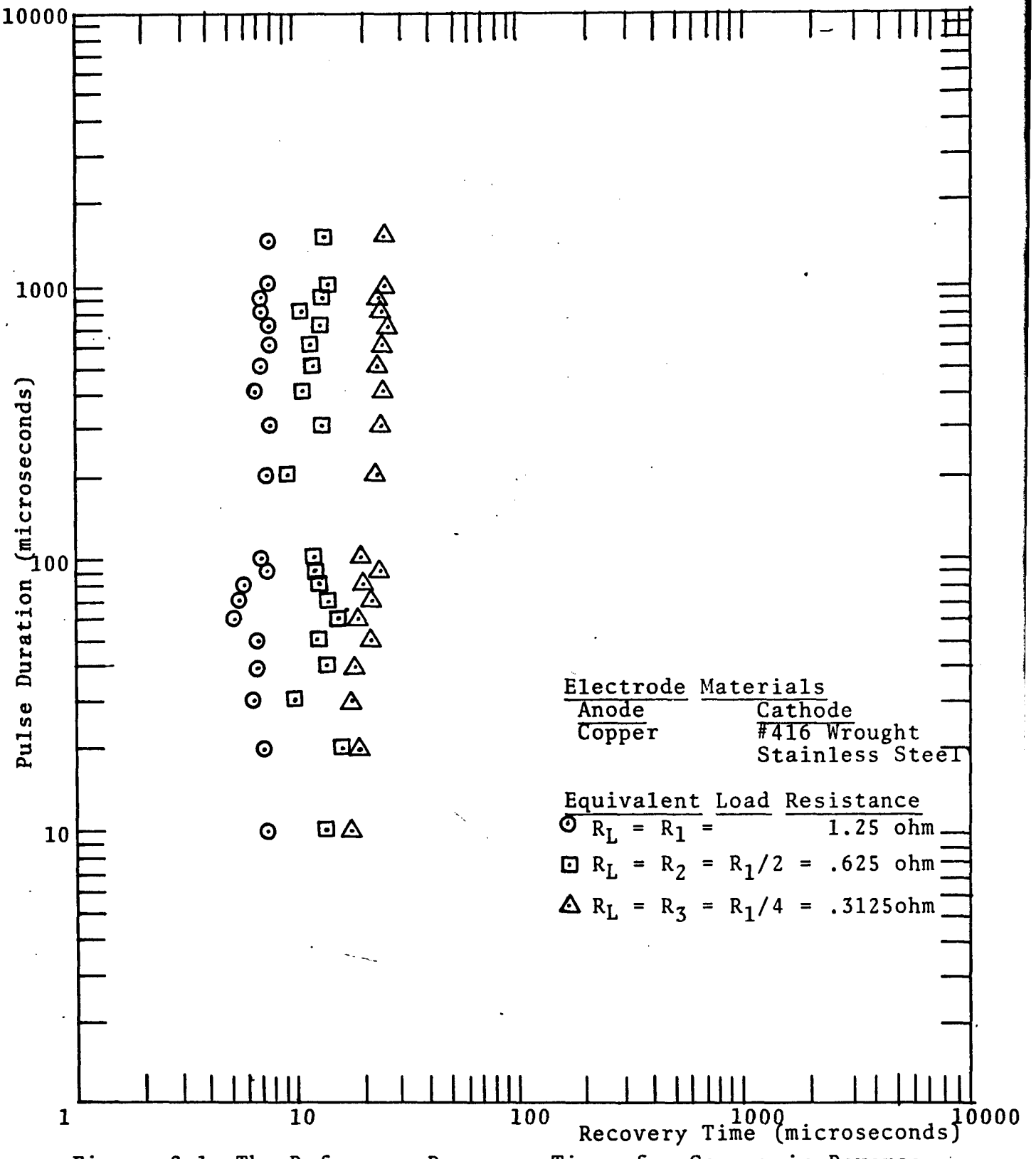

Figure 2.1 The Reference Recovery Times for Copper in Reverse Polarity with a Clean Gap and Texaco Code 499 EDM Fluid

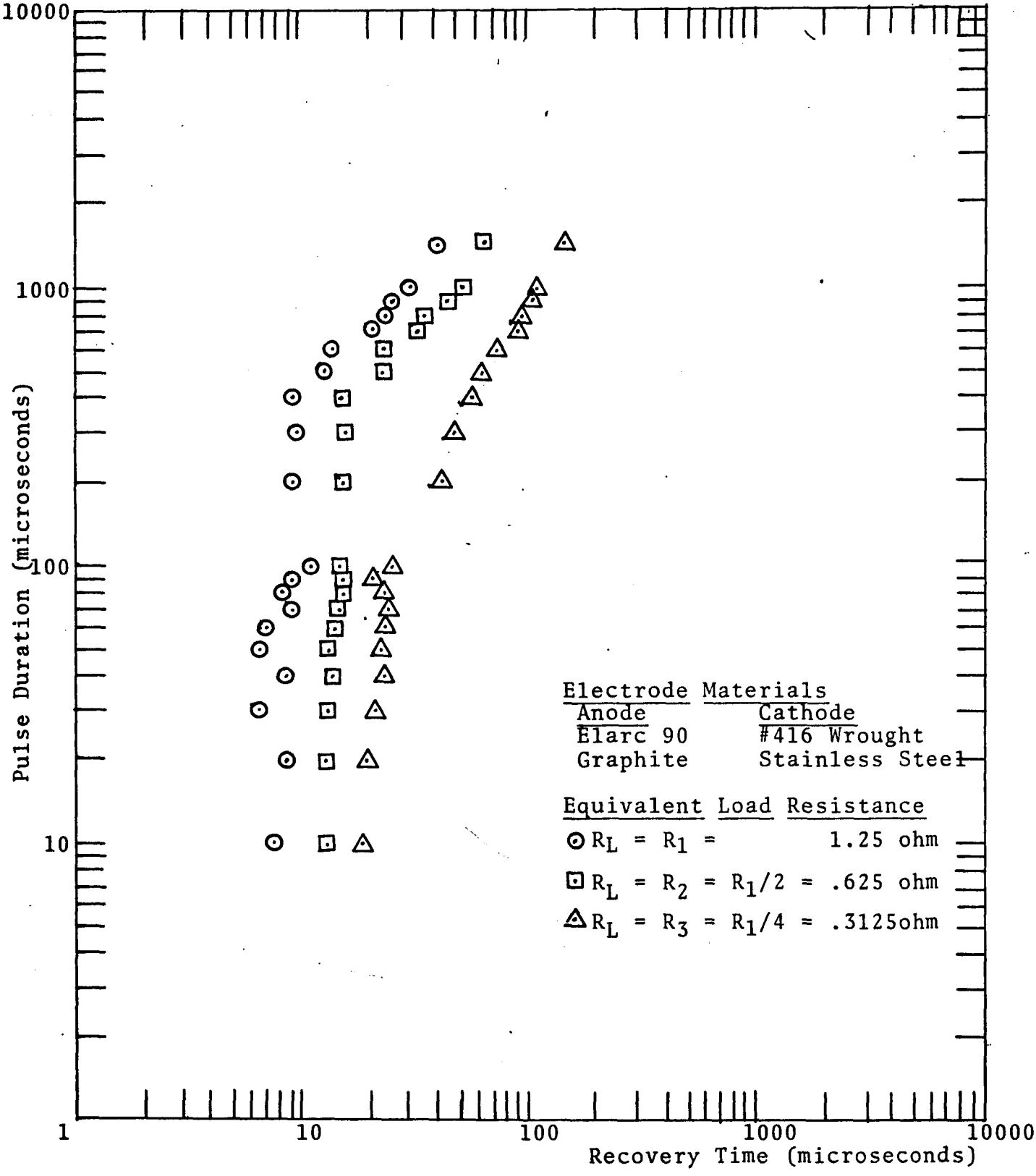

Figure 2.2 The Reference Recovery Times for Elarc 90 in Reverse Polarity with a Clean Gap and Texaco Code 499 EDM Fluid

time to exceed those of the gap gases. Therefore, the fast recovery observed for the lower pulse durations was possibly the gas thermal time constant. Eckman [41] has shown that the electron temperature, and hence the gas temperature [42], reaches a peak value in less than .1 microseconds after the discharge was initiated and then proceeds to cool to what appears to be an almost steady value, with the higher current discharges remaining at the higher temperatures. The higher current, and hence higher temperature discharges, would require a longer time for their ionized gases to cool. The longer cooling time then implies that as the discharge current increases so will the time necessary for the gap to recover.

The probable reason that higher recovery times are more evident at the longer pulse durations, is that the electrode's thermal capacity will absorb much more heat during the longer pulse durations. The long pulse durations then cause the thermal gradient into the electrode materials to become less severe and thereby slowing the conduction of the heat from the surface. The surface temperature of the discharge spot then becomes a greater influence on the recovery interval because its temperature remains higher longer.

2.) Normal Polarity, Clean Gap Reference Set Recovery Data

The next electrode arrangement investigated involved the same materials as were used for Figures 2.1 and 2.2. The copper is now the cathode and #416 steel is the anode. All other factors and conditions remained identical to the reverse polarity case. Several problems occurred while the recovery time data was being compiled for this case. With a

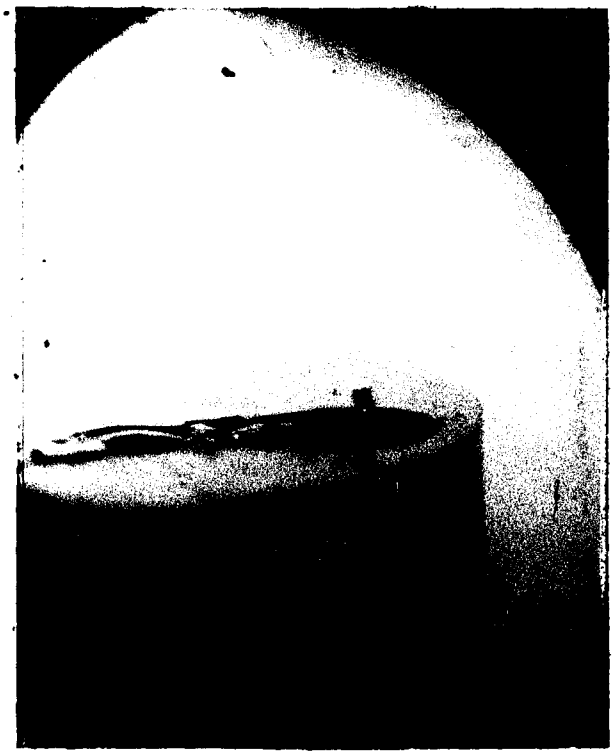

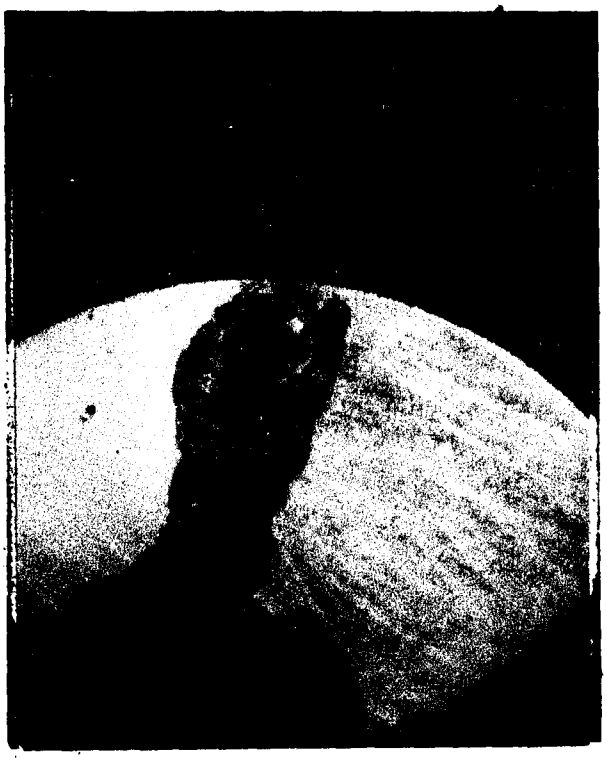

Anode: #416 Steel

Scale: Approximately 1mm/cm

Cathode: Copper

Scale: Approximately 1mm/cm

Figure 2.4 Photograph of Copper Cathode and the Opposing #416 Wrought Stainless Steel Anode with a Pillar of Steel Protruding from its Surface

clean gap, there was much difficulty in producing a current discharge, even with many gap breakdowns caused by the pilot pulse. However, as the gap became more contaminated, owing to the low current pilot pulse breakdowns, a high current discharge eventually occurred, which, in turn, made it easier to produce other power discharges. Contamination, however, was limited to a minimum in the clean gap case and the result was, that data was difficult to take and, to some extent, erratic, as can be seen in Figure 2.3.

Another problem occurred as the pulse duration was increased with copper as the cathode. With pulse durations greater than 1000 microseconds, there was a tendency for the gap to short during the discharge. In order to determine what was occurring in the gap that would cause a short circuit, the pulse duration was increased to 50 milliseconds. The photographs in Figure 2.4 show the results after 4 consecutive discharges. Notice that there is a small pillar of steel protruding from the steel anode surface. This pillar was apparently formed from the steel surface and bridged the gap during the discharge and caused the short between the anode and cathode. This protrusion appeared to be the result of a sliver of anode material being thrown upto the cathode. Further microscopic examination, during the numerous times this phenomena was observed, disclosed that a possible explosion on the anode surface expelled molten material to produce the pillar. When the anode surface was polished, it was observed that gas pockets had been trapped under the resolidified steel. It was, therefore, theorized that rapid heating of the gas pockets,

during a discharge, caused violent out-gassing or explosions on the surface that resulted in the shorted gap. Although the long duration of the discharge has enhanced the effect, this accounts for the gap being shorted during a discharge and also explains why copper on steel, in normal polarity, produces such erratic operation on most EDM machines. In fact, copper on steel - normal polarity - is rarely used at high pulse durations.

A possible explanation of why this phenomenon was not observed in reverse polarity was that there appeared to be no gas pockets trapped in the resolidified steel. The rapid heating of the gas pockets and the explosive out-gassing apparently are necessary to produce this phenomena. The reason gas is trapped in the resolidified metal when steel is the anode and not when it is the cathode can best be understood when a comparison of the surface texture of the machined steel electrode is made, see Figure 2.5. Figure 2.5 shows a side-by-side comparison of a steel electrode when it is machined as the cathode and as the anode. Notice that when the steel was the cathode, the surface texture is more smooth and regular, while the steel anode surface is very irregular and rough, even though the pulse durations used were the same in both cases. The surface texture of the steel anode would be more likely to produce trapped gas pockets under the resolidified metal, while the smoother steel cathode surface would not.

The recovery time data for the copper cathode case is shown in Figure 2.3. Again, the most noticeable result is the difference in recovery time as the current amplitude is

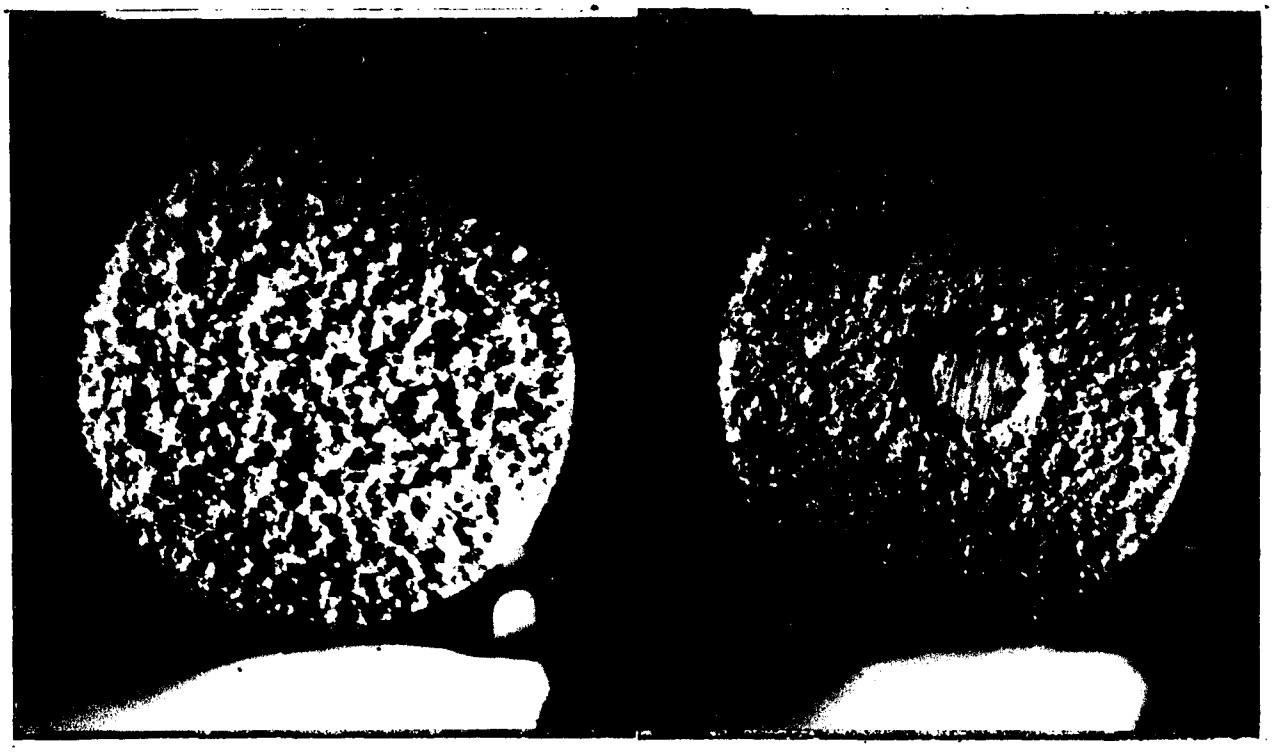

Normal Polarity

Scale: 1cm = .07 inch

Reverse Polarity

Scale: 1cm = .07 inch

Figure 2.5 Photograph of Surface of the #416 Wrought Stainless Steel Electrode Produced by Normal and Reverse Polarity Machining

increased. The recovery times with $R_L = R_1$ and R_2 are very similar to those with copper as the anode. The results with $R_L = R_3$, however, are more comparable to the highly contaminated gap case with copper as the anode which will be discussed later. The slight increase in recovery times observed when the copper electrode was changed from the anode to the cathode can be attributed to the greater current amplitudes available, in normal polarity, for this electrode combination, (see Figure 1.7). The greater current amplitudes would produce greater heating of the electrode crater area, thereby causing a longer thermal recovery time.

The Elarc 90 on #416 steel combination was studied again, but with Elarc 90 as the cathode; the clean gap results are shown in Figure 2.6. This normal polarity combination exhibited difficulties similar to those encountered when copper was used. Again, the machining gap was very reluctant to accept a current discharge, although there were many pilot pulse breakdowns observed. After numerous pilot pulse breakdowns, the gap again became slightly contaminated, and only then, was it relatively easy to produce current discharges. The current discharges were also observed to be very erratic and at times varied as much as 7 or 8 amps during the course of a discharge. A photograph of the erratic nature of the current can be seen in Figure 2.7, and some reference to the possible cause will be made later. These difficulties again cause a somewhat scattered appearance to the data on recovery time, although care was taken to exclude vastly varying current pulses from the data.

Scale: Vertical - 5 Amps/Division
Horizontal - 10 Milliseconds/Division
Equivalent Load Resistance
$R_L = R_1 = 1.25$ Ohm

Figure 2.7: Erratic Gap Current Waveforms Occurring When Elarc 90 and #416 Wrought Stainless Steel Are Used in Normal Polarity

The recovery time results for the clean gap case with Elarc 90 as the cathode are shown in Figure 2.6. The recovery times found for the shorter pulse durations, 10 to 80 microseconds, with the $R_L = R_2$ and R_3 current settings are much shorter than those measured for any of the previously mentioned electrode materials or polarities. This difference can possibly be explained by again referring to Figure 1.7 which shows the current waveforms for Elarc 90 as the anode. There is a very slow current rise with this electrode material as the cathode when compared to the other waveforms in Figure 1.7. The slow rise time could be attributed to the greater resistivity of the Elarc 90 and the higher machining voltage that occurs with graphites or carbons as the cathode material. The relatively constant value of recovery time that was observed for the various current settings and lower pulse dura-

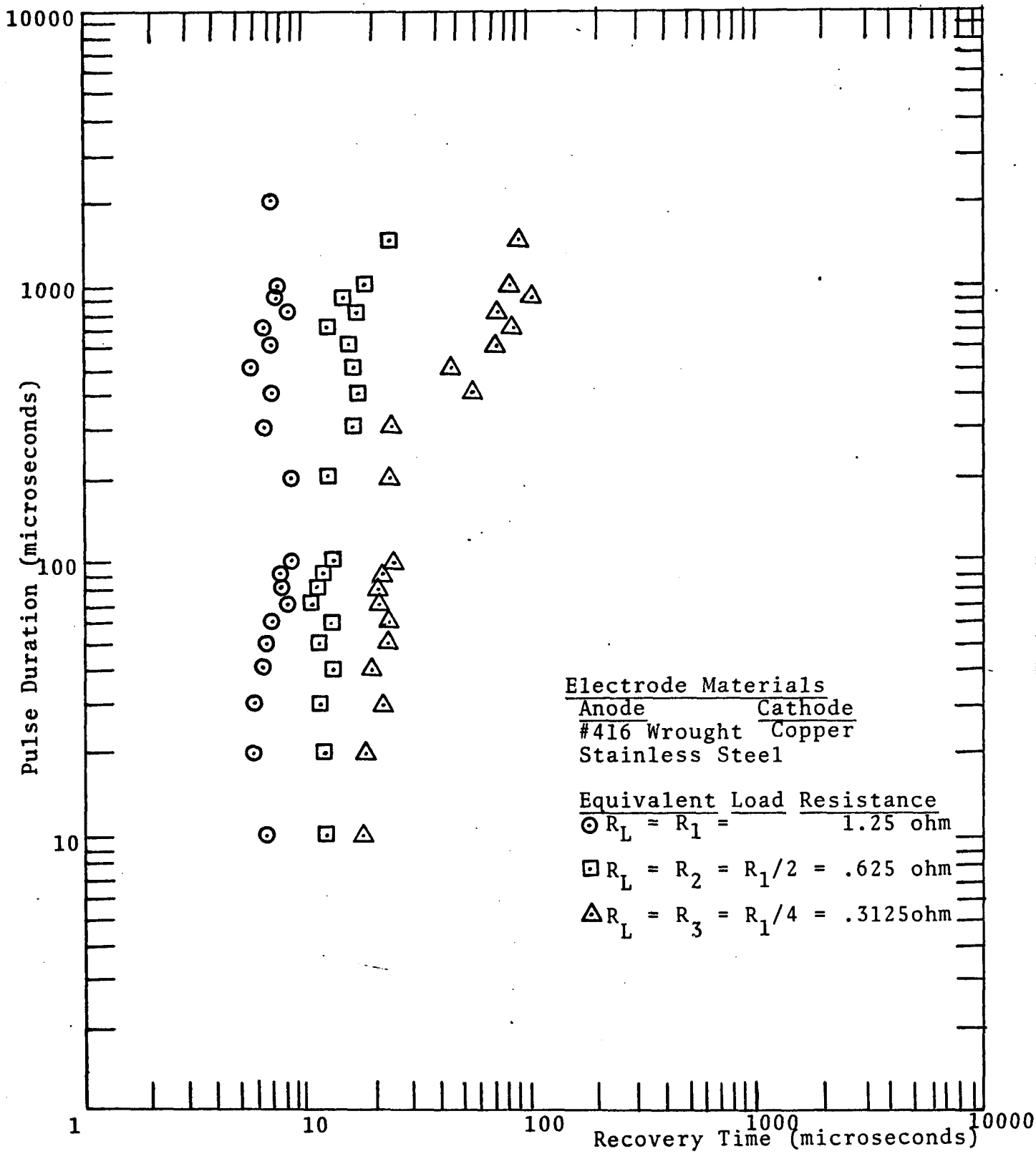

Figure 2.3 The Reference Recovery Times for Copper in Normal Polarity with a Clean Gap and Texaco Code 499 EDM Fluid

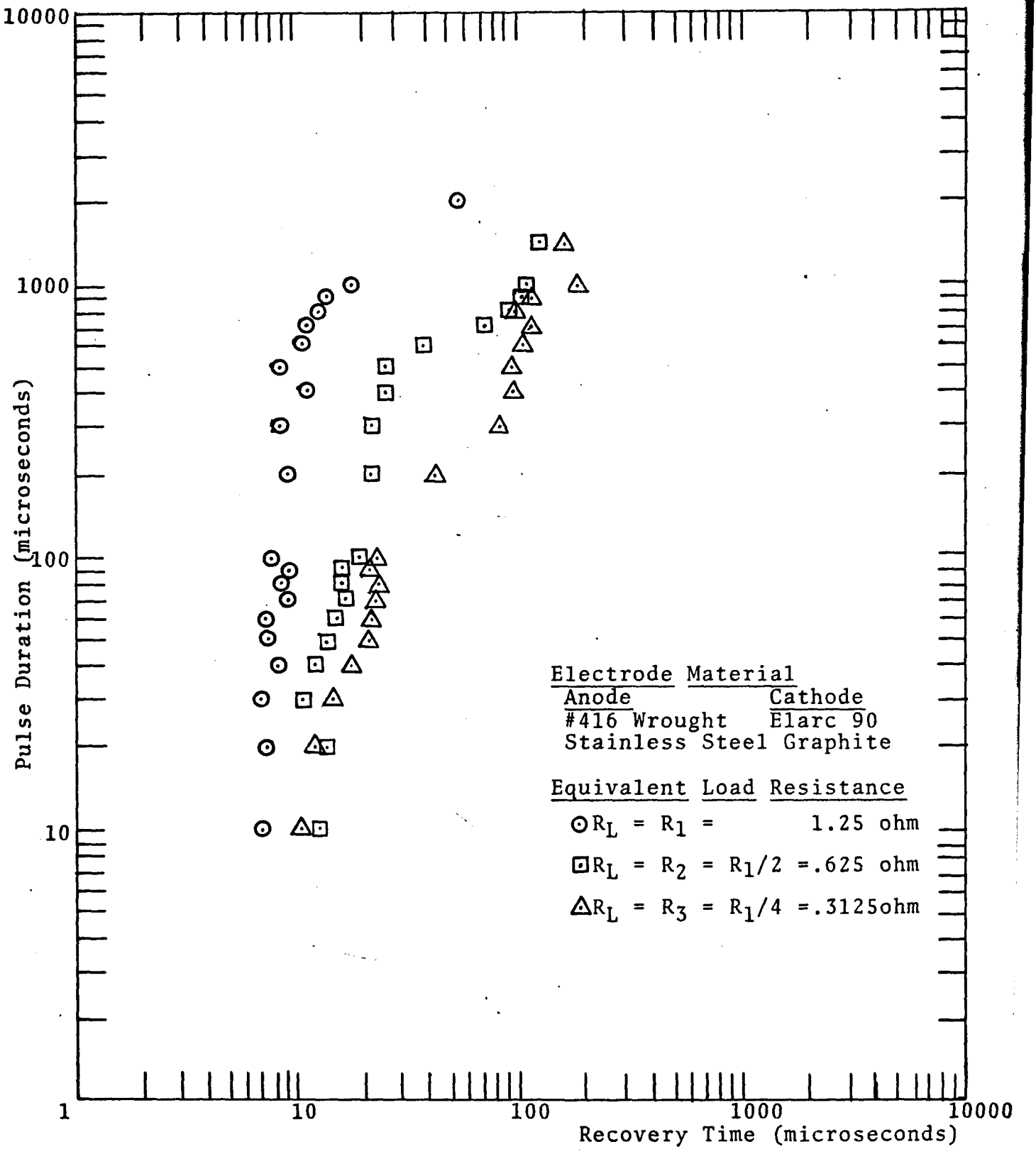

Figure 2.6 The Reference Recovery Times for Elarc 90 in Normal Polarity with a Clean Gap and Texaco Code 499 EDM Fluid

tions with other configuration and materials was not observed with Elarc 90 as the cathode resulting from this slow current rise time. If a way could be found to overcome this slow rise time, possibly the same relatively constant recovery times would have been observed in this case as it was in the other configurations.

3.) Reverse and Normal Polarity Contaminated Gap Reference Set Recovery Data

As was mentioned previously, no attempt was made to clean or flush the gap for the highly contaminated gap condition and all the debris and chemically cracked EDM fluid that was produced by the continuous sparking was permitted to remain in the gap space. The first electrode combination considered was copper on #416 Wrought Stainless Steel with copper as the anode. Figure 2.8 shows the recovery times associated with the same electrode configuration as Figure 2.1, except in this case the gap was permitted to become very contaminated. The highly contaminated gap case is not appreciably different from the clean case when $R_L = R_1$. However, with $R_L = R_2$ and R_3, there is a noticeable increase in the recovery time when compared to the clean gap case. With $R_L = R_2$, the recovery time appears to increase from 14 microseconds to about 16 microseconds when the pulse duration used is varied from 10 to 300 microseconds. At higher pulse durations, the recovery time appears to increase slightly with increasing current discharge durations, as occurs with $R_L = R_3$ with a highly contaminated gap. For the pulse duration range from 10 to 300 microseconds, the recovery times are very similar to the clean gap case. Above 300 microseconds,

the recovery times increase very noticeably with increasing pulse duration. The longer recovery time with a highly contaminated gap, could partially be attributed to the way the tests were conducted. The clean gap case had several seconds between successive discharges, while the highly contaminated case, had a minimum of 24 milliseconds between discharges. Although this time delay between successive discharges was made long and the discharge frequency made low to avoid mass electrode heating, it is possible that this succession of discharges could possibly change the temperature pattern of the entire electrode at higher current and longer pulse durations, thus affecting the rate at which the electrode discharge crater cools. Also, the large amount of debris on the surface of the electrodes, which contains carbon from the chemically cracked EDM fluid, could change the thermal properties of the ionized gas, thereby increasing its temperature decay time. There were also more noticeable amounts of steel plated* onto the copper cathode in the highly contaminated gap case than on the clean one, which would have also affected the thermal properties of the gap space.

The next case that was considered was the highly contaminated gap with Elarc 90 as the tool anode. Again the recovery time curve, shown in Figure 2.9, exhibits an increasing re-

---

* Steel plating is observed in the reverse polarity situations and it generally occurs at pulse widths greater than 100 microseconds. It involves the transport of steel from the anode to the cathode surgace, where it deposited as a gray or silvery coating upon the original electrode material.

covery time as the pulse duration is increased. The recovery times for $R_L = R_2$ and R_3, in the pulse duration range from 10 to 70 microseconds, appears to be slightly less than what they were when a clean gap was investigated. The results were checked and the data sequence repeated, but the results were about the same. The results with $R_L = R_1$ is slightly greater in the highly contaminated gap case, as occurred with the previous electrode configurations. With pulse durations greater than 70 microseconds, the data, again, becomes greater with a highly contaminated gap than with a clean one. The recovery times began to increase after 100 microseconds in the highly contaminated case, while in the clean case, the increase did not start until 400 microseconds for $R_L = R_1$ and R_2. For the current output with $R_L = R_1$ and R_2, the recovery times are noticeably longer for the upper range of pulse settings. With $R_L = R_3$, the difference is not as noticeable, but the highly contaminated case has slightly longer recovery times. The similarity of the clean and highly contaminated cases, with $R_L = R_3$, indicates that the gap and Elarc 90 electrode, possibly should have been cleaned more often in the clean gap case than after every second or third discharge.

Figure 2.10 shows the case of a copper cathode with a highly contaminated gap space. The recovery time curve again had a shape similar to those obtained with other materials and polarities. By comparing the contaminated case (Figure 2.10) with the clean gap case (Figure 2.3), it can be seen that the highly contaminated gap case is, again, very similar to the clean gap, except the clean gap recovery times were slightly

shorter. The recovery time data was less erratic in the highly contaminated case owing to the amount of contamination which was discussed earlier. However, recovery times, at pulse durations greater than 1000 microseconds, were nevertheless difficult to determine accurately. (See 1500 microseconds recovery time with $R_L = R_2$ - Figure 2.10).

The final recovery time reference set is the case with Elarc 90 as the cathode and #416 steel as the anode, which is shown in Figure 2.11. The recovery time curve again showed a shape similar to previously discussed curves for other configurations. However, if a comparison is made between Figure 2.11 and the previously mentioned curves, it can be seen that the case with Elarc 90 as the cathode exhibited the longest recovery times of all the reference materials considered. The most probable cause of the longer times is the greater heating effects that occur at the Elarc 90 electrode surface. The combination of the larger machining voltage drop, resistive heating, and thermal properties of the graphite material act to produce higher temperatures, as mentioned previously, and cause the temperatures to remain elevated longer than with the other reference materials. The higher temperatures and the longer thermal recovery times associated with graphite materials, and the fact that the Elarc 90 electrode was the cathode,or electron emitter, combine to produce a larger degree of thermal ionization and a longer lasting ionization effect than was observed with the other reference materials investigated. The longer thermal ionization times then could produce the longer recovery times.

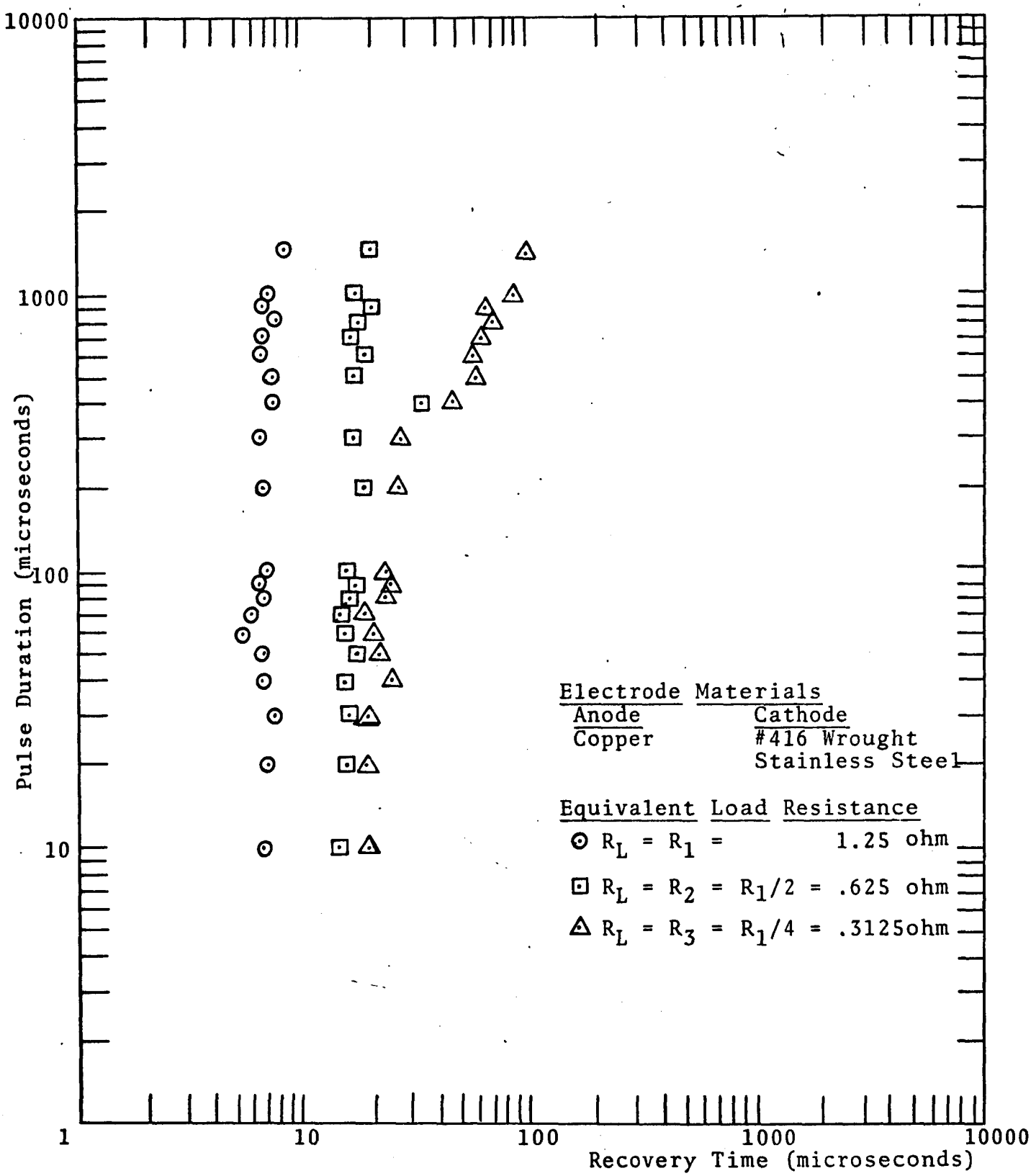

Figure 2.8 The Reference Recovery Times for Copper in Reverse Polarity with a Highly Contaminated Gap and Texaco Code 499 EDM Fluid

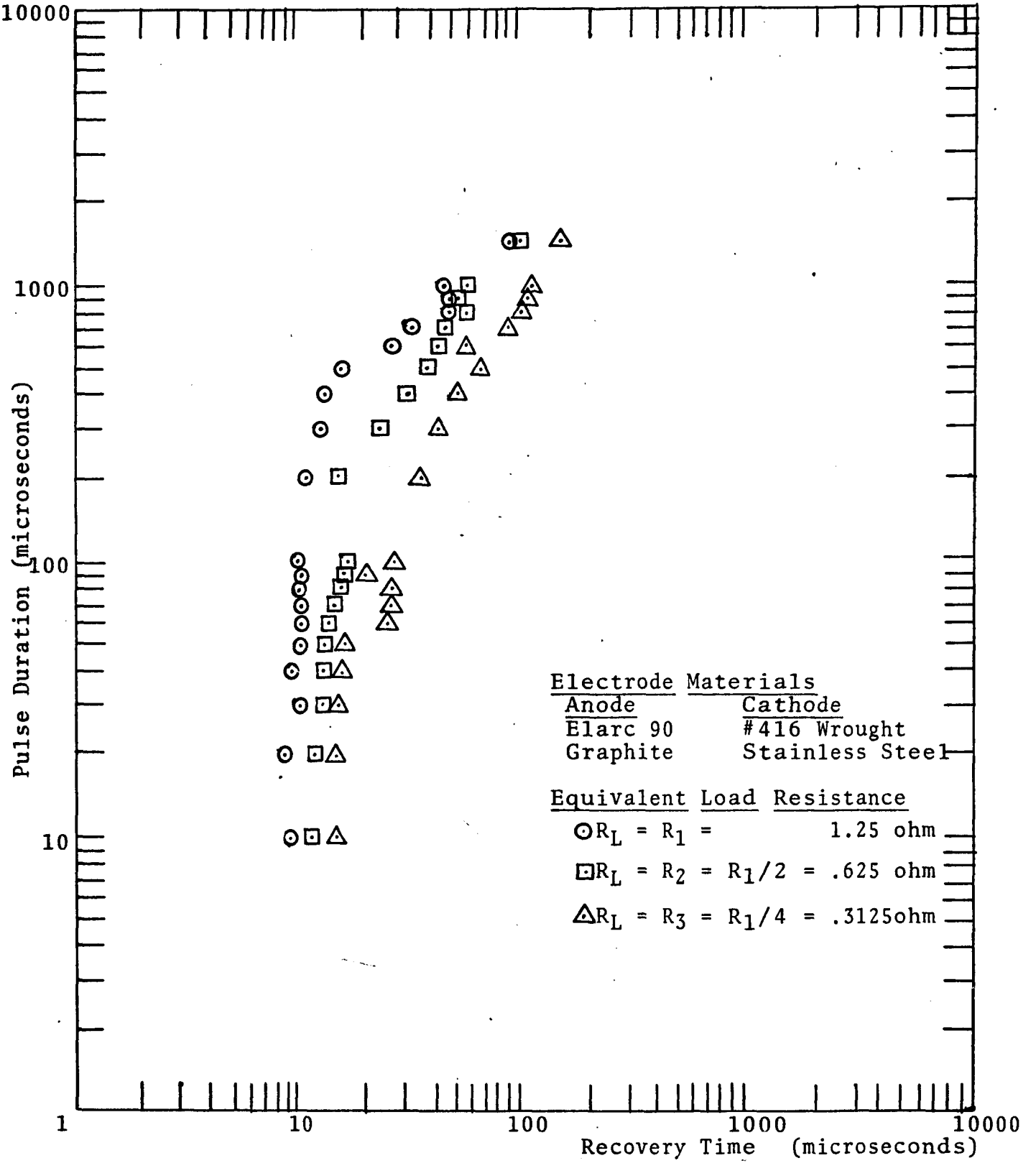

Figure 2.9 The Reference Recovery Times for Elarc 90 in Reverse Polarity with a Highly Contaminated Gap and Texaco Code 499 EDM Fluid

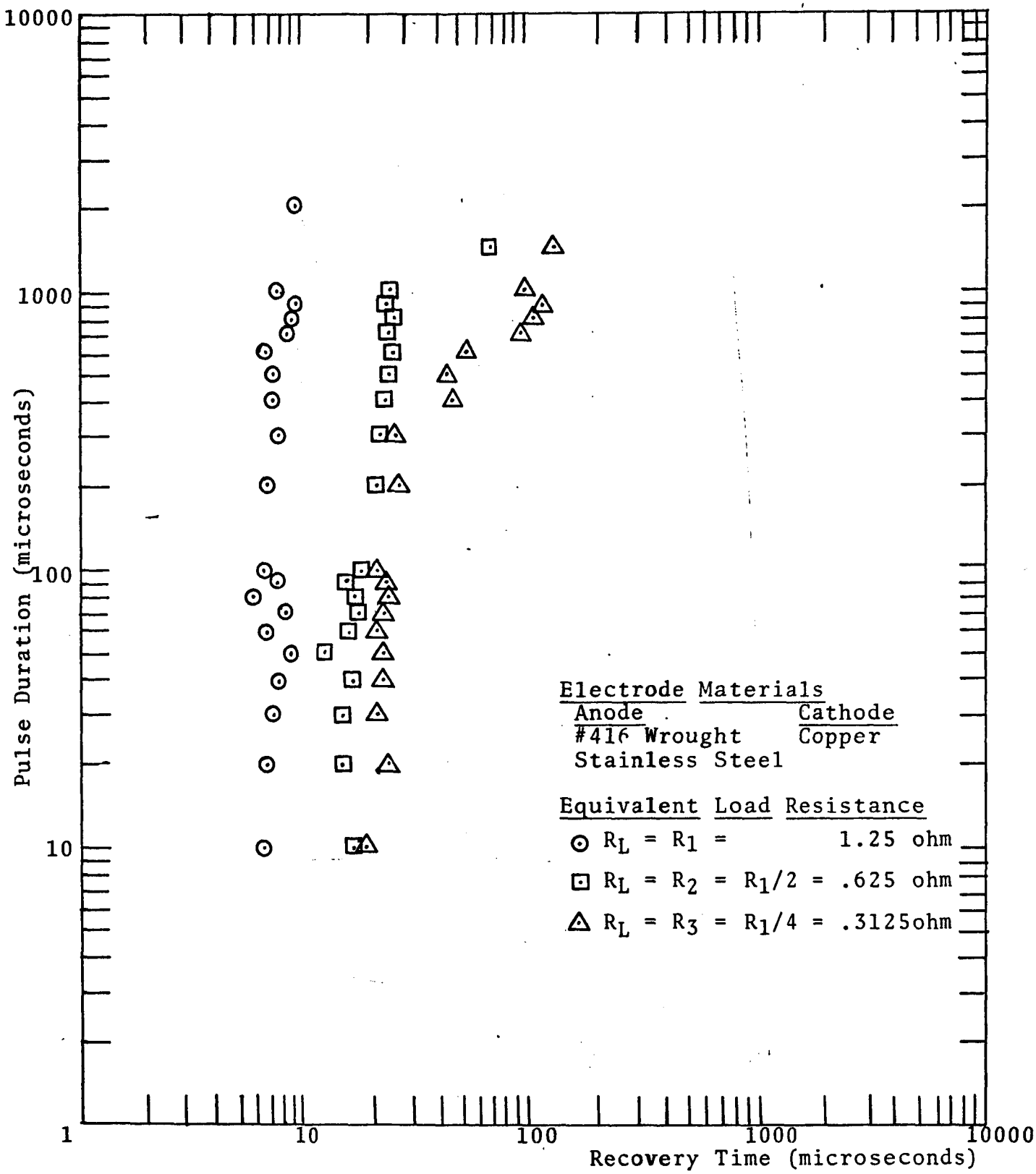

Figure 2.10 The Reference Recovery Times for Copper in Normal Polarity with a Highly Contaminated Gap and Texaco Code 499 EDM Fluid

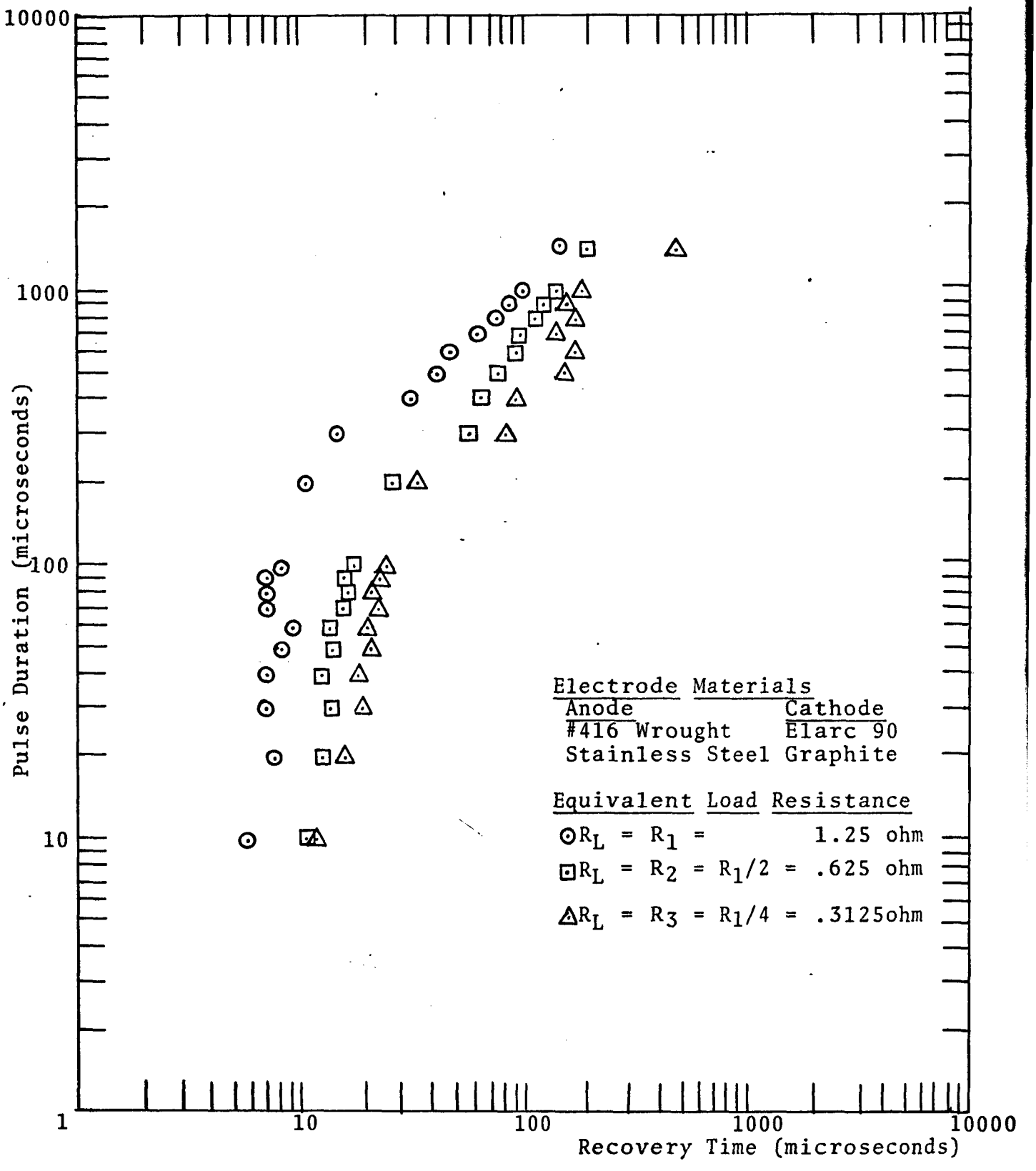

Figure 2.11 The Reference Recovery Times for Elarc 90 in Normal Polarity with a Highly Contaminated Gap and Texaco Code 499 EDM Fluid

4.) Discussion of the Recovery Time Results and some General Conclusions in Light of some Prior Findings

The general conclusion that can be formulated from the data on Elarc 90 and copper is that the recovery times increase when either of the following two parameters are increased: the magnitude of the current, or the duration of the current discharge. The longer recovery times are probably caused by the increased energy that is available to heat the electrodes and surrounding gases at these increased settings. Consequently, the more heat that must be removed from the electrodes, the longer it would take the electrode to cool and the longer the electrode can influence the gap. This effect is particularly noticeable at shorter gap spacings [38], which are inherent in the EDM process, because the temperature of the gases that are in close proximity to the electrode surface is dominated by the electrode temperature. Therefore, in the short EDM gap space, the gap gas temperature is dominated by the long term electrode effects. This conclusion, however, is somewhat contrary to that reached by some arc column researchers. They reasoned that there is very little influence on voltage recovery because of a current increase [43, 44]. The data for arc columns, however, was taken at very long pulse durations and their conclusions refer to these longer durations. The information that is available for shorter duration, comparable to EDM pulse duration is limited. Edels, et al., [10] did use arc durations as low as 100 microseconds and the data at the pulse duration does show a slight increase in recovery times with increasing current.

With #416 steel as the anode the recovery times are longer than reverse polarity for higher pulse durations. With Elarc 90 graphite as the cathode, the increased recovery times were attributed to the longer thermal recovery time found with graphite electrodes. [45] When graphite is the cathode, the higher temperatures (6940° - 6215°K for carbon and only 5900°K for copper [46]) associated with it and its lower thermal conductivities at these high temperatures [47] cause the spark column gases to remain hotter, therefore the gases remain ionized longer than other materials owing to the thermal ionization emissions* of electrons from the graphite cathode [48]. With copper as the cathode, the thermal ionization effects cannot last very long because of the rapid cooling of the copper. This reasoning explains why the normal and reverse polarity results with a copper electrode are very similar, with normal polarity requiring a slightly longer time to recover. Haswell [50] predicted the temperature rise and decay at the surface of a copper electrode caused by a single 20 microsecond discharge of 25 amps and found that the electrode surface takes between 5 - 10 microseconds to decay from the vaporization temperature to below 2000°K, which is in close agreement with the recovery times found here.

---

* Thermal ionization emissions - the thermal emission of electrons from the cathode surface require temperatures in excess of 2000°K [49]. For carbon, or graphite, the cathode can remain above the temperature for 100 to 500 microseconds, [9, 14], but copper cools more rapidly.

It is also noted from the recovery data that the Elarc 90 on #416 steel electrode combination required more time to recover than the copper on #416 steel configuration did, regardless of the electrode polarities. This generality is not strikingly noticeable at pulse durations below 100 microseconds, but for longer durations, the recovery times are measurably greater. These increased recovery times could probably be attributed to the temperatures and thermal phenomina that the Elarc 90 experienced during, and after, the discharge.

The similarity that all the electrode combinations and polarities exhibit at low pulse durations, below 100 microseconds, can be partially explained by lack of, or a minimal involvement of, the electrodes in the temperature decay of the ionized gap gases. At low pulse durations, the electrodes have, in all probability, not absorbed sufficient energy to cause their thermal decay time to exceed the decay time of the discharge column gases. Without the influence of the electrodes, only the thermal decay of the gas column could affect the recovery time and since the gas column should be somewhat similar in all cases, the decay time should be similar. The recovery data indicates that the electrodes (copper on #416 steel, both polarities,) did not enter in the gap recovery until 300 microseconds, while with Elarc 90, the electrode phenomena is noticeable for pulse durations as low as 100 microseconds.

The differences in recovery times, that occur at the longer pulse durations and higher currents can be attributed to the amount of energy absorbed by the electrodes. Since

more energy is absorbed at the higher settings, the heat content of the electrodes is increased to the point where the electrodes begin to influence the gap recovery times. Each electrode combination acts differently because of the different electrical and thermal properties of each material (i.e., thermal conductivity, melting point, vaporization temperature, resistivity, etc.). These properties all influence the temperature of the electrodes in some way, and hence, they will also affect the temperature of the gas column. The degree of ionization of the gap is determined by the temperature and, therefore, the recovery is also influenced.[10, 18] The higher the degree of ionization in the gap space, the lower the gap resistance would be. This same line of reasoning also explains why longer pulse durations and higher current amplitudes generally cause the recovery times to increase with all electrode materials and configurations.

Finally, there appears to be a noticeable increase in the recovery times when the level of contamination in the gap spacing increases. Although the possibility of cumulative heating effects exist in the highly contaminated gap case, as mentioned before, the type of materials in the gap space undoubtedly influence the composition of the ionized gas column and, therefore change its thermal properties. The exact nature of the change is not known and therefore, its influence could not be predicted or explained, except for the general conclusions of this paragraph.

B. Influence of Different Types of Graphite Electrode Material on the Recovery Time Results

Today, graphite is the most widely used electrode material in the EDM utilization art. The reasons for its popularity are:

(1) The metal removal rates associated with graphite are higher than the rates with other electrode materials,

(2) Graphite is usually easy to form into the desired shape of the tool electrode, and

(3) With the proper electrical conditions, the EDM process can proceed with little or no tool electrode wear when graphite is used.

The main purpose of this section of the recovery time study was to investigate the influence of different types of graphite electrode materials on the gap recovery time and to compare these times with the reference recovery times. The materials investigated are typical commercially used electrodes. The following types of carbon, or graphites were used: Poco 1 and Poco 3, which are molded graphites, made by the Poco Graphite Company, Electro-Carb 'EC-3' distributed by Mor-Wear Tools, and #6466 which is an experimental molded graphite or carbon material.

Poco 1 and Poco 3 are molded graphite electrode materials, which are high density and very fine grain size. Poco 1 is manufactured in a standard way, while Poco 3 has undergone a special process to fill its pores with carbon. Poco 3 is rated as the better of the two materials by the manufacturer. These two materials were subjected to the same test procedures followed with the copper and Elarc 90 electrode materials.

In order to draw a fair comparison between the various electrode materials, the current waveform associated with each material must be considered. A recovery time , current-magnitude relationship can then be drawn between the two or more materials that are to be compared. Figure 2.12 shows the current waveforms for Poco 1 on #416 stainless steel, both polarities, using the same load resistance settings employed previously. From these waveforms, a relationship can be established between the current oscillograms for Elarc 90 (shown in Figure 1.7) and those shown in Figure 2.12. The current waveforms with Poco 1 have a somewhat slower rise time than those with Elarc 90 under similar conditions. The peak current amplitudes are approximately the same with Poco 1 and Elarc 90 as the anode, but slightly less when the polarity is reversed.

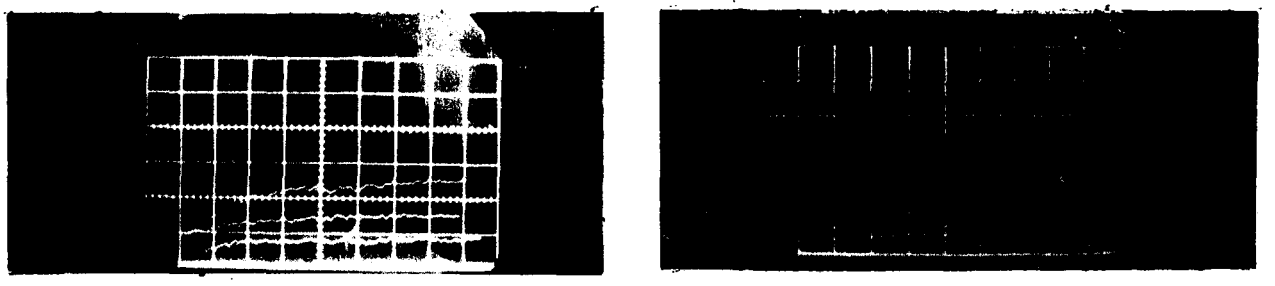

Reverse Polarity Normal Polarity

Scale: Vertical - 32 Amps/Division
Horizontal - 20 Microseconds/Division
Equivalent Load Resistance
$R_L = R_1 = 1.25$ Ohm (Lower Trace)
$R_L = R_2 = R_1/2 = .625$ Ohm (Middle Trace)
$R_L = R_3 = R_1/3 = .3125$ Ohm (Upper Trace)

Figure 2.12: Gap Current Waveforms Obtained with Poco 1 Graphite on #416 Steel

The recovery data for Poco 1 graphite on #416 steel are shown in Figures 2.13 and 2.14, with Poco 1 as the anode and cathode, respectively. When a comparison of Figure 2.13 and the results with Elarc 90 under similar conditions (Figure 2.9) is made, it can be seen that Poco 1 has a somewhat shorter recovery time in general, and depending on the equivalent load resistance and pulse duration, the Poco 1 recovery time can be 80% shorter than those for Elarc 90. Poco 1 exhibits the same general shape recovery time versus pulse duration curve as was found when Elarc 90 was used. There is an approximately constant recovery time for all three current settings for pulse durations below 100 microseconds, as was found in the case of Elarc 90. However, for Poco 1, this constant recovery time also existed at higher pulse durations. This difference between Elarc 90 and Poco 1, suggests that the thermal decay influence of the Poco 1 electrode material is less than the influence encountered in the case of Elarc 90. Nevertheless, electrode thermal influence for Poco 1 is observed for the $R_L = R_3$ current setting, for pulse durations greater than 500 microseconds. When the recovery time results for Poco 1 and Elarc 90 as the cathode are compared, the recovery times are again found to be shorter with Poco 1, but in this case, the Poco 1 recovery times were only, at the greatest difference, 30% shorter than those for Elarc 90. Some of the different results can be attributed to the lower current amplitudes found with Poco 1 . The lower currents are a direct result of larger gap voltages with Poco 1 (about 32 volts) as compared to Elarc 90 (28 volts).

The current waveforms for Poco 3 on #416 steel are shown in Figure 2.15. These waveforms are very similar to the waveforms of Poco 1 and they relate to those for Elarc 90 in a like manner. The recovery time graphs are shown in Figures 2.16 and 2.17. Figure 2.16 shows the results obtained for a highly contaminated gap with reverse polarity. Again, the graphs have the typical constant recovery times for lower pulse durations and increasing recovery times, as pulse duration increases, at the higher settings. The recovery times found for Poco 3 are shorter than those obtained using Elarc 90 under similar circumstances, again about 80% less at the point of greatest differences. The Poco 3 recovery times are also slightly shorter than those for Poco 1, but only about 5% to 10% less. The results with Poco 3 as the cathode (Figure 2.17) show that the recovery times for Poco 3 are 50% shorter than those for Poco 1, dependent on the pulse duration setting and the equivalent load resistance used. This difference in recovery times indicate that Poco 3 is the better graphite to use when shorter recovery times are important.

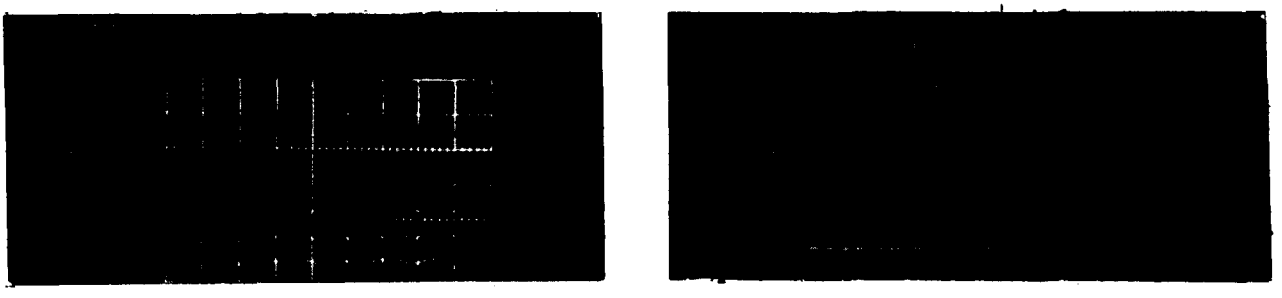

Reverse Polarity Normal Polarity

Scale: Vertical - 32 Amps/Division
Horizontal - 20 Microseconds/Division
Equivalent Load Resistance
$R_L = R_1 =$ 1.25 Ohm (Lower Trace)
$R_L = R_2 = R_1/2 =$ .625 Ohm (Middle Trace)
$R_L = R_3 = R_1/4 =$ .3125 Ohm (Upper Trace)

Figure 2.15: Gap current Waveforms Obtained with Poco 3 Graphite on #416 Steel

The next electrode material considered is Electro-Carb 'EC-3', which is a low-priced molded carbon electrode. The information available on 'EC-3' is shown in Table 2.1. Its thermal properties were not available and were therefore assumed to be similar to those of carbon, which are also shown in Table 2.1. The current waveforms for this electrode material are shown in Figure 2.18. The waveforms are very similar to those of the previously discussed graphite electrodes.

		Reference 52, 51, 53, 54	
Density		1.74 gms/cu cm	
Scleroscope Hardness		40 - 50	
Transverse Strength		5700 psi	
Electrical Resistance		.0007 ohm inch	
Maximum Grain Size		.003" dia.	
Method of Manufacture		Molded	
Carbon Properties			
Thermal Conductivity	360°C	.38	cal/cm sec °C
	500°C	.45	"
	1000°C	.55	"
	1500°C	.58	"
Specific Heat	20°C	.104	cal/gm°C

Table 2.1: Average Properties of Electro-Carb 'EC-3' Electrode

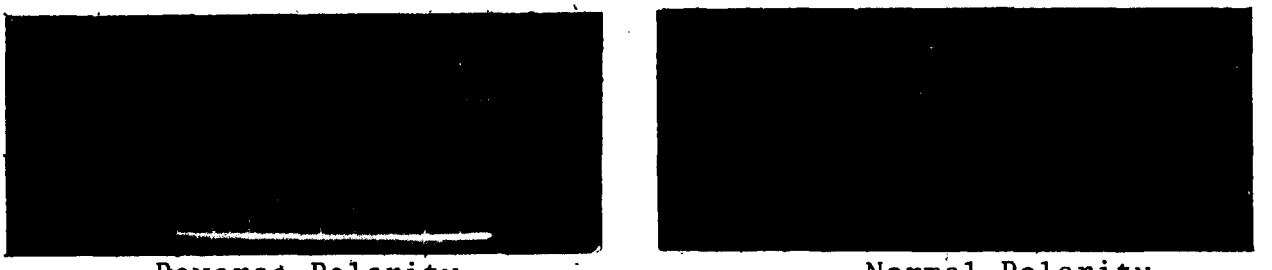

Reverse Polarity Normal Polarity

Scale: Vertical - 32 Amps/Division
Horizontal - 20 Microseconds/Division

Equivalent Load Resistance
$R_L = R_1 =$ 1.25 Ohm (Lower Trace)
$R_L = R_2 = R_1/2 =$ .625 Ohm (Middle Trace)
$R_L = R_3 = R_1/4 =$ .3125 Ohm (Upper Trace)

Figure 2.18: Gap Current Waveforms Obtained with 'EC-3' Carbon on #416 Steel

The recovery data obtained for 'EC-3' are shown in Figures 2.19 and 2.20. The graphs have the same general shape as the reference recovery time results. The 'EC-3' anode results exhibit similar recovery time data at lower pulse durations and, for the $R_L = R_1$, current setting, had shorter recovery times than Elarc 90 for discharge durations below 400 microseconds. However, at pulse durations greater than 400 microseconds, the recovery times are very much longer than those found with Elarc 90, about 5 times longer. This difference is apparently the result of the thermal properties of the electrode material because it cannot be totally attributed to current or gap voltage differences. The recovery times for 'EC-3' as the cathode are shown in Figure 2.20. In this case, the recovery times were considerably longer than the Elarc 90 data, as great as 5 times longer dependent on the conditions used. In conclusion, 'EC-3' requires more time to recover than any of the previously mentioned graphites.

The last tool electrode material investigated is an experimental molded graphite. It is classified as Number 6466 and no information is available about its properties. Its advantage over previously available molded graphite is a controllable uniformity and quality. The current waveforms for this material are shown in Figure 2.21. When this oscillogram is compared with that of Elarc 90 in Figure 1.7, it can be seen that the current amplitudes with #6466 as the anode are much less than those for Elarc 90, while with #6466 as the cathode, the current amplitudes are about the same. The current rise times with #6466 are also shown to be longer, in both polarities, than those

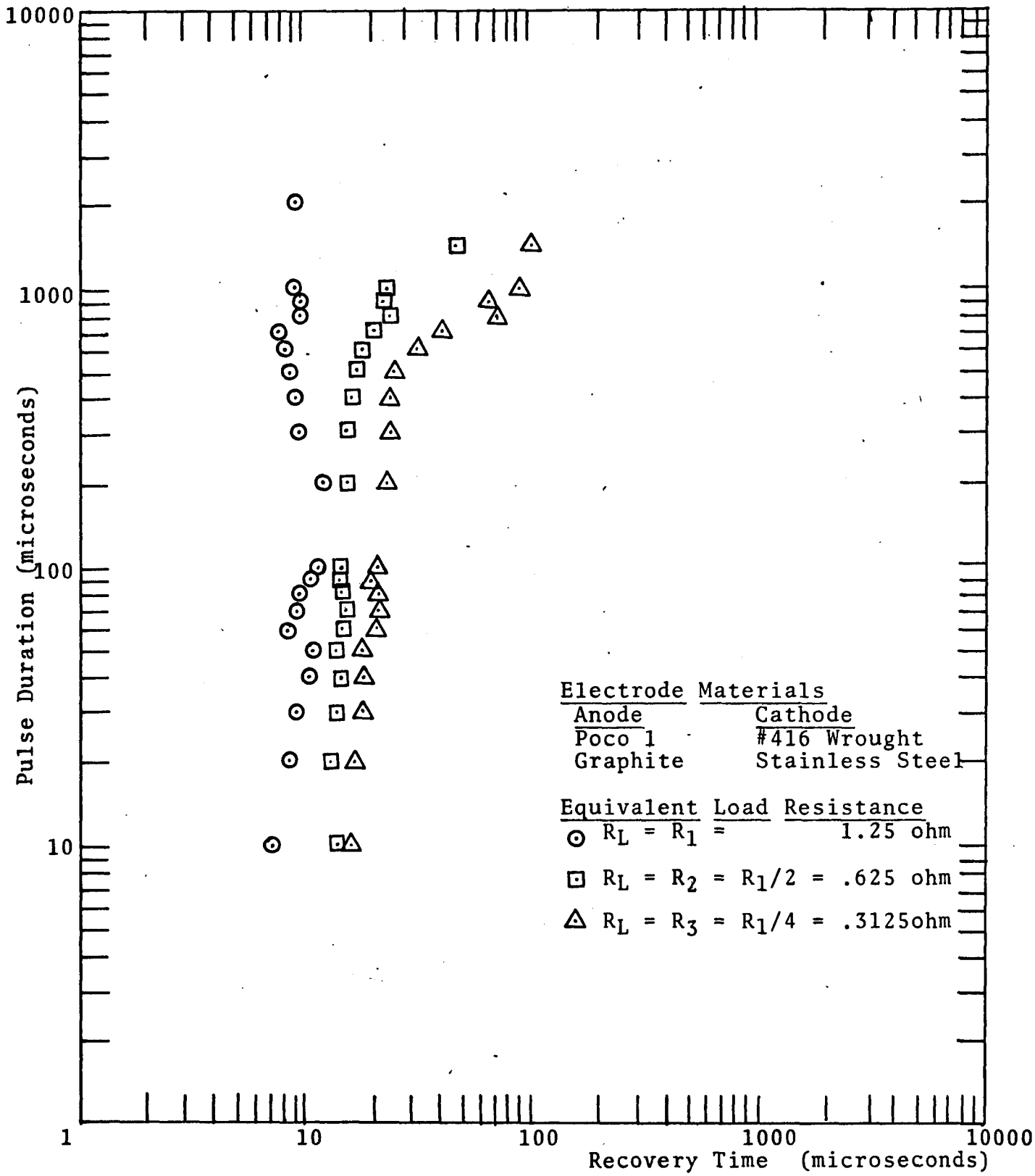

Figure 2.13. Recovery Times for Poco 1 in Reverse Polarity with a Highly Contaminated Gap and Texaco Code 499 EDM fluid

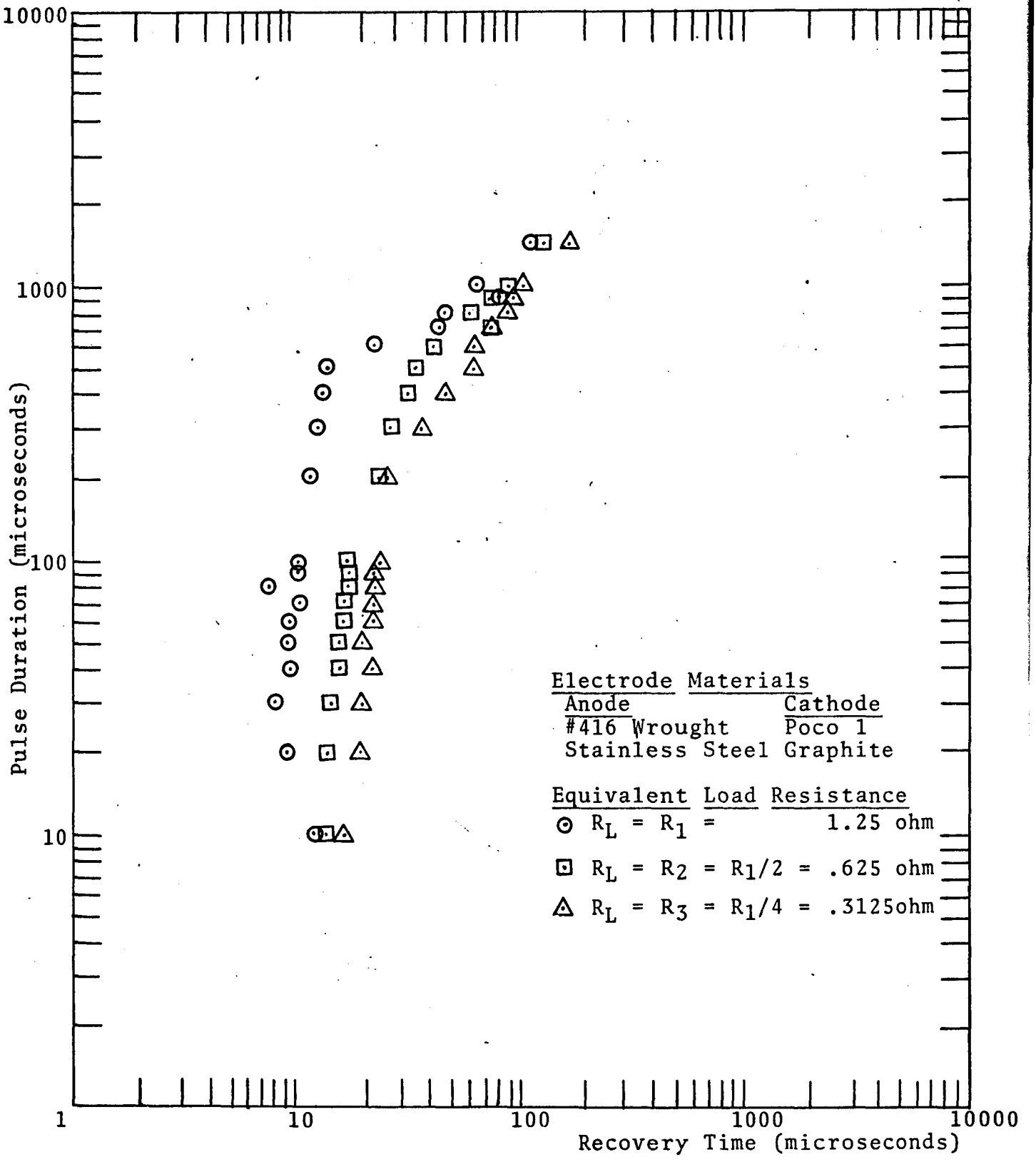

Figure 2.14. Recovery Times for Poco 1 in Normal Polarity with a Highly Contaminated Gap and Texaco Code 499 EDM Fluid

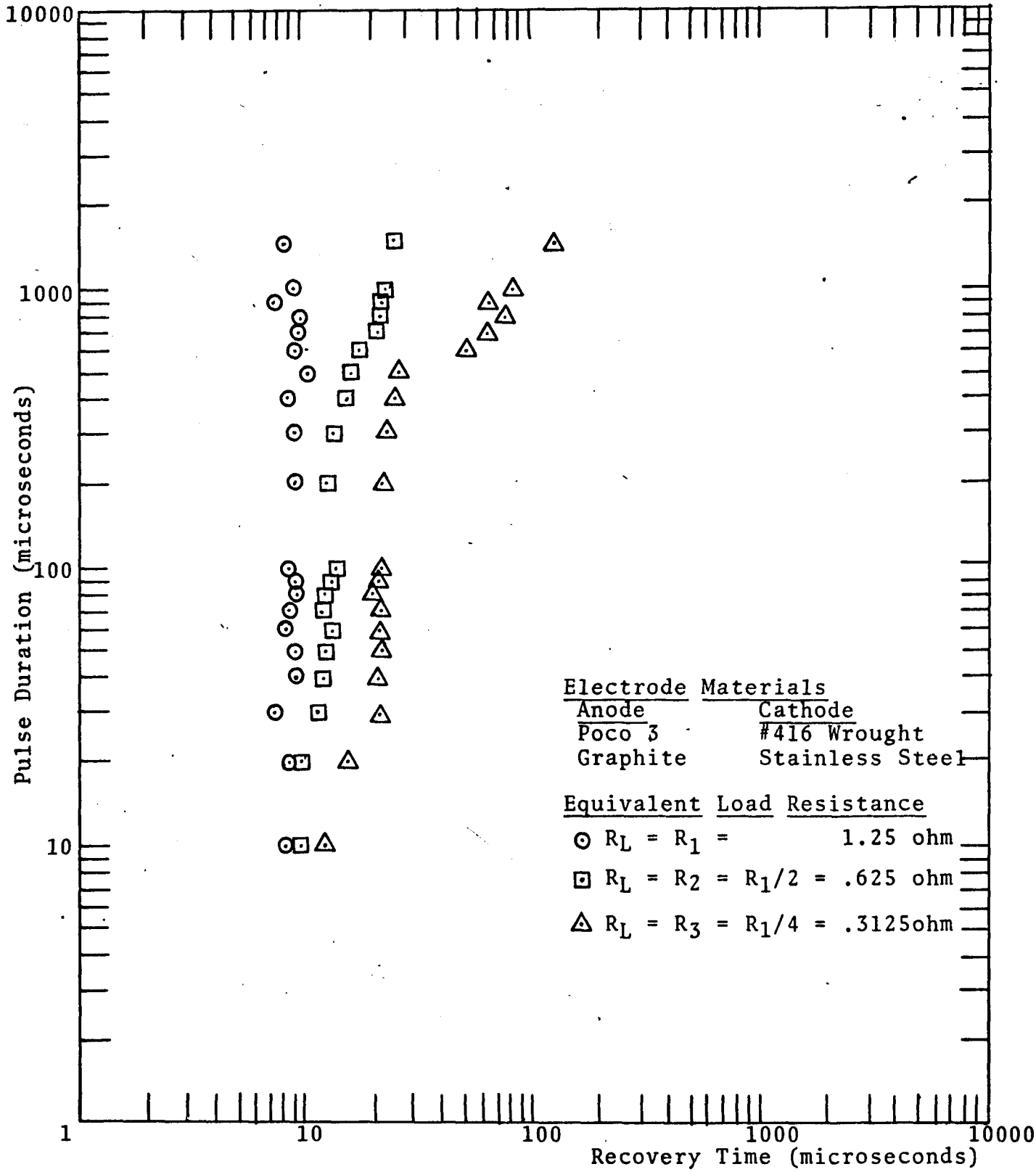

Figure 2.16 Recovery Times for Poco 3 in Reverse Polarity with a HIghly Contaminated Gap and Texaco Code 499 EDM Fluid

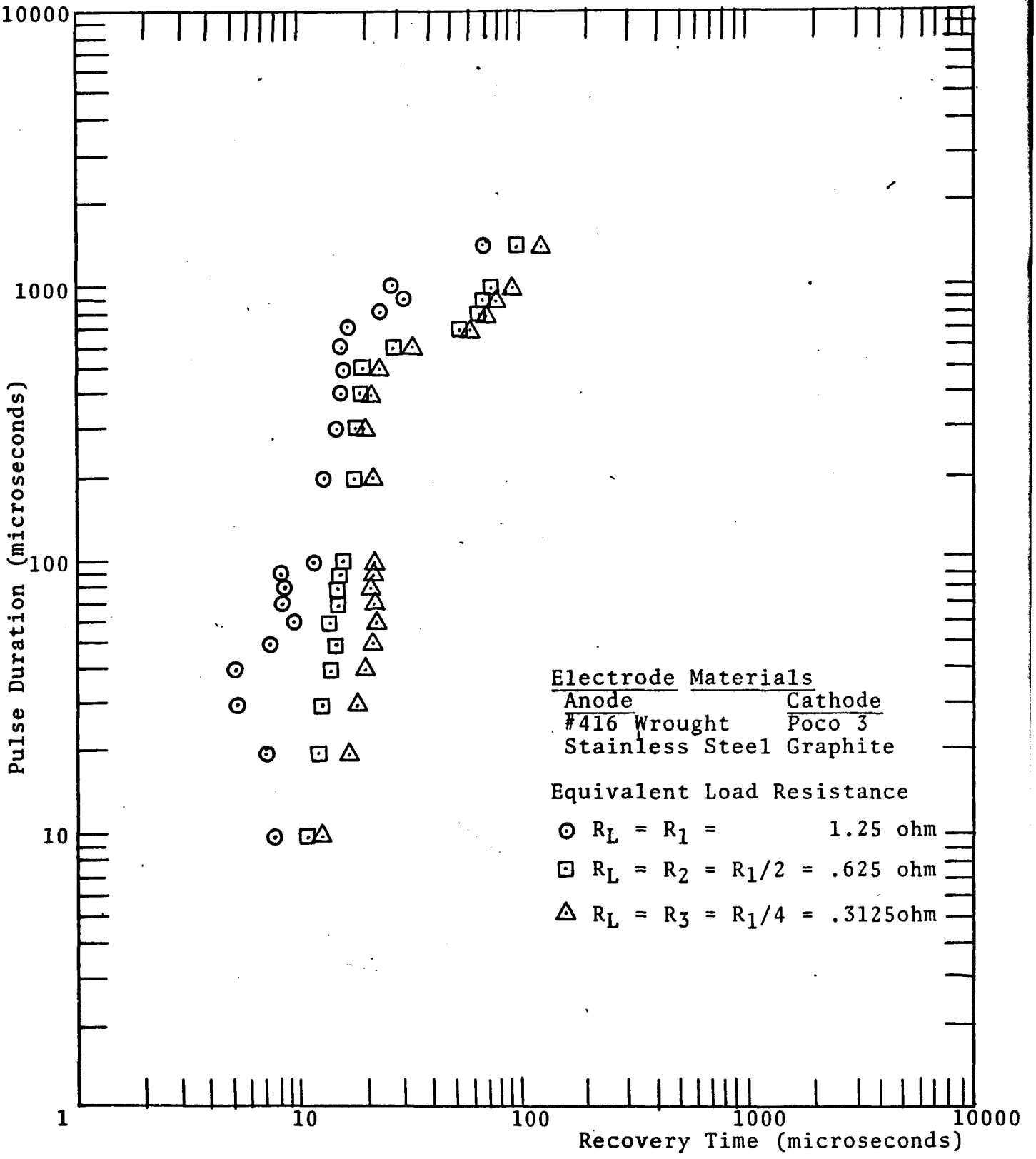

Figure 2.17. Recovery Times for Poco 3 in Normal Polarity with a Highly Contaminated Gap and Texaco Code 499 EDM Fluid

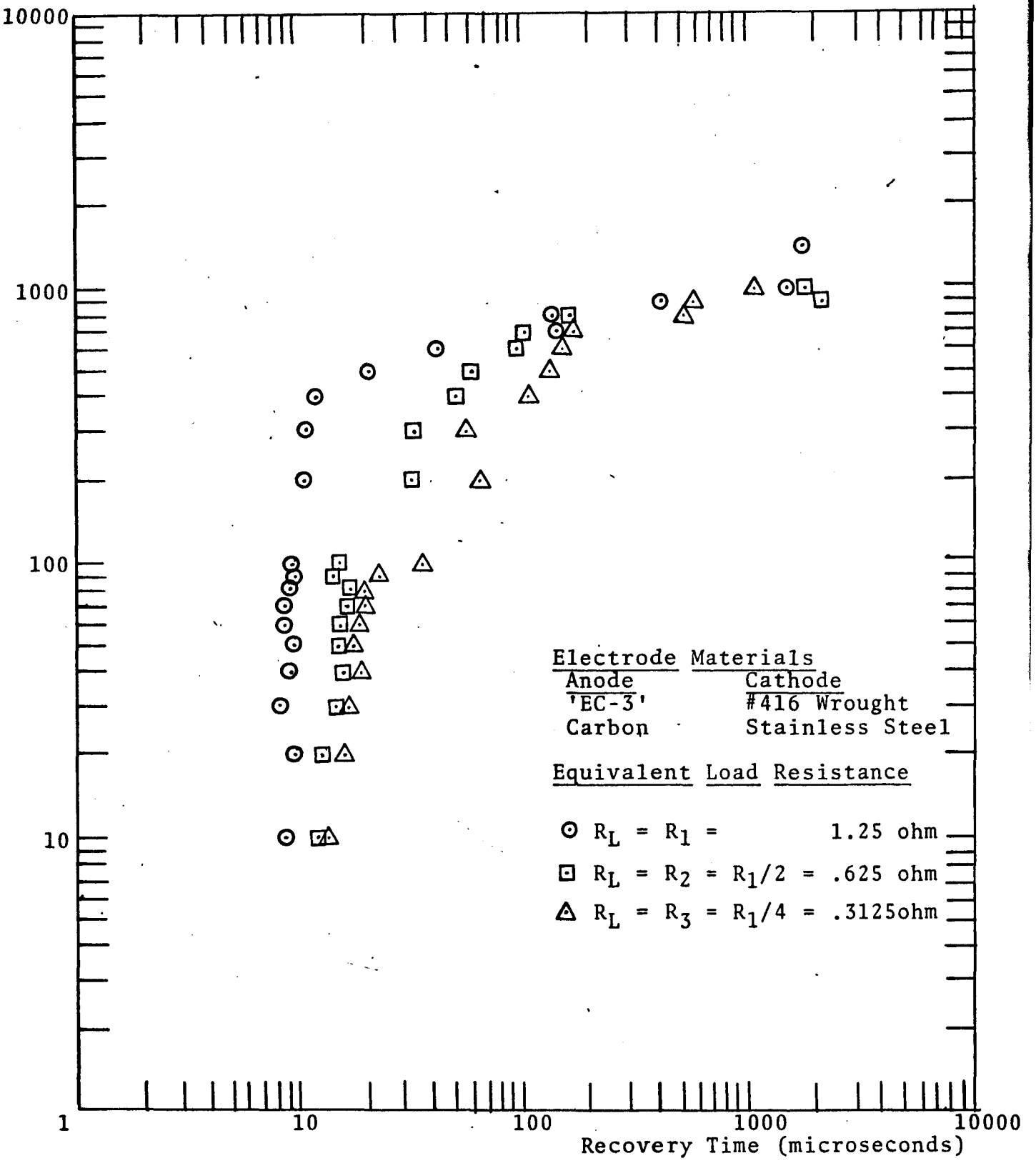

Figure 2.19 Recovery Times for 'EC-3' in Reverse Polarity with a Highly Contaminated Gap and Texaco Code 499 EDM Fluid

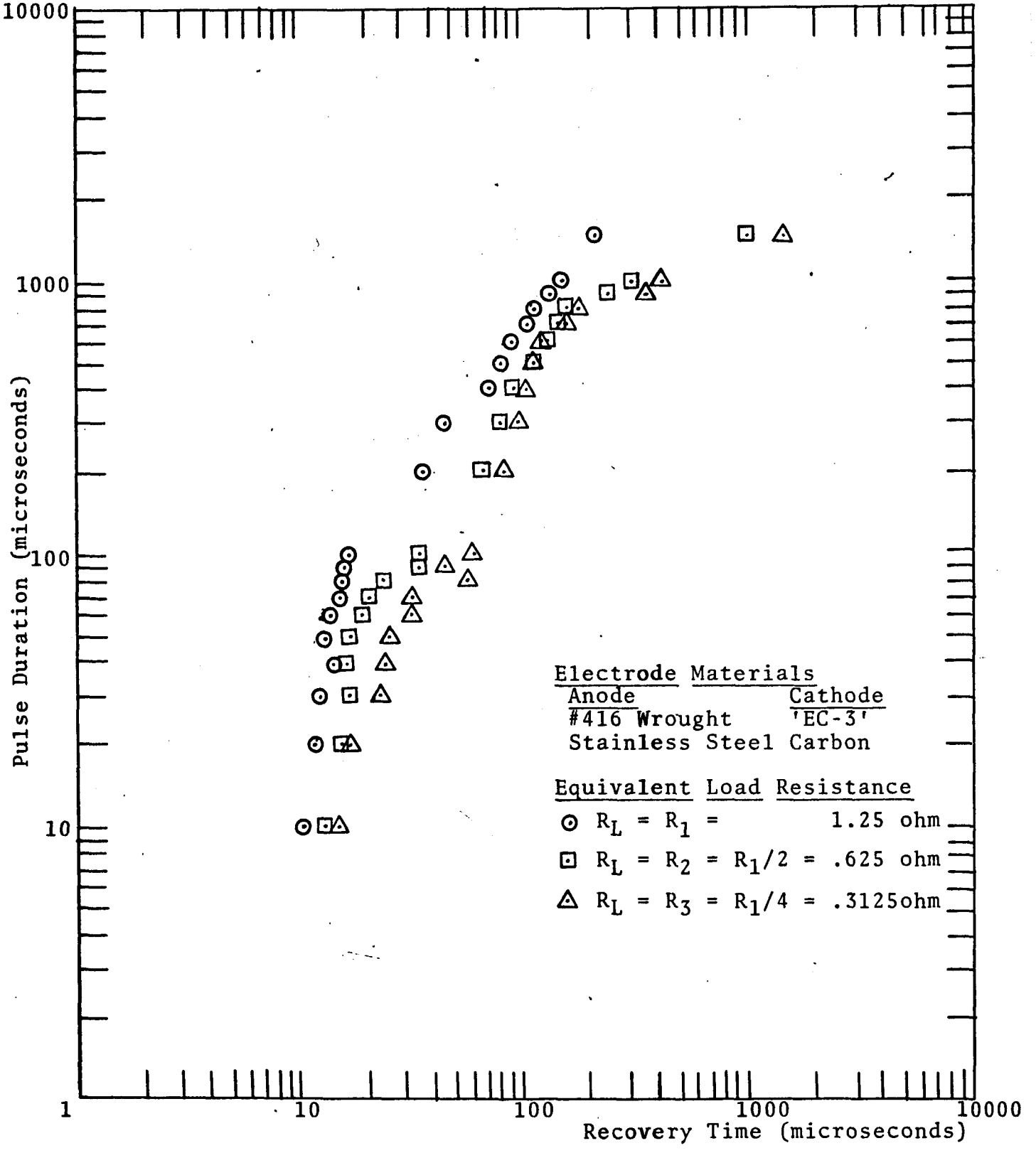

Figure 2.20. Recovery Times for 'EC-3' in Normal Polarity with a Highly Contaminated Gap and Texaco Code 499 EDM Fluid

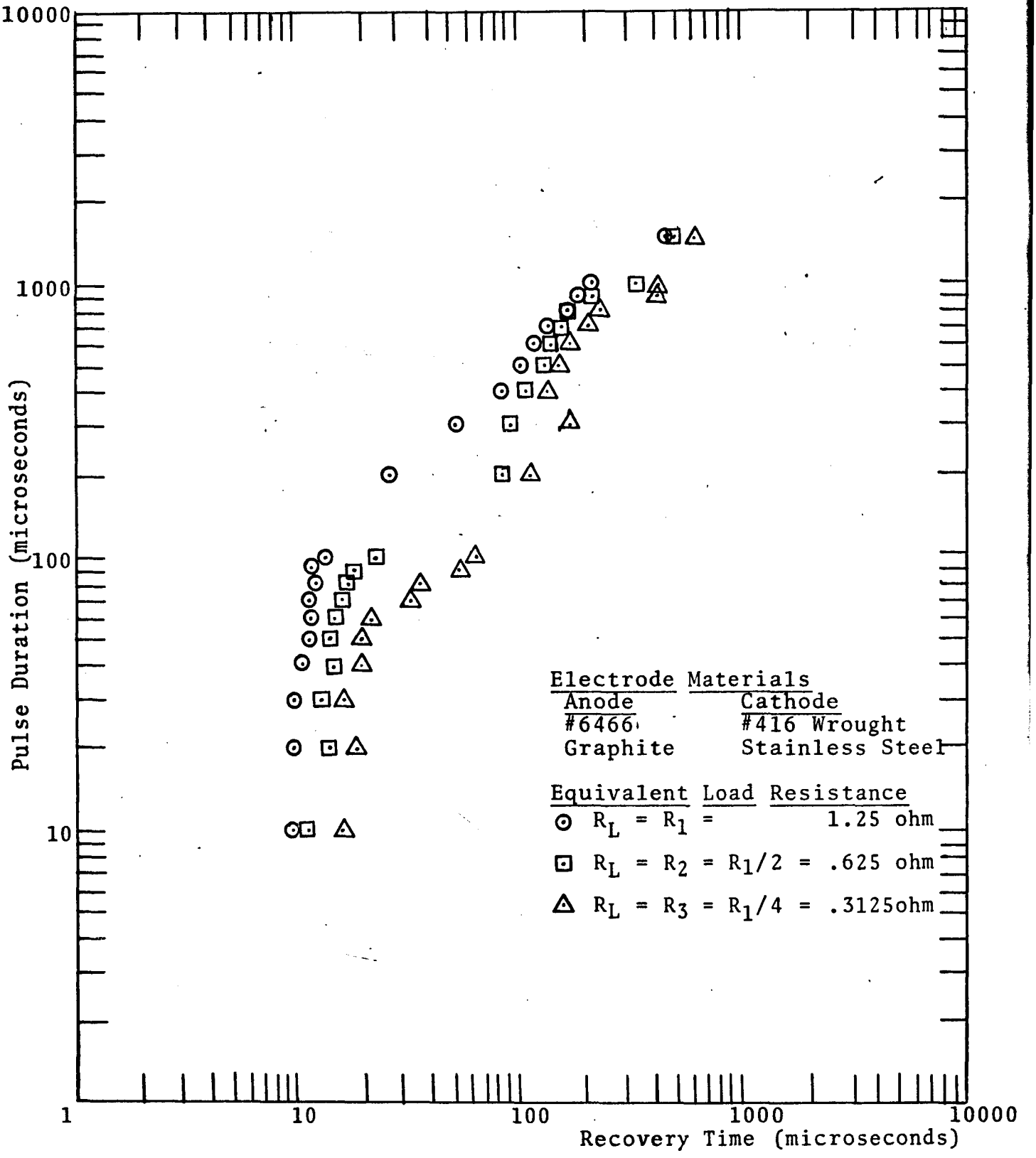

Figure 2.22 Recovery Times for #6466 Graphite in Reverse Polarity with a Highly Contaminated Gap and Texaco Code 499 EDM Fluid

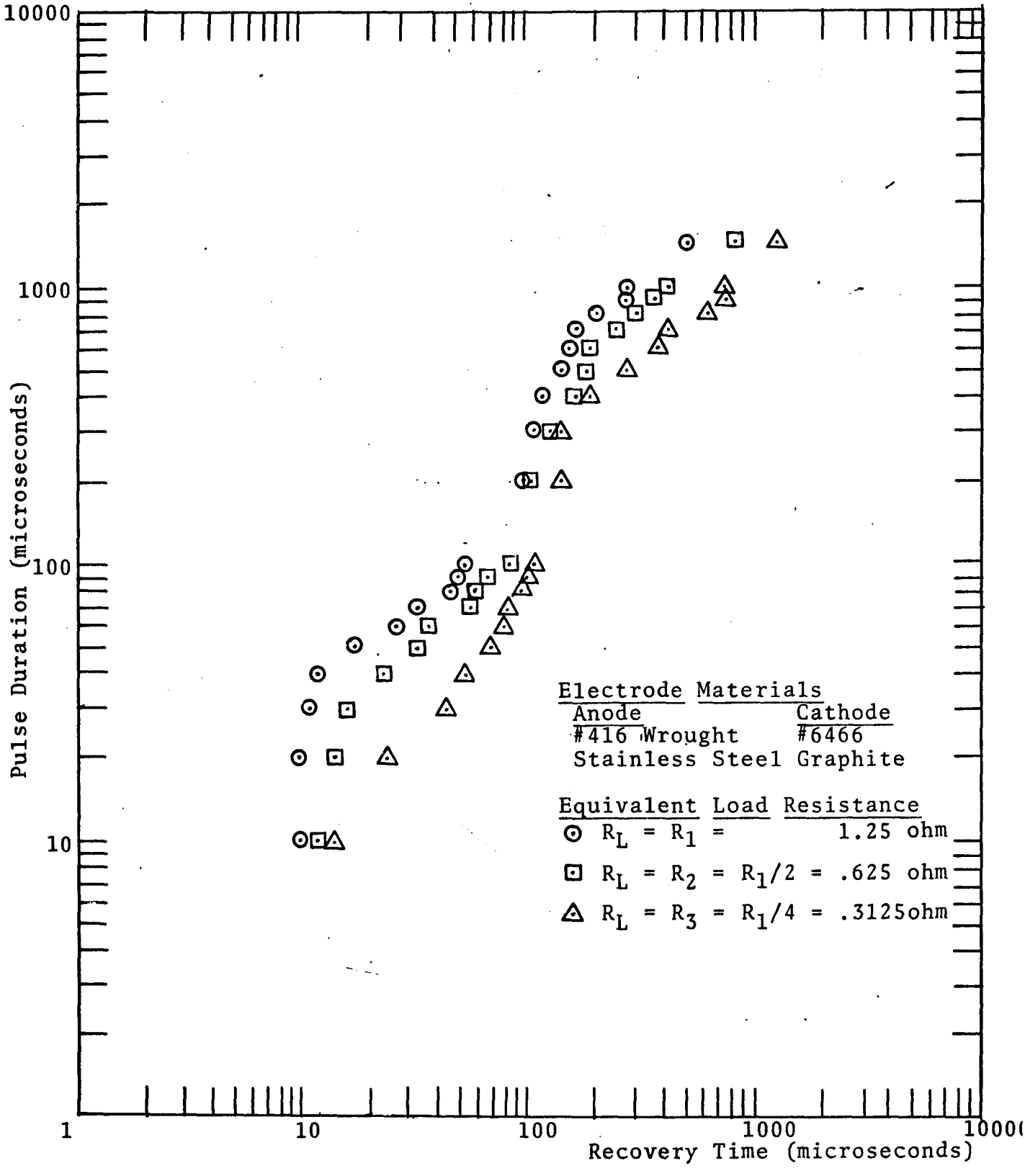

Figure 2.23 Recovery Times for #6466 Graphite in Normal Polarity with a Highly Contaminated Gap and Texaco Code 499 EDM Fluid

observed when Elarc 90 was used.

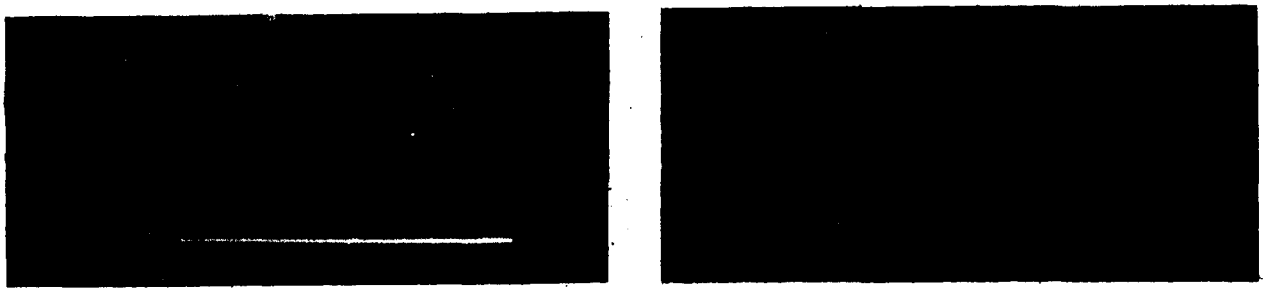

Reverse Polarity Normal Polarity

Scale: Vertical - 32 Amps/Division
Horizontal - 20 Microseconds/Division

Equivalent Load Resistance
$R_L = R_1 =$ 1.25 Ohm (Lower Trace)
$R_L = R_2 = R_1/2 =$ .625 Ohm (Middle Trace)
$R_L = R_3 = R_1/3 =$ .3125 Ohm (Upper Trace)

Figure 2.21: Gap Current Waveforms Obtained with #6466 Graphite on #416 Steel

The recovery time results for #6466 are shown in Figures 2.22 and 2.23. For the pulse durations below 100 microseconds, the results are again comparable to those of Elarc 90 and the other graphite materials. However, as occurred with 'EC-3', the recovery times are about 5 to 10 times longer than those for Elarc 90 at the upper end of the pulse durations range. Also, with #6466 as the anode, the current amplitude was about 20% to 30% lower than the current for Elarc 90, which indicates that the recovery intervals would possibly have been longer yet had the current amplitudes been the same.

C. Influence of Different Workpiece Materials on Recovery Time Results

The effect that changing the workpiece material had on recovery times was considered next. The first material investi-

gated was Hardtem B Tool-Steel, with an Elarc 90 Tool Electrode. The only current setting considered was that with an equivalent load resistance of 1.25 ohms. This current setting was used with all the workpiece materials, since the higher current settings generally had the same shape recovery-time curves, albeit with longer recovery times. The current oscillographs are shown in Figure 2.24. The wave shapes and current

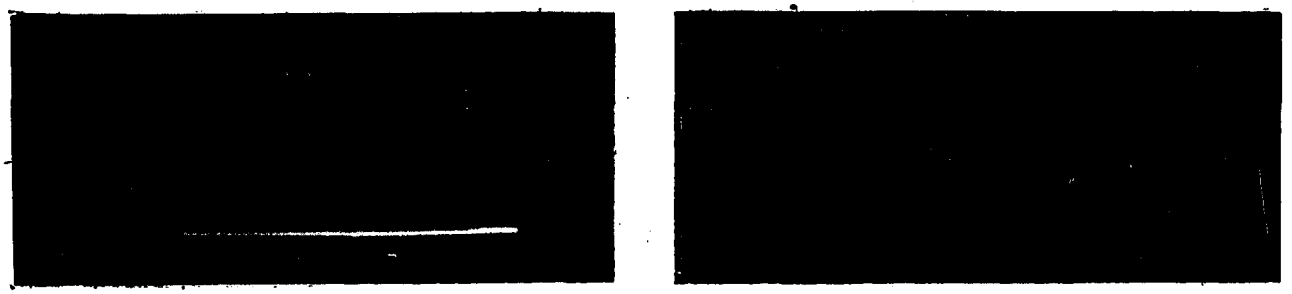

Reverse Polarity Normal Polarity

Scale: Vertical - 32 Amps/Division
Horizontal - 20 Microseconds/Division

Equivalent Load Resistance
$R_L = R_1 =$ = 1.25 Ohm (Lower Trace)
$R_L = R_2 = R_1/2$ = .625 Ohm (Middle Trace)
$R_L = R_3 = R_1/4$ = .3125 Ohm (Upper Trace)

Figure 2.24: Gap Current Waveforms obtained with Elarc 90 on Hardtem B Tool Steel

amplitudes are very similar to those obtained with Elarc 90 on #416 Wrought Stainless Steel. The recovery-time results for Hardtem B are shown in Figure 2.25 and 2.26. The results, again, exhibit the typical graphic pattern, i.e., constant recovery times for lower pulse durations, while at greater durtions, the recovery time increases. The results with Hardtem B show a recovery time about twice as long as the recovery time found with Elarc 90 on #416 steel. The thermal conductivity of #416 steel and Hardtem B are fairly similar at 20°C,

indicating similar recovery times, but the specific heat coefficients are very different. The higher value of specific heat for #416 steel indicates a greater ability to absorb the heat produced by a discharge and could explain the shorter recovery times observed.

The next workpiece material considered was Armco Iron. The available data concerning the physical properties of this metal are shown in Table 1.2. The current waveforms for the case of Armco Iron are shown in Figure 2.27. The rise times and current amplitudes are similar to those obtained with Elarc 90 on #416 steel. The recovery time data is shown graphically in Figures 2.28 and 2.29. The reverse polarity results of Figure 2.28 are very similar to those obtained for #416 steel. At the lower pulse duration settings, the erratic nature of the recovery times makes a comparison somewhat difficult. The normal polarity results shown in Figure 2.29 are somewhat longer than the recovery times found for #416 steel (about 1.3 times longer) when higher pulse durations are used, but the data is similar at the lower settings. The thermal conductivity of Armco Iron is, as occurred with Hardtem B, higher than that of #416 stainless steel. One possible explanation for the longer recovery times found with Armco Iron is that its specific heat is less than that of #416 steel, indicating possibly faster heating of Armco Iron. The faster the initial electrode heating, the sooner the electrode influenced recovery times would become evident in the gap recovery interval.

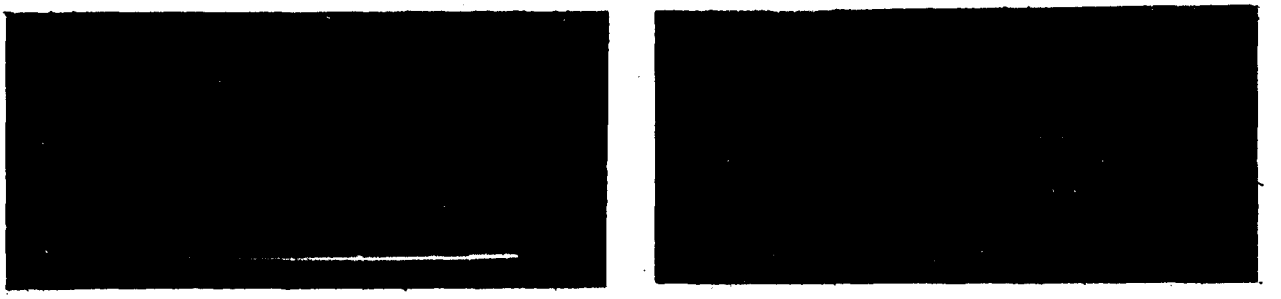

Reverse Polarity Normal Polarity

Scale: Vertical - 32 Amps/Division
Horizontal - 20 Microseconds/Division

Equivalent Load Resistance
$R_L = R_1 =$ 1.25 Ohm (Lower Trace)
$R_L = R_2 = R_1/2 =$ .625 Ohm (Middle Trace)
$R_L = R_3 = R_1/4 =$ .3125 Ohm (Upper Trace)

Figure 2.27: Gap Current Waveforms Obtained with Elarc 90 on Armco Iron

The last workpiece material investigated was Gray Cast Iron*. Gray Cast Iron is a name given to a class of cast irons which are generally characterized by a high carbon content (3% to 3.35% by weight) and a high silicon content (2% to 2.4%). This material is of interest here owing to the many problems encountered when it is used in a conventional EDM machine. The current oscillograms that resulted when Gray Cast Iron was used as a workpiece material are shown in Figure 2.30. The current rise times are somewhat slower than those for the case of #416 steel, but the current amplitudes when Gray Cast Iron was the cathode, appear to be larger. With a Gray Cast Iron anode, the current amplitudes are smaller than the amplitudes obtained with #416 steel. The recovery times are shown in

*Gray Cast Iron - also known as Gray Iron or Gray Metal.

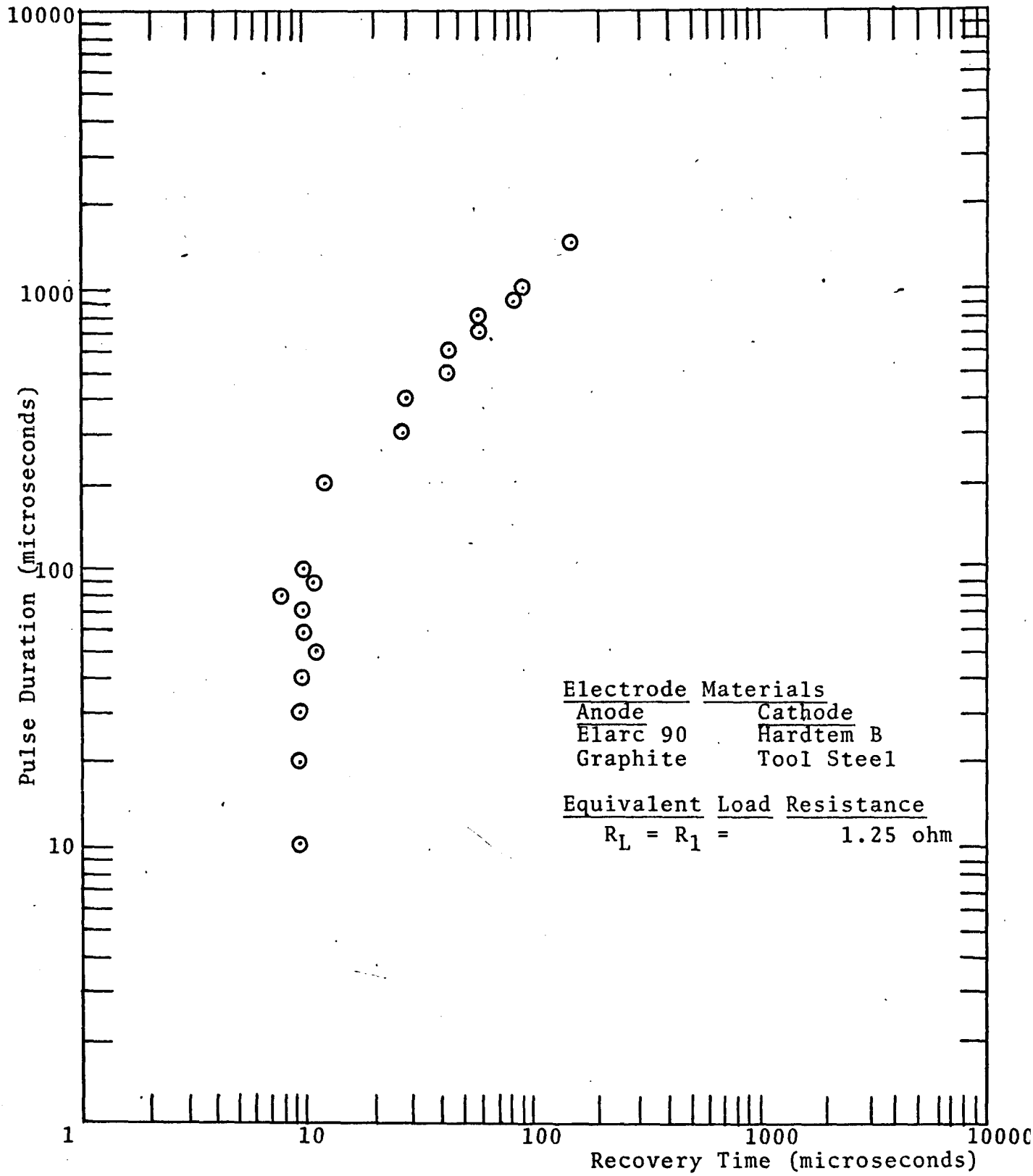

Figure 2.25 Recovery Times for Elarc 90 on Hardtem B in Reverse Polarity with a Highly Contaminated Gap and Texaco Code 499 EDM Fluid

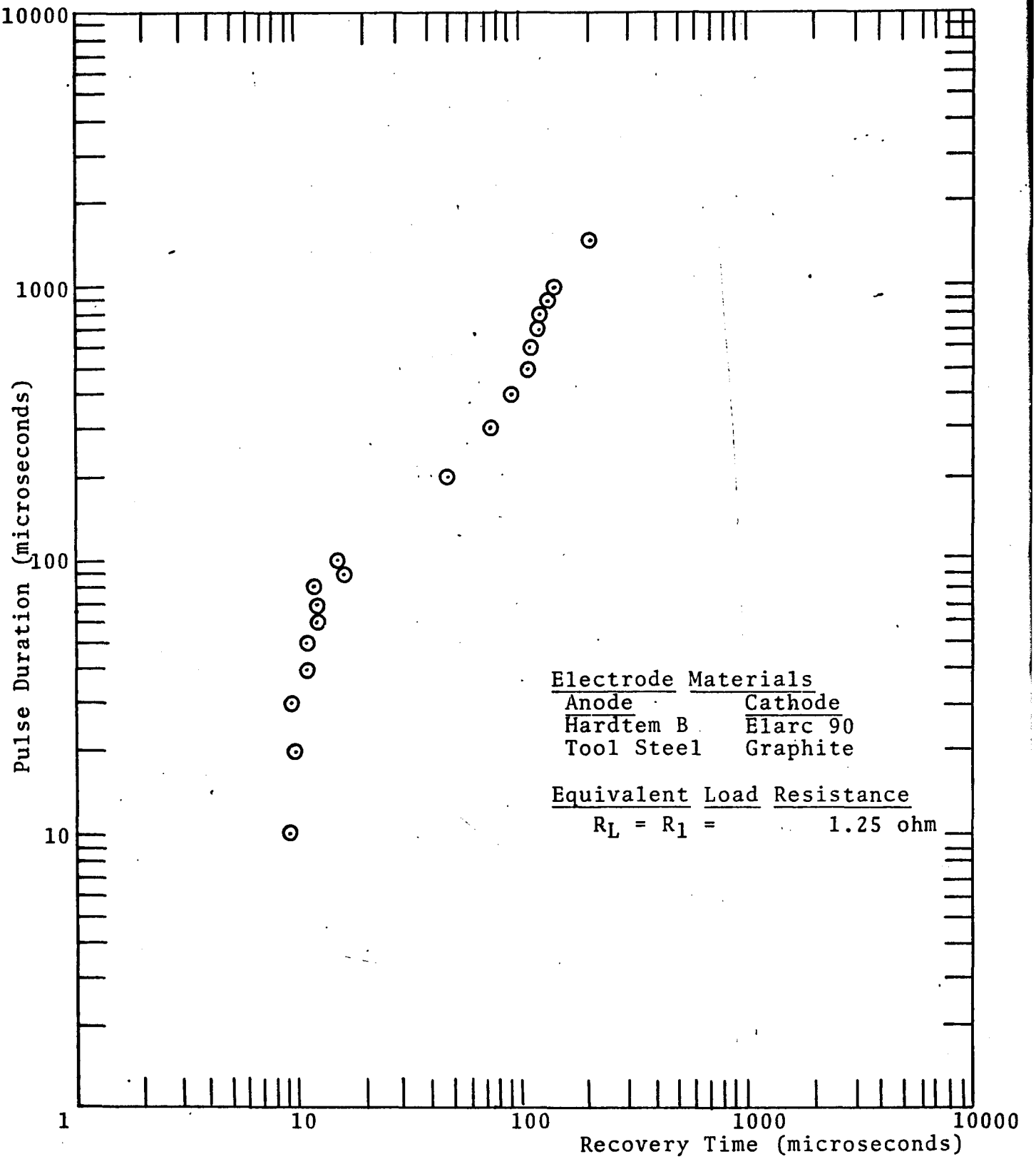

Figure 2.26 Recovery Times for Elarc 90 on Hardtem B in Normal Polarity with a Highly Contaminated Gap and Texaco Code 499 EDM Fluid

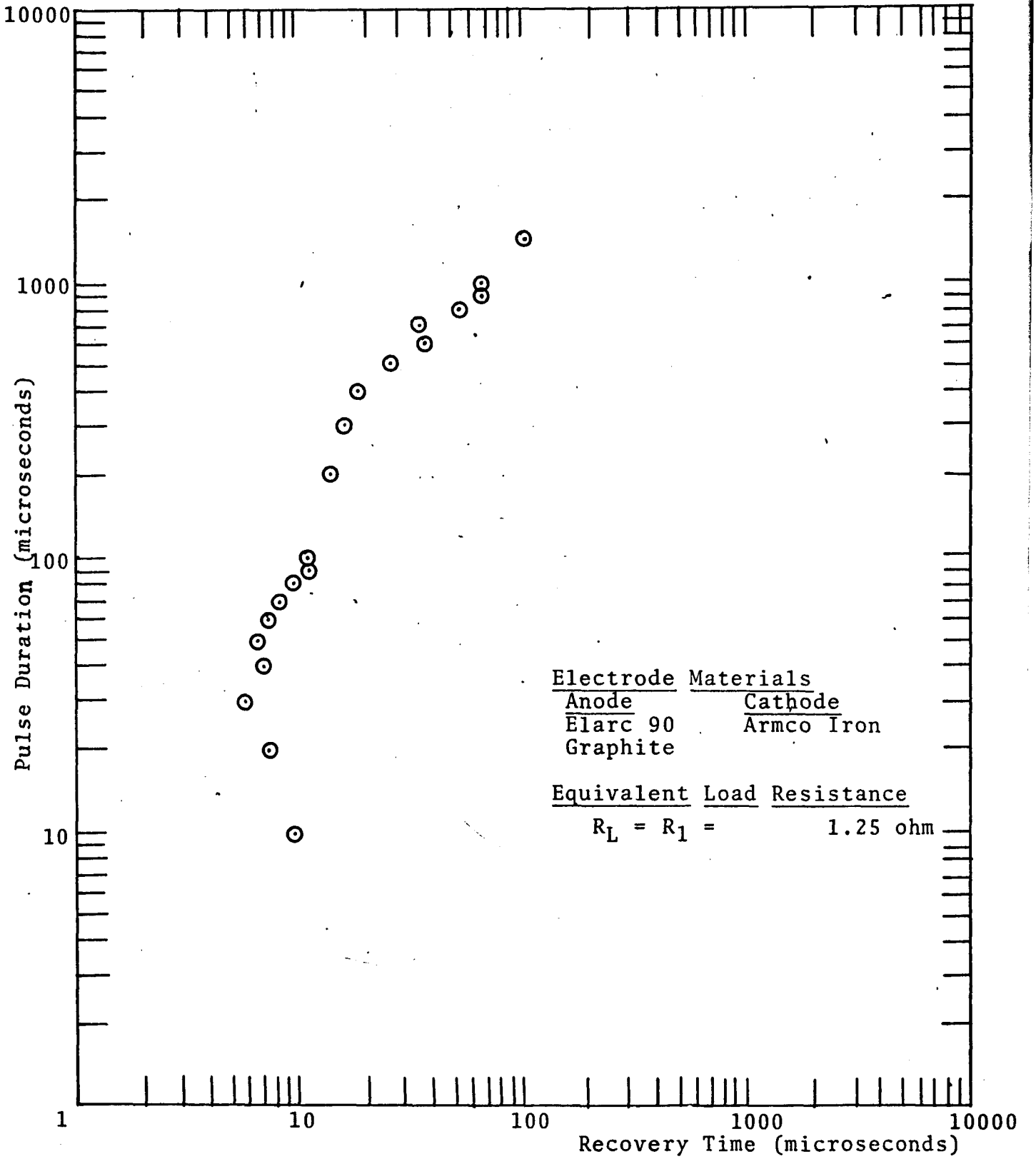

Figure 2.28 Recovery Times for Elarc 90 on Armco Iron in Reverse Polarity with a Highly Contaminated Gap and Texaco Code 499 EDM Fluid

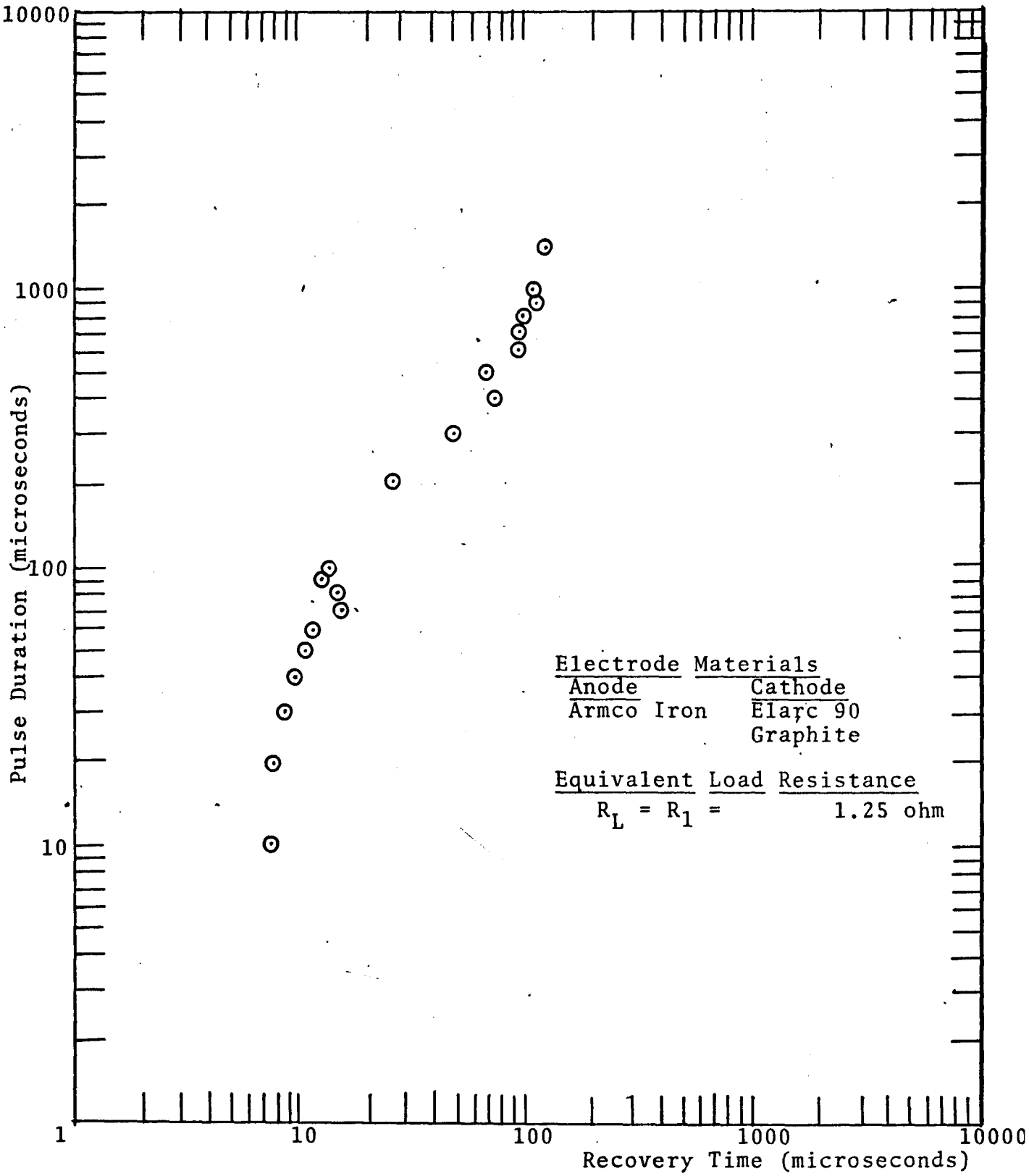

Figure 2.29 Recovery Times for Elarc 90 on Armco Iron in Normal Polarity with a Highly Contaminated Gap and Texaco Code 499 EDM Fluid

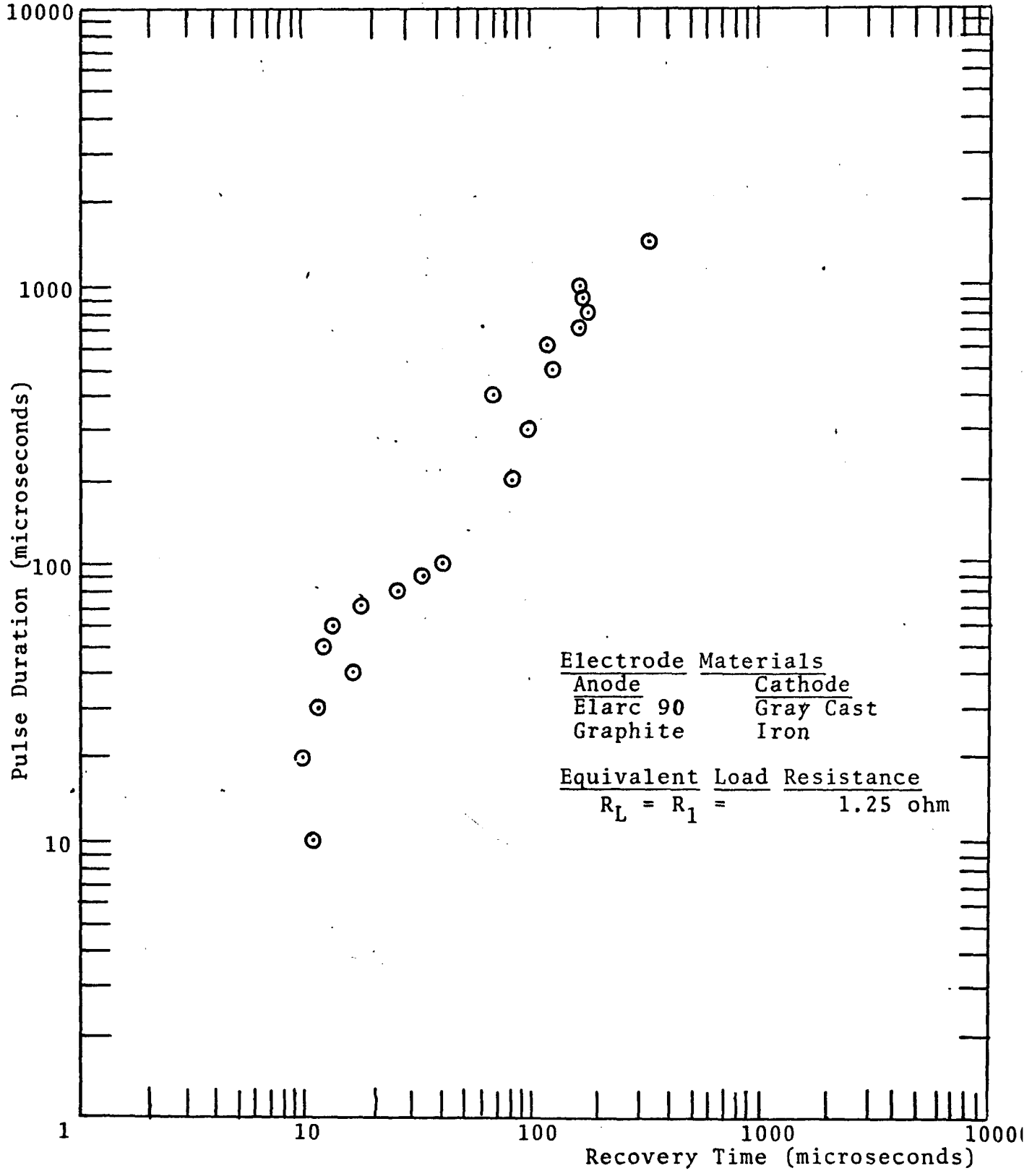

Figure 2.31 Recovery Times for Elarc 90 on Gray Cast Iron in Reverse Polarity with a Highly Contaminated Gap and Texaco Code 499 EDM Fluid

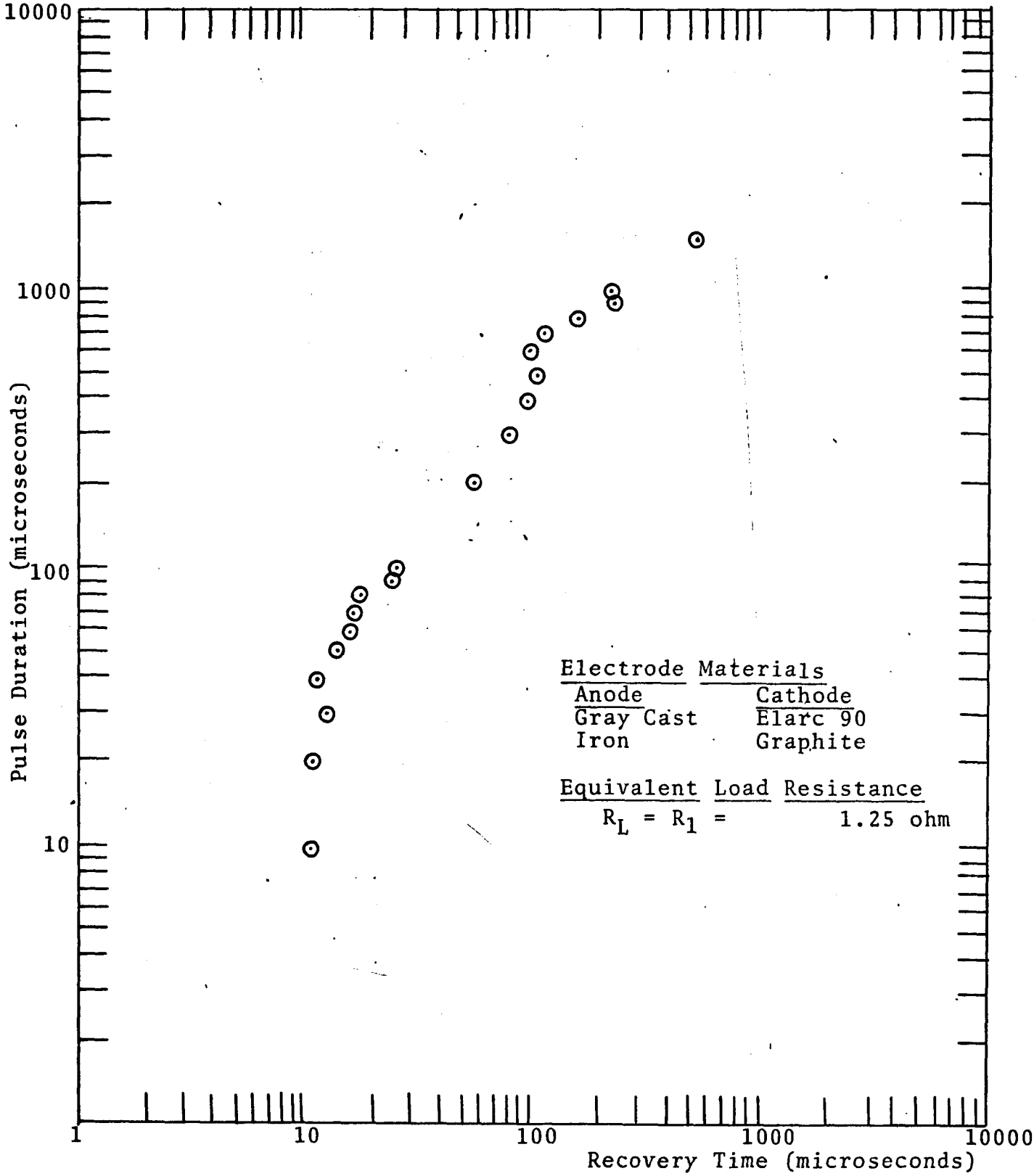

Figure 2.32 Recovery Times for Elarc 90 on Gray Cast Iron in Normal Polarity with a Highly Contaminated Gap and Texaco Code 499 EDM Fluid

Figure 2.31 and 2.32. The recovery times with the Gray Cast Iron are slightly longer than those obtained with #416 steel over the entire pulse duration range investigated. Even at the low pulse settings, where the current amplitudes are smaller than those with #416 steel, the recovery times are about 2 to 3 times longer. The longer recovery times indicate possible problems when this material is used in an EDM machining operation, which is in agreement with available machining experiences.

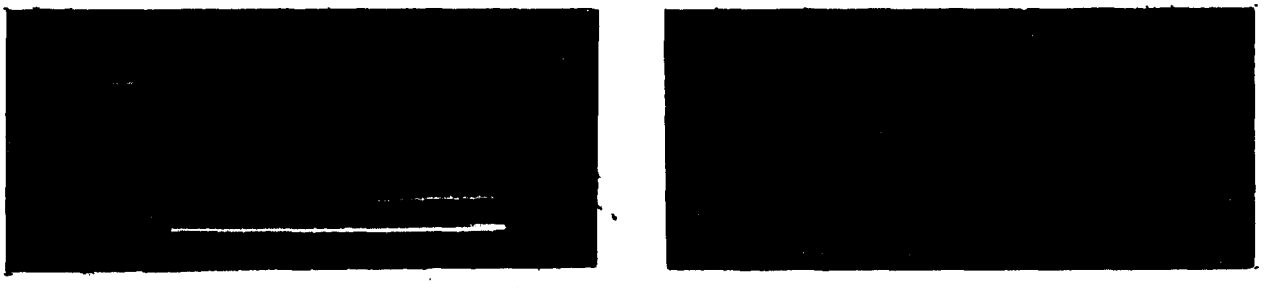

Reverse Polarity Normal Polarity

Scale: Vertical - 32 Amps/Division
Horizontal - 20 Microseconds/Division

Equivalent Load Resistance
$R_L = R_1 =$ 1.25 Ohm (Lower Trace)
$R_L = R_2 = R_1/2 =$ .625 Ohm (Middle Trace)
$R_L = R_3 = R_1/4 =$ .3125 Ohm (Upper Trace)

Figure 2.30: Gap Current Waveforms Obtained with Elarc 90 on Gray Cast Iron

D. Influence of the Different Types of EDM Fluid on Recovery Time Results

The majority of fluids tested for this section were commercially available fluids intended for use in EDM machines. Very little information was available from the manufacturers regarding the composition of their brand of fluid. The majority of the fluids tested are basically hydrocarbon and are

generally a specially treated kerosene. The properties of kerosene were given previously in Table 1.3. Pure silicone fluid and various mixtures of hydrocarbon and silicone fluids were also tested. A list of the EDM fluids and their manufacturers is shown in Table 2.2

All the fluids, except the pure silicone, were tested by using the highly contaminated gap condition and with less pulse duration detail than was considered with previous electrode materials. All of the pure hydrocarbon fluids were tested in both reverse and normal polarity with Elarc 90 and #416 Wrought Stainless steel, with pulse durations from 10 - 1500 microseconds. The results disclosed that as far as recovery time is concerned there is virtually no differences between the hydrocarbon fluids and they are all similar to the recovery times found previously with Texaco Code 499 Fluid. Since this data was found to offer no new information, it has been excluded from this paper.

The mixtures tested were Silicone 40, 80, 100, and 200. The graphic representation of the recovery data for these mixtures is shown in Figures 2.33 and 2.34. The recovery times exhibit the typical curve shape with initially constant recovery times followed by increasing recovery times as the pulse duration is increased. The results with Elarc 90 as the anode are very similar to the times obtained when Texaco Code 499 was used, and the Elarc 90 cathode results are about 10% lower. With the silicone mixtures, in normal polarity, the recovery times begin to increase at a lower pulse duration (50-60 microseconds) than with Texaco fluid or the other hydro-

carbon fluids (100-200 microseconds), but in the upper end of the pulse duration range, the recovery times are about 5% to 10% lower. These two previously mentioned conditions indicate that the rate of recovery time increase is less with the mixtures than with the other fluids. The slower rate of recovery time increase indicates that a possible lower recovery time advantage exists when these fluids are used at pulse durations greater than 1000 microseconds. However, for the pulse duration range of interest in this investigation, very little difference was found between the silicone mixtures and the pure hydrocarbon fluids.

The investigation of the pure silicone fluid was made more extensive owing to the recent amount of literature published regarding its machining qualities. The silicone fluid used in this investigation was SF-96(5) made by General Electric. It was chosen because of the close similarity of viscosities between it (5 centistokes) and regular EDM fluids (2.68 centistokes). The clean and highly contaminated gap case results for Elarc 90 as the anode are shown in Figures 2.35 and 2.36. The results for Elarc 90 as the cathode are shown in Figures 2.37 and 2.38. The gap machining voltages and currents are very similar to those found with Texaco Fluid. There are slight differences between the clean and highly contaminated case recovery times, as was found when Elarc 90 and #416 steel were used with Texaco EDM Fluid, but again, the curve shape is similar. The clean gap condition, however, maintains a low recovery time and does not begin to increase until a pulse duration of 200 microseconds, while the highly contaminated

Type	Manufacturer
510	Wolf's Head Oil Refining Co. Oil City, Pa.
Amoco M S O	American Oil Co.
#499	Texaco
Shell EDM	Shell Oil Co. New York, N.Y.
Factopure T30	Boron Oil Co. Cleveland, Ohio
Mineral Seal Oil LR-6128	
Citgo No. 90109	City Service Oil Co. Cranbury, N.J.
Silicone EDM 200	Chem-Cool Co. Maywood, Ill.
Silicone EDM 100	"
Silicone EDM 80	"
Silicone EDM 40	"
Pure Silicone SF-96(5)	General Electric Silicones Waterford, N.Y.
Florochemical FC-77	3M Company, Chemical Div. St. Paul, Minn.

Table 2.2: EDM Fluids Tested and Manufacturers

case begins to increase between 60 to 100 microseconds, regardless of the polarity. The results with Elarc 90 as the cathode have a very scattered appearance which is caused by discharge and contamination difficulties similar to those encountered previously with Texaco fluid and Elarc 90 as the cathode.

The most noticeable difference between the Texaco fluid recovery times and those of pure silicone is the smaller increase in recovery time that occurs when the current amplitude is increased. This nominal increase can best be seen at the lower pulse duration settings. With $R_L = R_1$, the recovery times are approximately the same as those for Texaco fluid with pulse durations below 50 microseconds. However, with $R_L = R_2$ and R_3, the recovery times are about 10% shorter for pulse durations up to 100 microseconds.

The silicone fluid has an oxygen and a silicon radical present in its chemical make-up, besides a hydrocarbon CH_3 radical. [55] In all likelihood, hydrogen and methane are produced [56] just as with hydrocarbon fluids, but what happens to the silicon and the oxygen atoms, and their role in the eventual gap recovery is not clear.

At higher pulse durations, the recovery data for silicone is similar to that of the other hydrocarbon fluids tested, indicating that the electrode is again dominating the recovery interval. However, the typical bend, or knee, of the recovery time versus pulse duration curves, occurs at a pulse duration about 10 microseconds shorter than that found with hydrocarbon fluids. The lowering of the bend could probably be attributed to the slightly higher viscosity of the silicone fluid, which

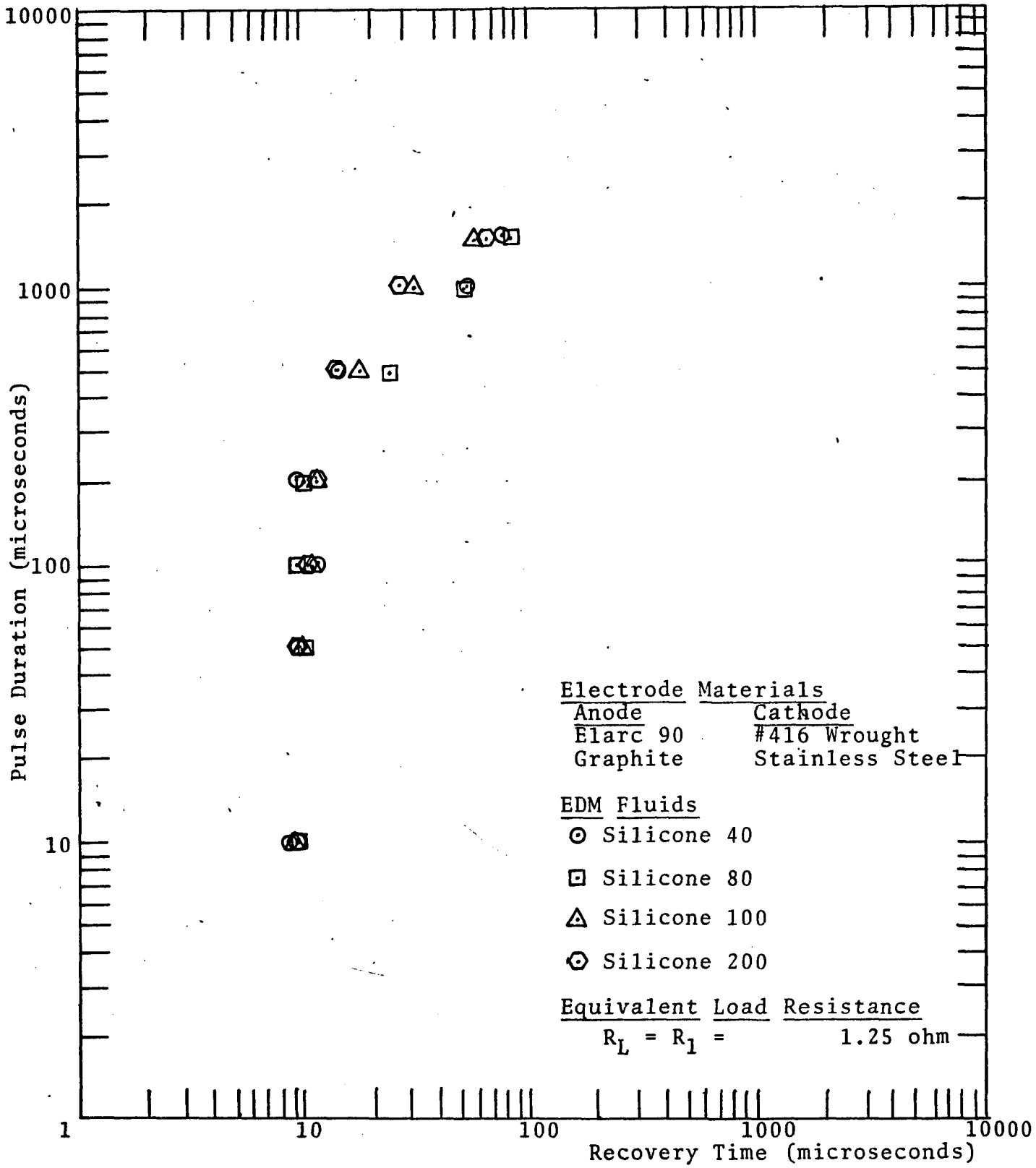

Figure 2.33 Recovery Times for Elarc 90 on #416 Wrought Stainless Steel in Reverse Polarity with a Highly Contaminated Gap and Using Silicone 40, Silicone 80, Silicone 100, and Silicone 200 EDM Fluid

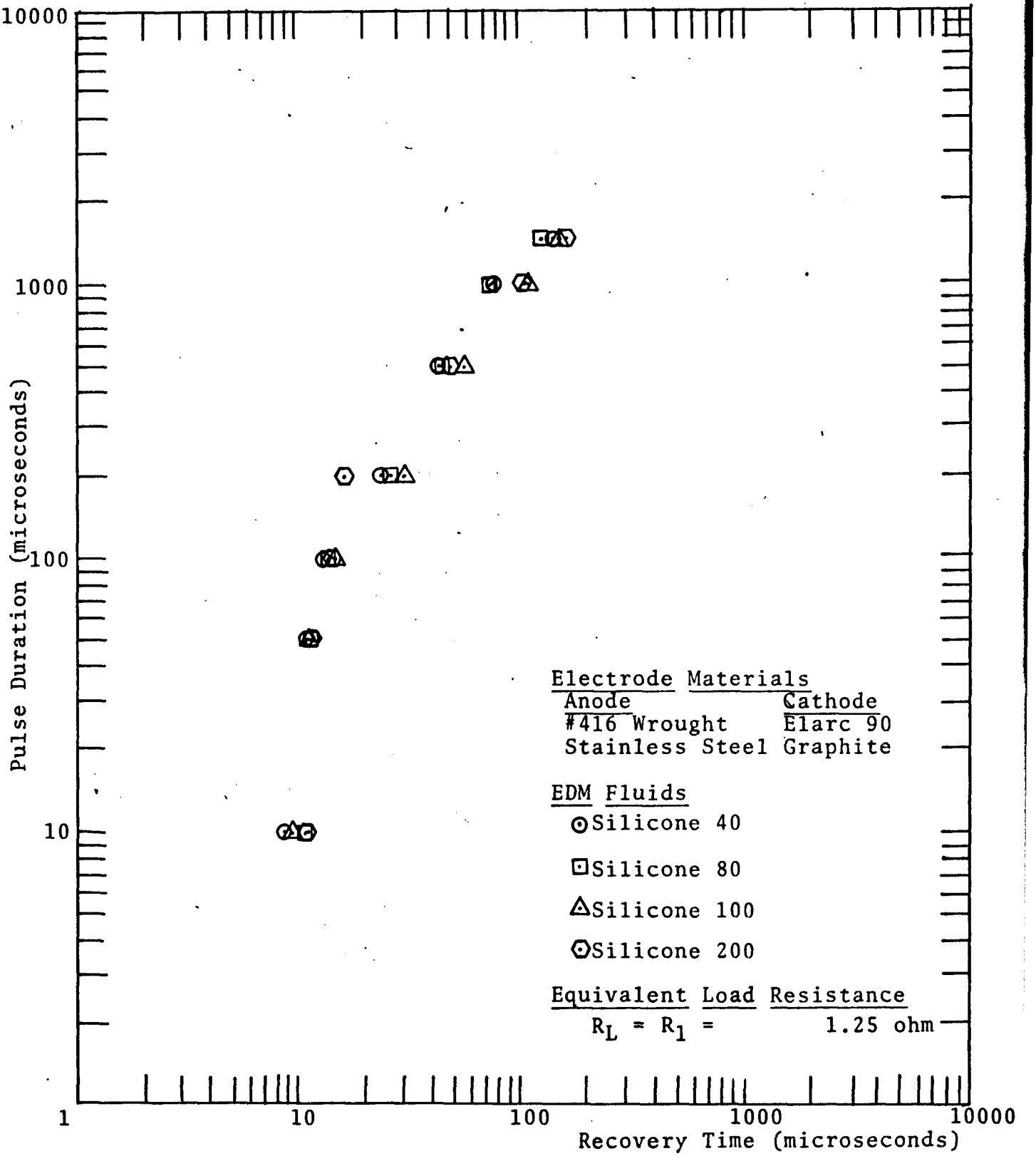

Figure 2.34 Recovery Times for Elarc 90 on #416 Wrought Stainless Steel in Normal Polarity with a Highly Contaminated Gap and Using Silicone 40, Silicone 80, Silicone 100, and Silicone 200 EDM Fluid

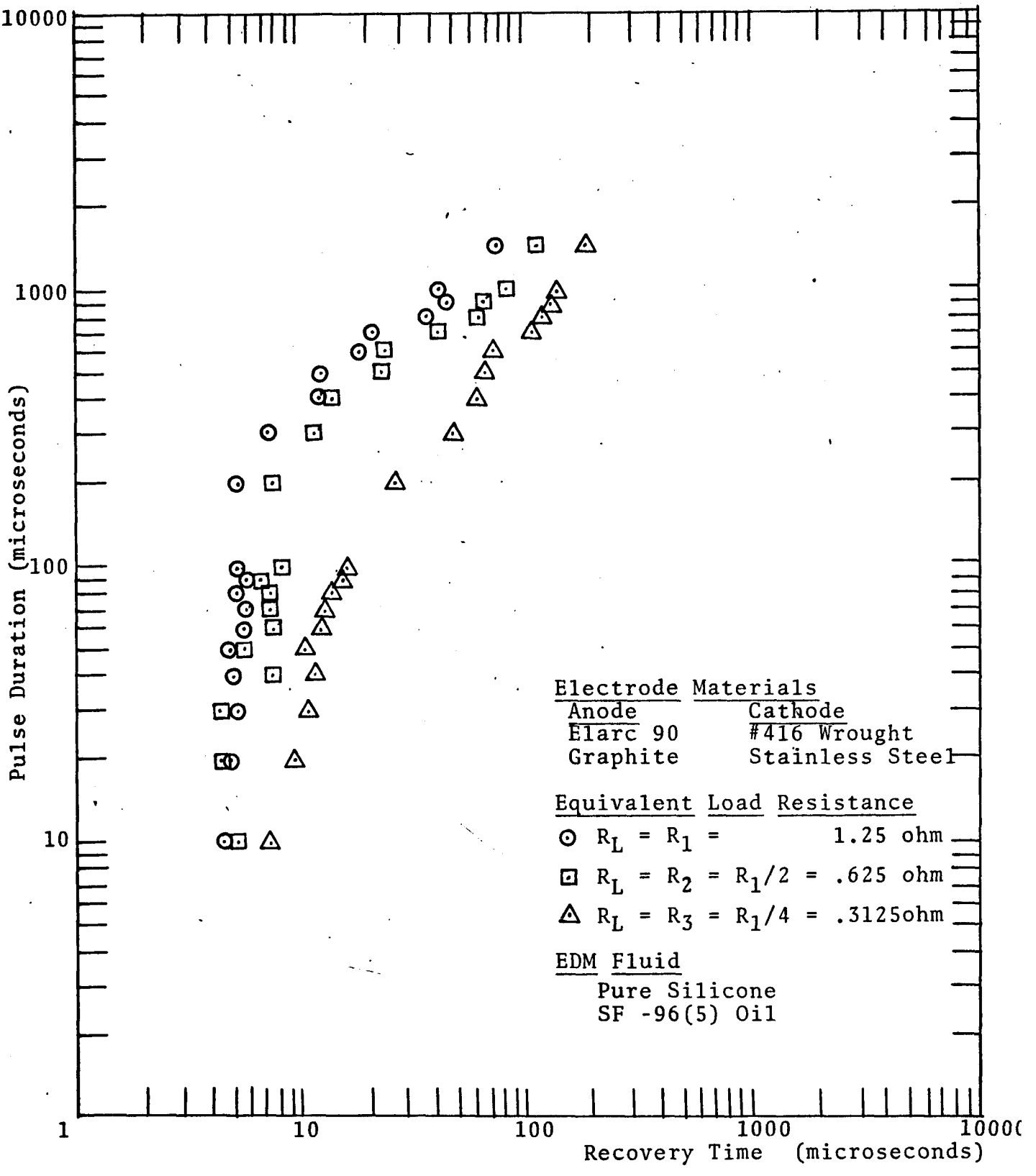

Figure 2.35 Recovery Times for Elarc 90 on #416 Wrought Stainless Steel in Reverse Polarity with a Clean Gap and Pure Silicone SF-96(5) Oil

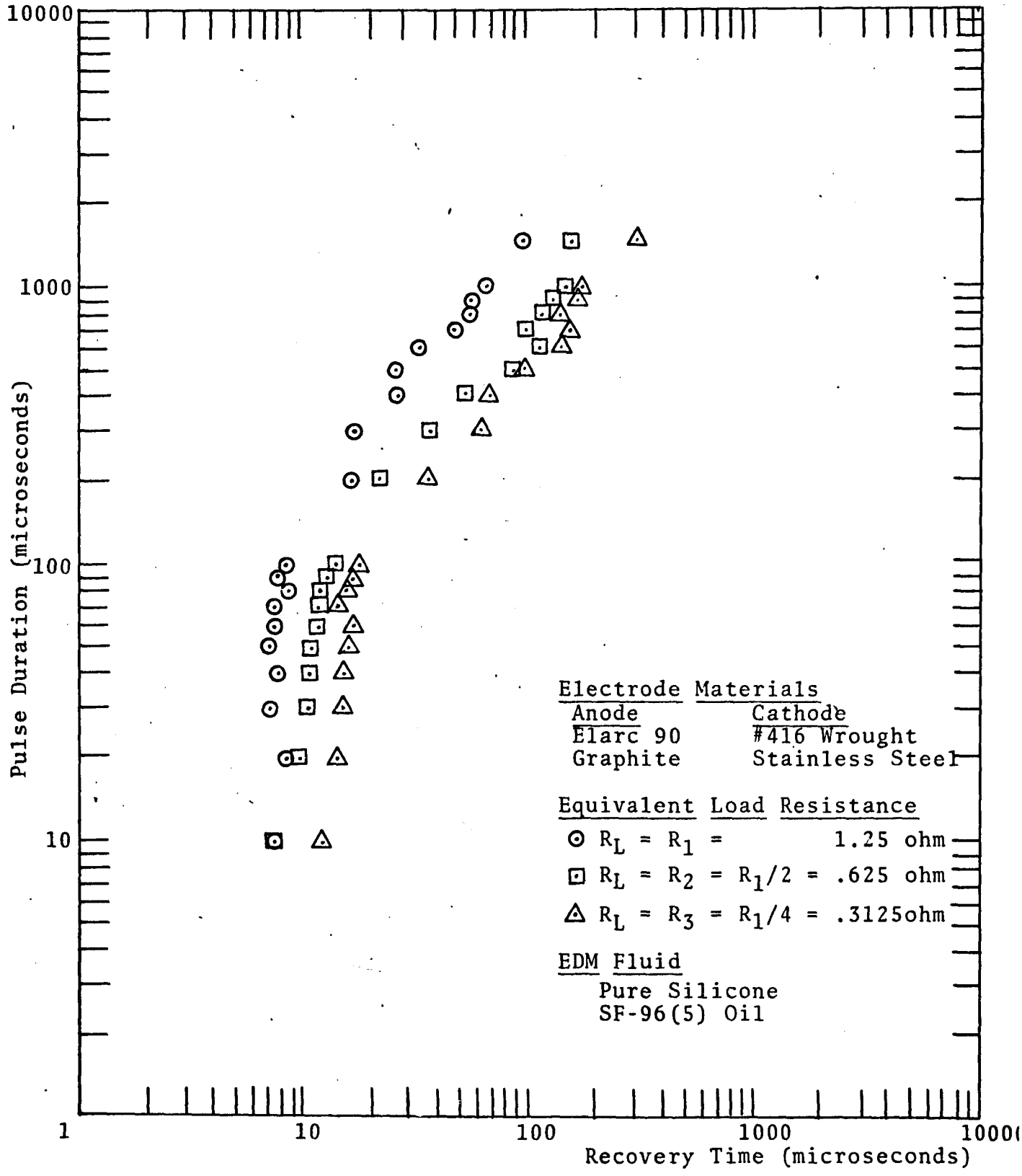

Figure 2.36 Recovery Times for Elarc 90 on #416 Wrought Stainless Steel in Reverse Polarity with a Highly Contaminated Gap and Pure Silicone SF-96(5) Oil

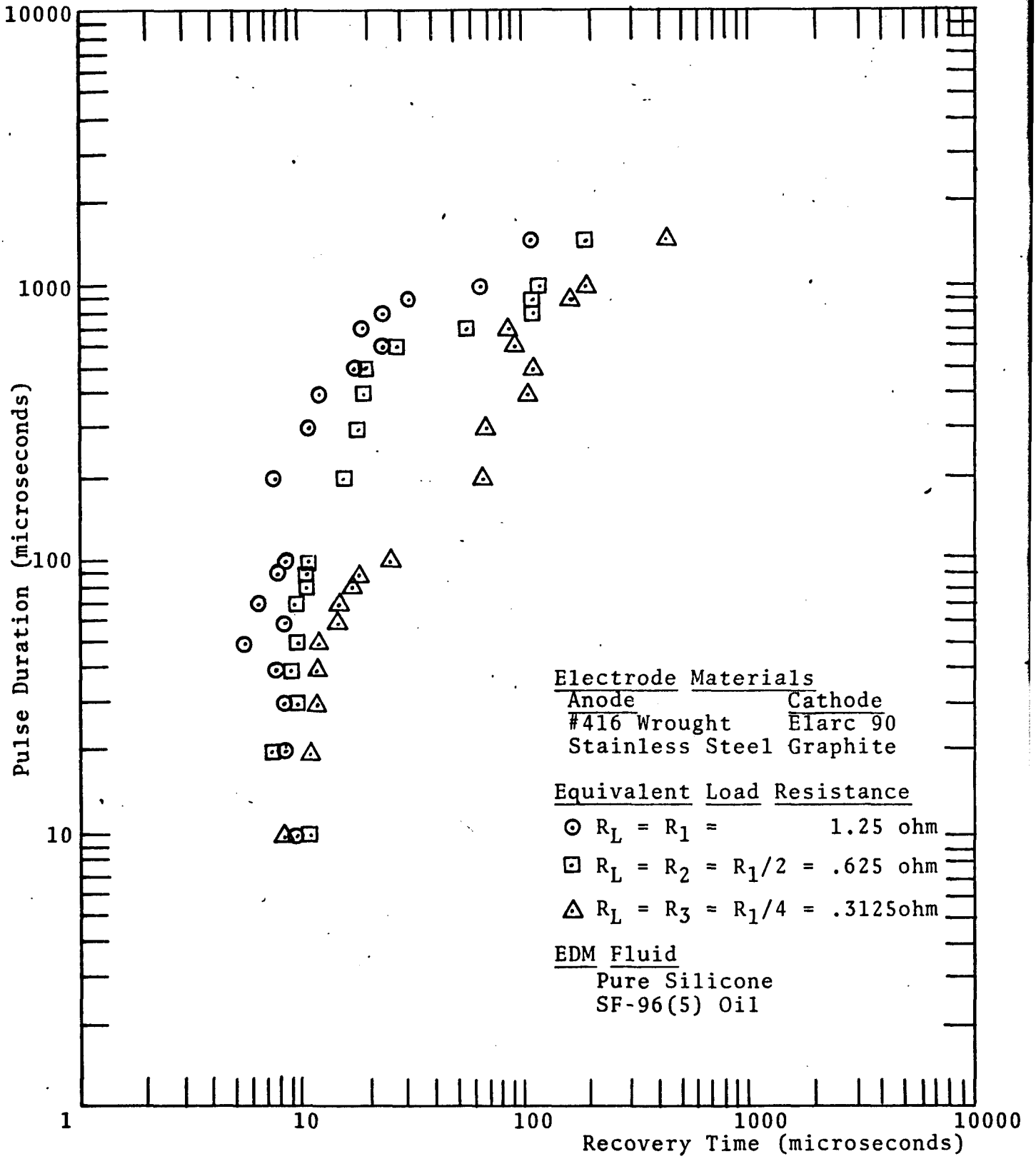

Figure 2.37 Recovery Times for Elarc 90 on #416 Wrought Stainless Steel in Normal Polarity with a Clean Gap and Pure Silicone SF-96(5) Oil

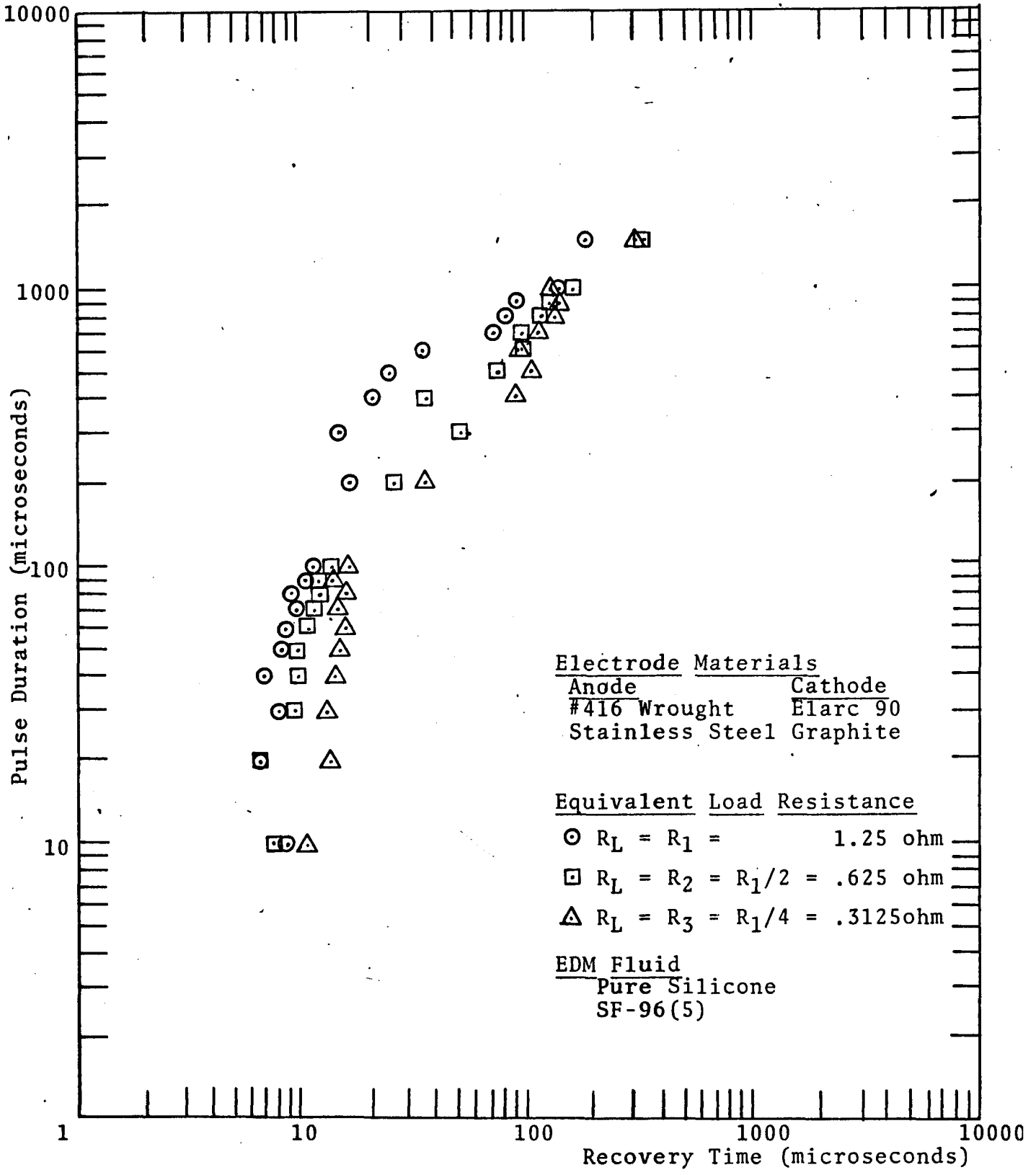

Figure 2.38 Recovery Times for Elarc 90 on #416 Wrought Stainless Steel in Normal Polarity with a Highly Contaminated Gap and Pure Silicone SF-96(5) Oil

will cause the radial expansion of the discharge column to be slower [57]. The slower expansion could result in the faster heating of the electrode crater area, thereby, allowing the electrode thermal influence to appear at a lower pulse duration.

E. Discussion and Conclusions Regarding the Recovery Time Results

Once a self-sustaining discharge* has been formed and the ionized channel established, the discharge current can proceed to rise. In general, the temperatures associated with the current-carrying column are very high. Temperatures as high as 5000 - 10,000°K [59] have been measured. The temperature is dependent on the electrode materials, gap space, arc duration, current amplitude, and thermal properties. The high temperatures are established in the discharge column in less than .1 microseconds [60] and cause further ionization and vaporization of the dielectric fluid which surrounds the initial spark channel. The vaporized EDM fluid forms a bubble around the discharge column which expands and contracts as described by Hockenberry. [61] The discharge channel also expands as described by Eckman. [60] The high temperature causes the electrodes to heat up, and the temperature at the electrode terminus of the discharge quickly reaches the vaporization temperature

---

* A self-sustaining discharge is one that has sufficient voltage and current from its internal power source to maintain an ionized channel when all sources of external ionization are removed. It is necessary to have the proper field, pressure, and gap, such that each electron, leaving the cathode, establishes a secondary process, which, in turn, causes a new electron to leave the cathode. [58]

of the electrode material [62] and remains there for the duration of the discharge.

The temperatures associated with the discharge column are sufficient to cause thermal ionization* which maintains the discharge. The thermal ionization is established and maintained by the energy given up to the gas particles due to collisions with the ions and electrons in the column.[64]

When the power source is removed from the discharge, current can no longer flow and the discharge is extinguished. There are, however, many events that must take place before the gap can be termed recovered. Again, there is disagreement among the various investigators concerning the processes involved and their importance in the gap's eventual recovery. Churchill et al., make a generalized statement regarding the recovery of a spark gap.[65]

"The rate of spark gap recovery, after the passage of a discharge, is a function of the initial discharge characteristics and the processes taking place in the channel after current zero. Depending upon the relative importance of the various ionizing and deionizing processes in the decaying channel, the gas in the electrode space slowly recovers to its full dielectric strength. Energy is lost through recombination and diffusion, conduction, convection and radiation, and on this basis, recovery is complete when the energy losses, after current zero, are equal to the energy contained in the channel at current zero."

---

* Thermal ionization is a general term applied to the ionizing action of molecular collision occurring in gases at very high temperatures.[63]

It can be noted then, that there are many processes involved in the recovery of the spark gap and that numerous factors can influence the recovery time. Much of the work on the recovery of arc columns has shown the effects of various parameters. The type and size of the electrodes and their temperature decay were shown to influence the reignition voltage.[10, 66] Gap spacing was also important to the recovery of the gap[10, 65]. It was found, that the shorter the gap distance, the faster the ionized gas would cool due to thermal effects of the electrodes [67]. However, the closer the two electrodes are spaced, the more the thermal recovery of the electrode surface influences the total temperature decay. Then, as was indicated by Edels, et al.,[38] in their paper on arc reignition, there was an initial fast decay of the ionized gas temperature to the temperature of the electrode surface, followed by a slower thermal decay dictated by electrode thermal coefficients, provided the decay time constant of the electrode was longer than that of the gas[38], and that the electrode heat content is high enough to prevent its temperature decay to ambient before the gas column reached the electrode temperature[68]. It, therefore, seems reasonable to expect in the EDM process that there could be an initial fast recovery time followed by a longer time dependent upon the electrode materials.

Most of the reasoning mentioned regarding recovery was taken from literature concerning arc voltage recovery, but it seems reasonable that the factors that influence reignition voltage in arc gaps, could also influence the resistive recovery of the EDM machining gap. Although, the EDM process

takes place under a liquid, the recovery phenomena takes place within a gas bubble, which is similar to the conditions used in the arc research.

Edels, Churchill, and other arc researchers were mainly interested in determining how to avoid the 'Slepian race phenomena'* [69] and its relationship to the construction of improved contactors, circuit breakers, and switches. However, in EDM, the important consideration is not the relationship of the re-applied voltage to the restriking potential of the gap, but how re-application of voltage affects the random nature necessary in the EDM process. The previously mentioned arc investigations were concerned with the recovery interval's relationship to reignition of the arc no matter where the new arc appeared on the electrode surfaces, but in the EDM process, the recovery interval is important only in regard to its influence upon the random machining operation.

The generalized conclusion regarding the different graphite and carbon materials tested is that certain molded tool electrode materials appear to have shorter recovery times than other molded varieties. The longer recovery times found with certain molded materials suggest that the manufacturing processes for these electrodes could have a greater tendency to cause a condition referred to as 'coking', which will be discussed in Chapter III, and from actual machining experiences, this is indeed the case.

---

* 'Slepian race' is a relation between the re-application of voltage to a set of contacts and the restriking voltage of the contacts. If voltage is reapplied to the contacts too quickly, it could exceed the restriking voltage and result in an arc.

An exact explanation of the variation in recovery times that occurred when the tool electrode material was changed, cannot be given owing to insufficient data regarding the difference between the materials on the limited experimental information obtained. The recovery times are definitely linked to the thermal properties of the electrode materials and how these properties affect the temperature of the gap gases following a discharge, as has been mentioned by many arc researchers [70]. The influence on recovery times, that various properties of the graphite materials have, is not known and a more controlled study would be necessary to make an exact determination. Changes in the graphite grain size, porosity, binder type, uniformity, density, etc., all affect the thermal characteristics of the electrode, and hence, the events occurring in the gap spacing. The data available is, therefore, insufficient to develop any specific reasoning for the increases in recovery times that were mentioned.

When the workpiece material was varied, other problems arose. Some of the thermal properties of the metals tried were available and are shown in Table 1.2. The recovery results, however, did not vary according to the conclusions drawn in many of the arc research papers, i.e., the material with the highest thermal conductivity will recover the fastest.[71] However, the results for the metals tested indicated almost exactly the opposite reasoning, which is similar to some of the results reached by Parker, et al.,[72] in their investigation of electrode surface temperature and its role in spark gap recovery. Parker, et al., found that a material with

a lower thermal conductivity than copper caused the gap to recover faster than it did when copper was used. They reasoned that the reduced recovery times were the result of changes in the cathode surface due to the arc. The changes caused a reduction in the secondary Townsend ionization coefficient* and hence, the faster recovery interval resulted,[73] but they offer no explanation of what changes could cause this reduction.

The conclusions reached by the arc researchers, reflect the nature of the current discharges they investigated. They considered mostly long-duration arcs where steady state thermal gradients could be established in the electrodes. The thermal capacity of the electrodes was almost saturated because of the long arcs and the effect of thermal capacitance was reflected when the size of the electrodes was increased (also increasing thermal capacitance) and the gap was found to recover faster.[74] Therefore, for short duration current discharges, the initial thermal capacity, or the specific heat, seems to be of greater importance in regards to gap recovery times. A material that is capable of absorbing heat quickly, should recover faster than one which absorbs heat slowly. The specific heat should, therefore, be the governing factor when short-duration discharges are investigated, and thermal conductivity would become more

---

* Townsend proposed the first fairly satisfactory explanation of the ionization phenomenon that occurred during a current discharge. His idea was based upon the assumption that current increase, during the course of breakdown, was the result of ionization by "collision". He used two ionization coefficients to explain the process: The First Coefficient designated the number of ionization collisions per centimeter due to electrons that have gained sufficient energy from the gap field. The Second Coefficient related to ionization caused by the positive ion formed by electron collisions, that had gained sufficient energy from the gap field to ionize the gas by collision.

important as the pulse duration increased. This reasoning was partially supported by the previously presented data on the different workpiece materials. The specific heat of #416 Wrought Stainless Steel was larger than that of any other metal workpieces considered and the recovery times with #416 steel were the lowest of all the workpiece materials considered. However, data regarding the specific heat of Gray Cast Iron was not readily obtainable. The literature available seemed to imply that the addition of carbon to iron increased the thermal capacity, but no specific statement to this nature was found.

The generalized conclusions regarding the workpiece metals tested are limited because of the scope of the materials tested. The results indicate that the Gray Cast Iron required the longest times to recover, while Armco Iron and Hardtem B both required about the same times. Number 416 steel had the shortest recovery times and would, therefore, be classified as the best workpiece material tested when fast recovery times are important.

There have been numerous claims made by both users and manufacturers of EDM fluids regarding the merits and advantages gained when a certain type of fluid was used in the machining process. These people, however, have little information with which to back up their claims and generally have only a few reasons why they claim the fluid was best. There have been several comprehensive studies[79] attempted to determine if there actually was a difference between the various brands of EDM fluids and light oils used with the process. A Japanese group[75] investigated many different fluids and oils, but they came to no definite conclusions

regarding which type was the best for the EDM process. Another study was conducted by the Cincinnati Milling Machine Company[76] to understand the function of the EDM fluid in the machining process. The Cincinnati report does reach some conclusions regarding the different fluids tested. They state that ordinary hydrocarbon fluids do not breakdown easily enough to insure the formation of a current discharge after each breakdown and that a mixture of triethylene glycol, water, and monoethyl ether of ethylene glycol exhibited the best overall performance of all the fluids tested.[77] Both the previously mentioned investigations apparently were concerned with actual machining operations to gather information. Owing to the use of a specific type of EDM machine and the skill of the machine operator, this method allows other factors to influence the data. In order to reach a meaningful conclusion regarding the available fluids, the influence the fluid has upon various aspects of the machining operation and the effects the fluid properties impose upon the process should be understood first.

Hockenberry[78] investigated the effects that fluid viscosity had upon the erosion of electrode material during a single discharge, and concluded that the higher the fluid viscosity, the smaller each single discharge crater area would be. The smaller crater areas then indicate a lower machining rate. This conclusion implies that higher viscosity fluids would produce poorer machining rates than lower viscosity ones. This study, however, was concerned with only one small aspect of the differences between the various fluids and others must follow Other authors have investigated the effects of the EDM fluid

by observing the resultant craters[23, 60] and the gap voltages and currents during the discharge.[80]

It was found in the present investigation that the different fluids had little noticeable effect upon the recovery interval following the discharge. Only the silicone mixtures and the pure silicone appeared to have any effect whatsoever. These results are understandable when the nature of the gases in the gap spacing are considered. These gases play an important part in the thermal properties and the eventual recovery of the gap spacing.[81] In the case of the pure hydrocarbon fluids, which were all essentially kerosene, the gases were in all likelihood very similar, if not the same. Therefore, there was no reason for the recovery times to differ appreciably. However, in the case of the hydrocarbon-silicone mixtures, and pure silicone fluids, the possibility exists that the gap gases could have been different* and therefore, the gap spacing thermal decay properties would have been different. The influence of the gap gases would be most noticeable at low pulse durations where electrode influences were at a minimum and with pure silicone, there was a noticeable lessening of the recovery times at the lower durations. This effect was not detectable with the fluid mixtures owing to probable dominance by the hydrocarbon gases. The gap

---

* The chemical formula for the dimethyl-silicone fluid used in this study is:

$$\left(\text{-SI(CH}_3\text{)-O-}\right)_x$$ [55] as compared to the hydrocarbon of $$\left(\text{-C(H)-}\right)_x$$

Therefore with the silicon and oxygen radical available, the evolved gases should be different, although no study of the evolved gases could be found.

gases evolved from both the mixtures and the pure silicone also affected the thermal decay of the electrodes. The effect was observed when the rate of recovery time increase was less than that found when pure hydrocarbon fluids were used.

The generalized conclusions regarding the recovery time of the various different fluids tested are:

(a) There appears to be no advantages gained by the use of any of the different hydrocarbon fluids tested.

(b) The silicone-hydrocarbon mixtures and pure silicone fluids do cause a change in the recovery times, but an appreciable difference was never found. Although, silicone possible would have an advantage at higher pulse widths, where its recovery time would possibly be shorter than those of the hydrocarbon fluids.

CHAPTER III

COMPARISON OF RECOVERY TIME MEASUREMENTS WITH CERTAIN DELETERIOUS EDM MACHINING RESULTS

A. Carbon Growth on the Tool Electrode and Workpiece Surfaces

One of the most destructive phenomena that occurs in the EDM art is the uncontrollable growth of a carbon material on the EDM electrodes, or what is termed the coking condition. Coking comes into existence when there is a concentration of discharges in approximately the same physical location on the workpiece and usually results in the complete destruction of the workpiece. This concentration results in the growth of stalagmite and stalactite formations from the workpiece and tool electrodes, with the largest growth occurring on whichever electrode happens to be of negative polarity. The most efficient way to eliminate the coking growths once they are established is to interrupt the machining and physically remove them. Several photographs of these coking growths are shown in Figure 3.1. Note that these growths occur in all sizes and in Figure 3.1 (b), a detectable spiralling can be seen. This spiralling was often noticed when coking occurred. Typically damaged test workpiece and tool electrodes are shown in Figure 3.2. Figure 3.2-c), d), and e) show 4 typical workpiece damage from a coking condition. Notice that in Figure 3.2-c) the surface finish is relatively smooth as a result of comparably short pulse durations, and still a coking case managed to occur. Figure 3.2-d) and e) show the irreparable damage than can result from the coking condition, and e) - several coking cases

a) Typical Coking Growths of Varying Size
Scale: Approximately 1/2 Actual Size

b) Spiraling Coking Growths
Scale: Approximately 1/2 Actual Size

Figure 3.1 Photographs of Coking Growths

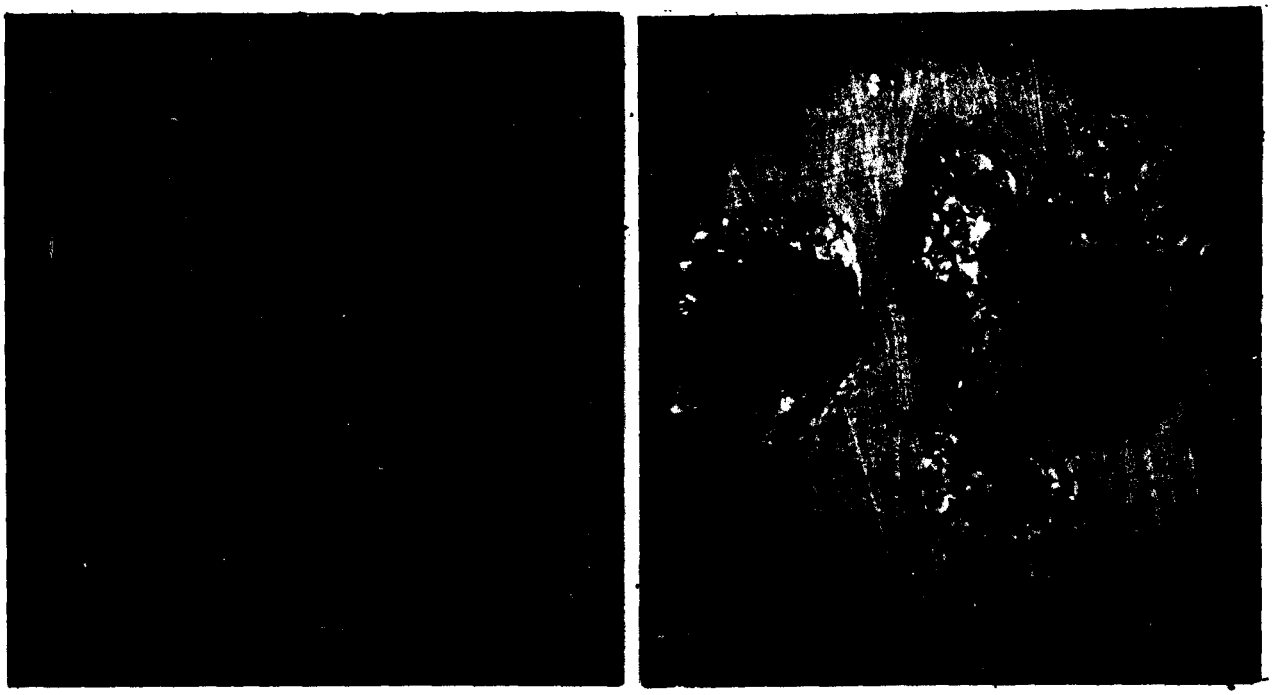

Elarc 90 Anode Hardtem B Cathode
Scale: Approximately 1cm/2mm

a) Reverse Polarity, $R_L = R_1 = 1.25$ ohm, and Texaco EDM Fluid

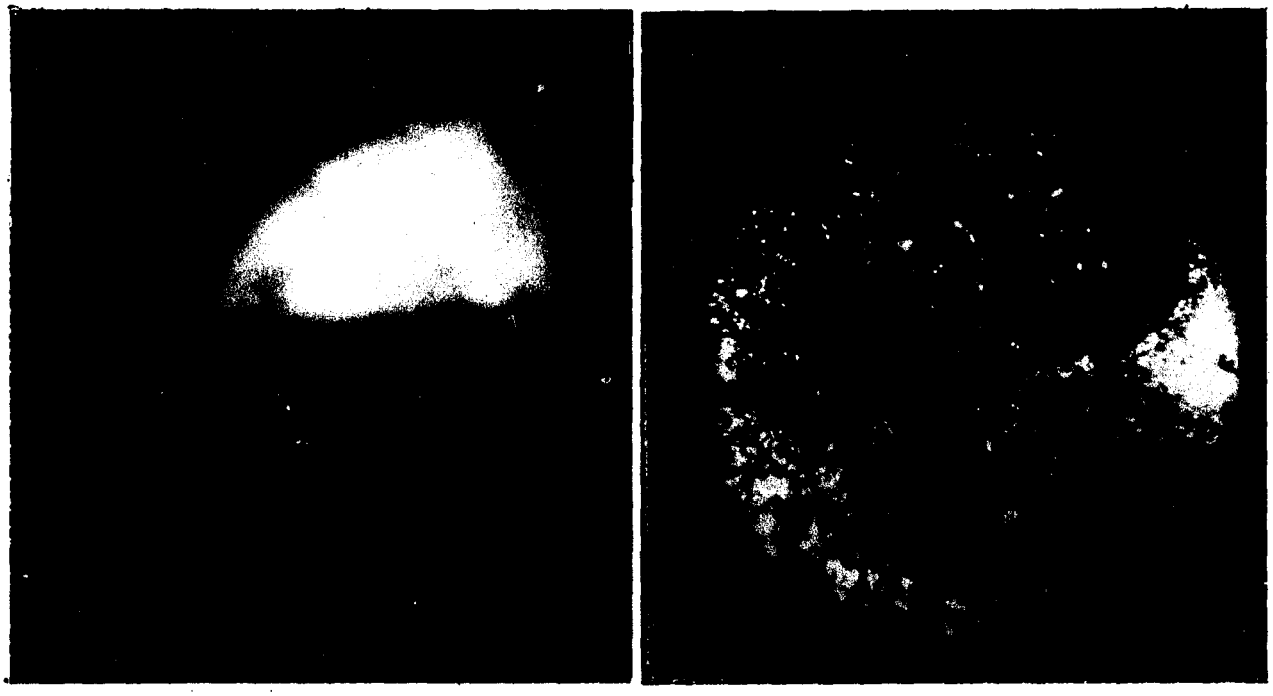

Elarc 90 Cathode Hardtem B Anode
Scale: Approximately 1.5cm/2mm

b) Normal Polarity, $R_L = R_1 = 1.25$ ohm, and Texaco EDM Fluid

Figure 3.2 Typical Damage Done When a Coking Condition Occurs During an Actual Machining Test

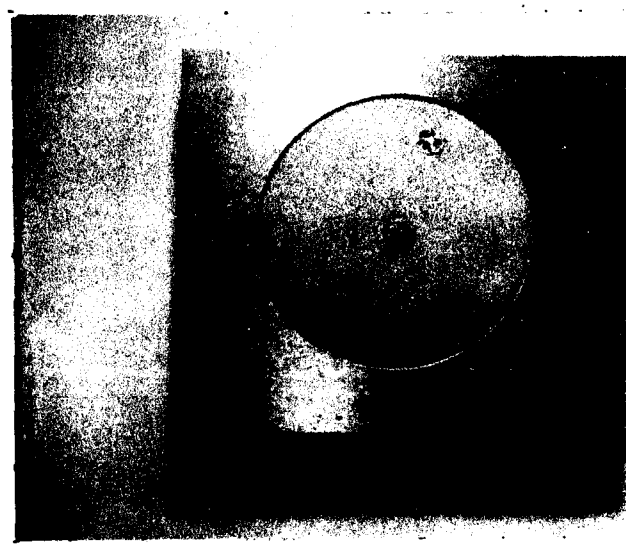

c) Coking Damage Can Occur When Low Power Pulses are Being Used

Scale: Approximately 0.9 Actual Size

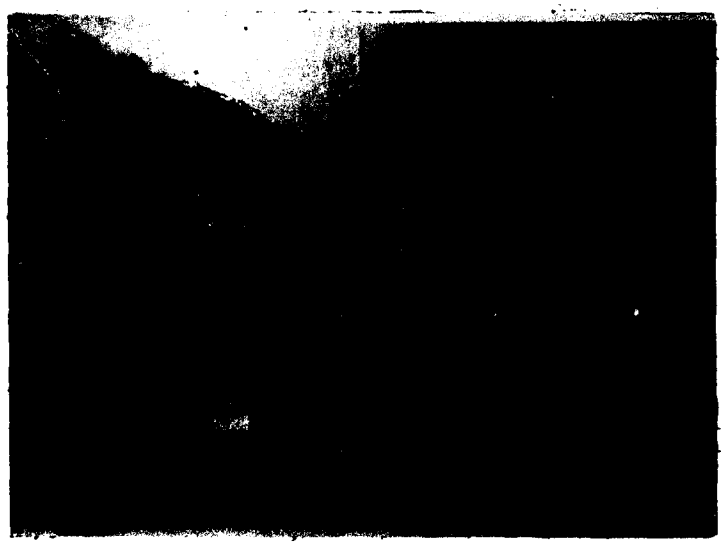

d) Damage to Hardtem B Workpiece When Coking Occured with an 1 1/2" Carbon Tool Electrode

Scale: Approximately 0.9 Actual Size

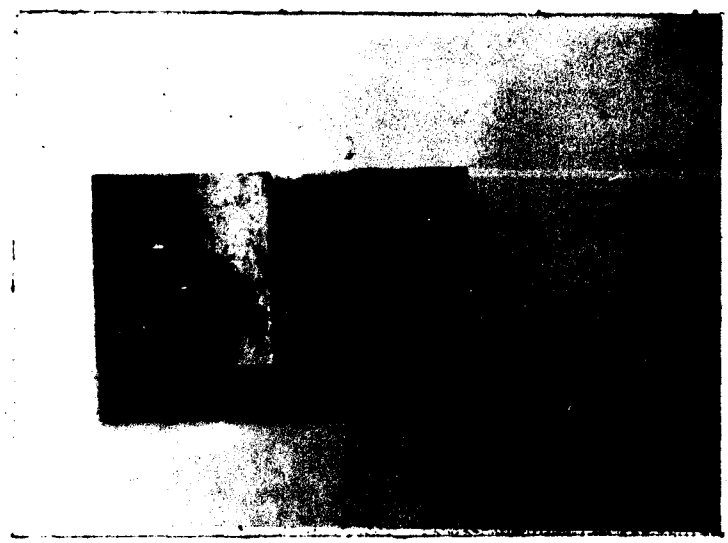

e) Multiple Damaged Areas Occuring During A Single Machining Test

Scale: Approximately 0.9 Actual Size

Figure 3.2(con't) Typical Damage Done When a Coking Condition Occurs During an Actual Machining Test

occurred during a single machining operation, resulting in multiple damaged areas on the workpiece. In many cases where coking occurs, the damage causes a substantial financial loss to the user. It is, therefore, desirable to understand the coking condition, to determine what possibly causes it, and how it can be eliminated. The purpose of this section was to gain a better understanding of the coking condition.

Until recently there has been very little, if any, published information regarding the coking condition. Prior to this time, EDM operators had to rely totally upon experience to tell them which combination of parameters should be made on their particular machine to avoid coking and, more often than not, the operator still had to constantly watch the operation to insure that coking did not occur. Generally, once coking developed on a machine, the procedure followed by the operator was to reduce the duty cycle and current output of the machine, which in turn, reduced the overall efficiency of the EDM operation.

The knowledge accumulated by the machine operators has, as a result of the trial and error procedures, provided several clues as to when coking occurs. There is a greater tendency for coking to occur when carbon or graphite electrodes are used in normal polarity, although coking has also been observed with reverse polarity and with copper electrodes. Higher duty cycles also seem to cause the condition to occur more frequently than lower duty cycles. Very seldom is this condition ever observed for pulse durations below 20 microseconds, even with high duty cycles. Also, certain electrode material combinations are apparently more prone to this condition than others are.

There are several other properties of the coking condition that distinguish it from normal machine operation besides the obvious ones mentioned previously. When coking is occurring in the gap spacing, there is a marked decrease in the machining pulse gap voltage, an increase in the discharge current, and generally a remarkably stable machine operation, lacking the erratic tool electrode movements typical of most machining situtions. The oscillograms in Figure 3.3 show typical gap voltage and current waveforms for normal machining and for a coking condition. The pulse duration was extended, in some cases, to enhance the differences. Figure 3.3 - a) shows the lower machining voltage and higher currents found when the coking condition exists as compared to a standard machining situation. Note that the gap current and voltage waveforms for the coking case are smooth and fairly noise-free when compared to the regular machining waveforms. The current and voltage waveforms, with normal polarity, had the same differences, but not as noticeable, as those for reverse polarity, and are, therefore, not shown here. The remainder of Figure 3.3 shows regular and coking current waveforms for different pulse duration settings. The rise times with coking pulses are somewhat slower, in both polarities, than those of the regular case.

Several other interesting observations were made during the course of the coking study, using both a 'self-timed' EDM machine and the test circuitry discussed earlier. When the test apparatus was set to produce very long pulse durations, it was observed that the coking condition could come about during a single discharge. (See Figure 3.4) It can be seen,

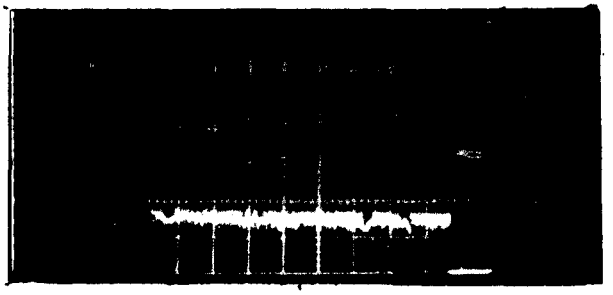

1) Regular Machining Voltage Pulse
2) Regular Machining Current Pulse

Scale:

	Vertical	Horizontal
1)	10 volts/div	5 millisec/div
2)	6.66 amp/div	5 millisec/div

a) Reverse Polarity, Elarc 90 on Hardtem B, $R_L = R_1 = 1.25$ ohm, and Using Texaco Code 499 EDM Fluid

Regular Machining Current Pulse

Scale:

Vertical	Horizontal
6.66 amp/div	20 microsec/div

b) Reverse Polarity, Elarc 90 on Hardtem B, $R_L = R_1 = 1.25$ ohm, and Using Texaco Code 499 EDM Fluid

Regular Machining Current Pulse

Scale:

Vertical	Horizontal
6.66 amp/div	10 microsec/div

c) Normal Polarity, Elarc 90 on Hardtem B, $R_L = R_1 = 1.25$ ohm, and Using Texaco Code 499 EDM Fluid

Figure 3.3 Typical Machining Voltage and Current Waveforms Observed When Correct Machining and a Coking Condition Occurs

by looking at Figure 3.4, that when the change occurred during a single discharge, there was a definite decay from the standard machining voltage, to a lower voltage and a corresponding rise in current. In other occurrences of this phenomena, the rise and decay of the pulse current and voltage exponential in form, indicating possible heating effects in the electrodes. When coking develops, consecutive current discharges occur in the same general location, causing an accumulative heating effect, that apparently results in the lowering of the gap machining voltage and the further formation of the coking growths.

Reverse Polarity

Electrode Materials:

Elarc 90 on Hardtem B - Texaco 499 Fluid

Scale:

a) Vertical - 10 Volts/Division
   Horizontal - 5 Milliseconds/Division

b) Vertical - 6.66 Amps/Division
   Horizontal - 5 Milliseconds/Division

Equivalent Load Resistance:

$R_L = R_1 = 1.25$ Ohm

Figure 3.4: Photograph of Gap Current and Voltage Waveforms that Converts from a Standard Machining Pulse to a Coking Pulse

The reason the discharges tend to accumulate in one small area is the key to determining why coking occurs. As was seen in Figure 3.2, the coking condition generally occurs at the edge of the electrode machining surface. Although with large machining surface areas, the condition can arise anywhere over the machining surface. Grachis[82] has shown that the least amount of fluid flushing occurs at the edges of the machining surface for the case of center pressure flushing. Therefore, the greatest amount of fluid contamination exists at the edges. As was shown in the previous photographs of the damage done to a workpiece because of the coking condition, the coking case usually occurs at the edge of the machining surface which suggests a possible relationship between the contamination level and coking.

In general, previous investigators have found several processes that cause the deposition of carbon upon a surface. Examination of these processes is worthwhile because they appear to be related to the coking process in EDM. Two such processes are the growth of carbon whiskers and the formation of pyrolytic carbon. Carbon whiskers have a very small diameter - about .01 to .020 microns[83] - and they are grown in a D.C. graphite arc under the high pressure of an inert gas. During the process, a carbon rod (anode) is allowed to vaporize and re-deposit upon a carbon block (cathode), but a detailed explanation of the process is not given and apparently not known. The carbon deposited on the block is termed by Bacon[84] as a "boule", in which the graphite whiskers are imbedded. The "boule" was observed to have a growth rate of about .5 inches per minute[84], which is roughly the

growth rate of many observed coking growths. Figure 3.5 shows a photograph of a graphite whisker made by Davis, et al.[85] Notice the marked similarity to Part b) of Figure 3.1, with the only major difference being the dimensions, i.e., the graphite whisker was about 1 micron across, while the coking growth can be as large as 1/8 to 1/4 inch across. The coking growths, however, occur on both electrode surfaces, and when the electrode materials are copper and steel, neither electrode can provide sufficient carbon to sustain the coking growth. Therefore, another process must also have been taking place in the EDM gap spacing.

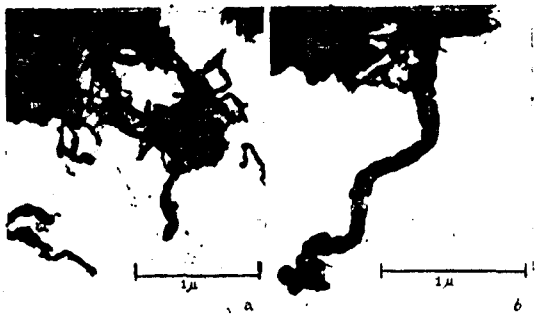

(a) Carbon growth in firebrick after 30 hr. in carbon monoxide at 450° C., showing mass of characteristic vermicular threads. (b) Large vermicule formed by coalescence of smaller threads

Figure 3.5: Photomicrograph of a Graphite Whisker from "An Unusual Form of Graphite" by Davis, Swanson, and Rigby - Published in "Nature" Volume 171, 1953, pg. 756.

Another process which may aid in explaining the coking process is the method of producing pyrolytic carbon. Pyrolytic carbon films are produced over the surface of a suitable refractory and chemically stable object placed within a heated enclosure in the presence of a hydrocarbon gas or vapor. The film is the result of pyrolysis, or "cracking", or thermal decomposition of the gas or vapor. The temperatures involved are in the range

from 975°C. to 1300°C.; the temperature is indicated as the most important condition which determines the rate of carbon deposition.[86] The hydrocarbon gas used most often in this process is methane, although others are used. As can be seen in Table 3.1, several researchers have found appreciable quantities of methane and other hydrocarbon gases present in the EDM vapors.

Neither of the previously described carbon growth processes occurs under the exact conditions that are encountered in the EDM machining process. The description given of the pyrolytic process makes no mention of voltage polarities or an arc being involved in the process, and the graphite whiskers process descriptions make no mention of the effect hydrocarbon gas would have upon the growth mechanisms. Since both processes require conditions that are known to be present in the gap spacing, it seems logical to conclude that some combination of the two growth mechanisms occur during the EDM coking condition.

Since the coking conditions is accompanied by a concentration of discharges at the same physical location, it can be expected that thermal effects would cause a lengthening of the recovery time. Coking causes an accumulative heating effect, which in itself would cause the recovery times to increase because of longer thermal recovery times. The coking growths become the effective electrodes. Moreover, the thermal effects are very strong owing to the small diameter of the growths. The growths are carbon in composition and, therefore, will produce a higher temperature ionized gas column than most other electrode materials. One would expect that the effects of the higher temperatures and longer electrode thermal influence would combine to cause longer recovery times.

Compound	Ref. 87 Berghausen (EDM)	Ref. 88 Perchuro (Pulsed Arc)	Ref. 89 Grodzinski (Low Current)	Ref. 90 Chepilov (.3 msec Pulse)
Hydrogen (H_2)	1 - 2%	58%	56%	68.8%
Methane (CH_4)	8 - 9%			3.8%
Acetylene (C_2H_2)	23 -24%	30%	32%	
Ethylene (C_2H_4)	38 -40%	7% (C_nH_{2n})	8.5% (C_nH_{2n})	
Ethane (C_2H_6)	10 -11%	5% (C_nH_{2n+1})	3.5% (C_nH_{2n+1})	
Propane (C_3H_8)				
Other				11.4%
Unidentified	12 -20%			15.8%

Table 3.1: Typical Composition of Gases Evolved from Various Types of Discharges

Normally on an EDM machine, the coking condition develops most frequently when high currents, long pulse durations, and high duty cycles are employed. These conditions proved to be too taxing for the experimental apparatus used for measuring the recovery times. However, it was discovered, that a coking case would occur at lower settings, provided the stalagmite and stalactite growths were induced by some other means. It was also discovered that these growths could be produced by using a small 'seed' piece of a previous coking growth. Moreover, when a 'seed' is placed in a conventional EDM machining gap, a coking condition cannot be avoided. The 'seed' procedure was successfully used to produce coking with all the graphite and carbon electrodes tested on various metal workpieces. However, absolutely no success was achieved when copper was used as the tool electrode even though coking has been observed with a

copper electrode on a commercial EDM machine. These findings regarding seeding suggests another way that the coking case might develop in a machining operation. Poorly filtered dielectric fluid could possibly contain particles from previous coking growths, which, when forced through the machining gap could cause the coking condition.

The maximum current capabilities of the experimental apparatus limited the recovery measurements to the investigation of a 'cold coking case' as opposed to the case where many discharges occur in rapid succession and heat up the coking growths. The test procedure was similar to that used previously, except in this instance, each series of measurements were begun at long pulse durations and decreased to the shortest instead of vice versa. The longer pulse durations acted to maintain the growth situation initially while low pulse durations slowly eliminated the coking growths.

The coking condition was investigated by using several different workpiece materials and various tool graphites immersed in different EDM fluids, with both normal and reverse polarity. The recovery time results are very similar in all cases tested. This similarity can be explained by certain features of the coking condition. Whenever coking was observed, the coking growths and not the base metal were actually acting as the opposing electrodes; the original electrode surfaces merely served as an electrode holder of sorts. Since the electrode termini of the discharge were similar, if not the same, in all polarity cases, the results would be expected to be similar. The reverse and normal polarity results using Elarc 90 on Hardtem B with Texaco Fluid,

Poco 3 on #416 Steel with Texaco Fluid, and Elarc 90 on #416 Steel with pure silicone fluid, are shown in Figures 3.6, 3.7, 3.8, 3.9, 3.10, and 3.11, respectively. A quick comparison of these results shows that they were very similar and all exhibited a constantly increasing recovery time with increasing pulse duration. The recovery times were also much longer than those found previously, which was again caused by the electrode configuration - a carbon growth on another carbon growth. The results with pure silicone fluid were somewhat difficult to obtain. Numerous attemtps were made to establish a coking condition, using all the previously mentioned methods, but with no success. A coking condition would not form with silicone as it did with EDM fluid. It was necessary to remove the silicone fluid and to establish the coking growths using a hydrocarbon fluid. The electrodes and fluid containers were then cleaned to eliminate any traces of hydrocarbon fluid without disturbing the coking growths. The pure silicone fluid was then introduced and the coking condition was found to maintain itself in silicone once the growths were established. The recovery results were again similar to those with hydrocarbon fluid. An analysis of the gases created when a discharge occurs under silicone fluid was not available, but a glance at the chemical formula for silicone shown previously, suggests the strong possibility of hydrocarbon gases.[88] The presence of hydrocarbon gases would support the growth mechanisms commented on earlier.

The coking phenomena is undoubtedly the worst condition that can occur at the machining gap owing to its extremely long recovery times and the damaging results. However, the recovery

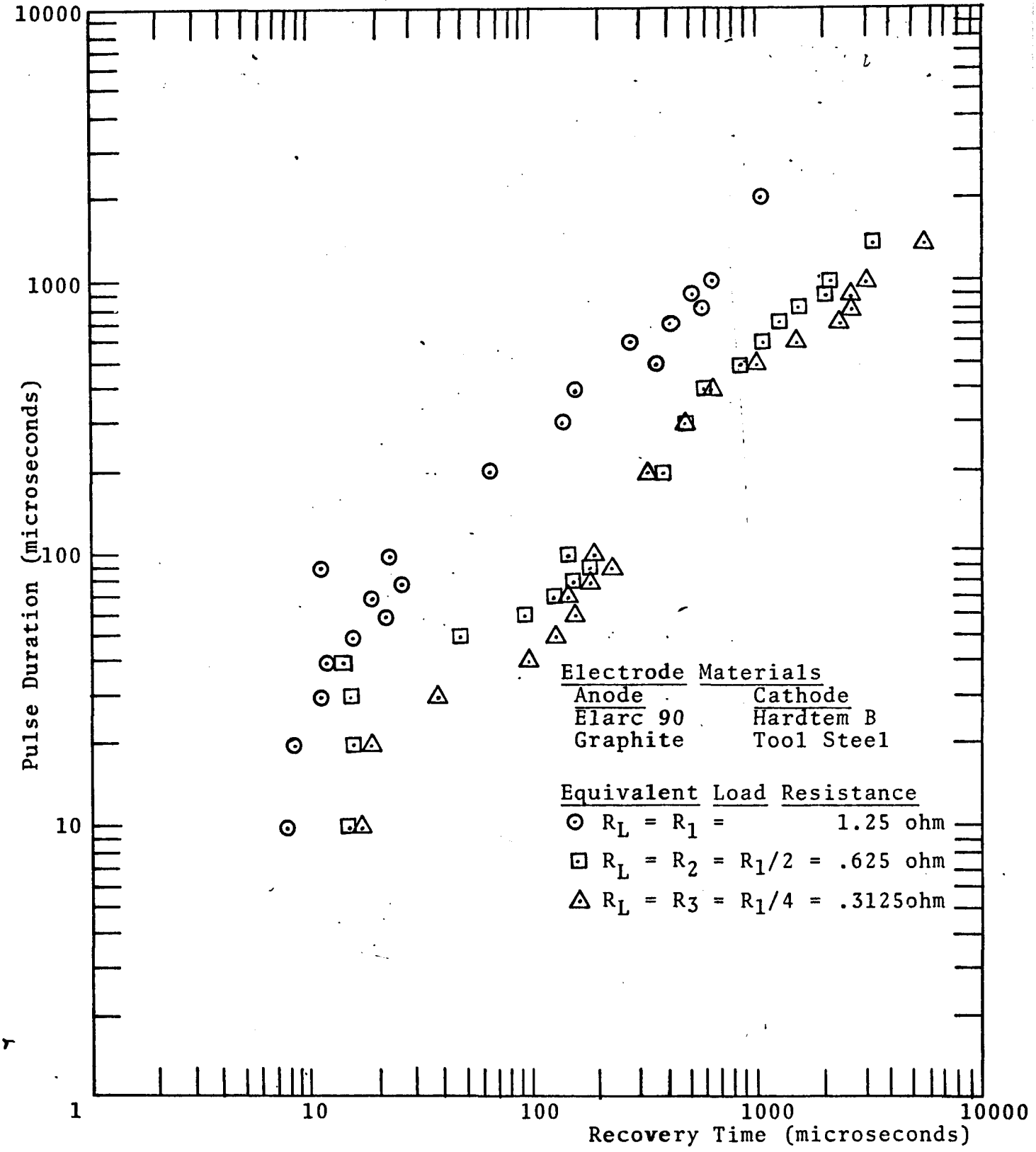

Figure 3.6 Recovery Times for Elarc 90 on Hardtem B Tool Steel in Reverse Polarity with a Coking Condition and Texaco Code 499 EDM Fluid

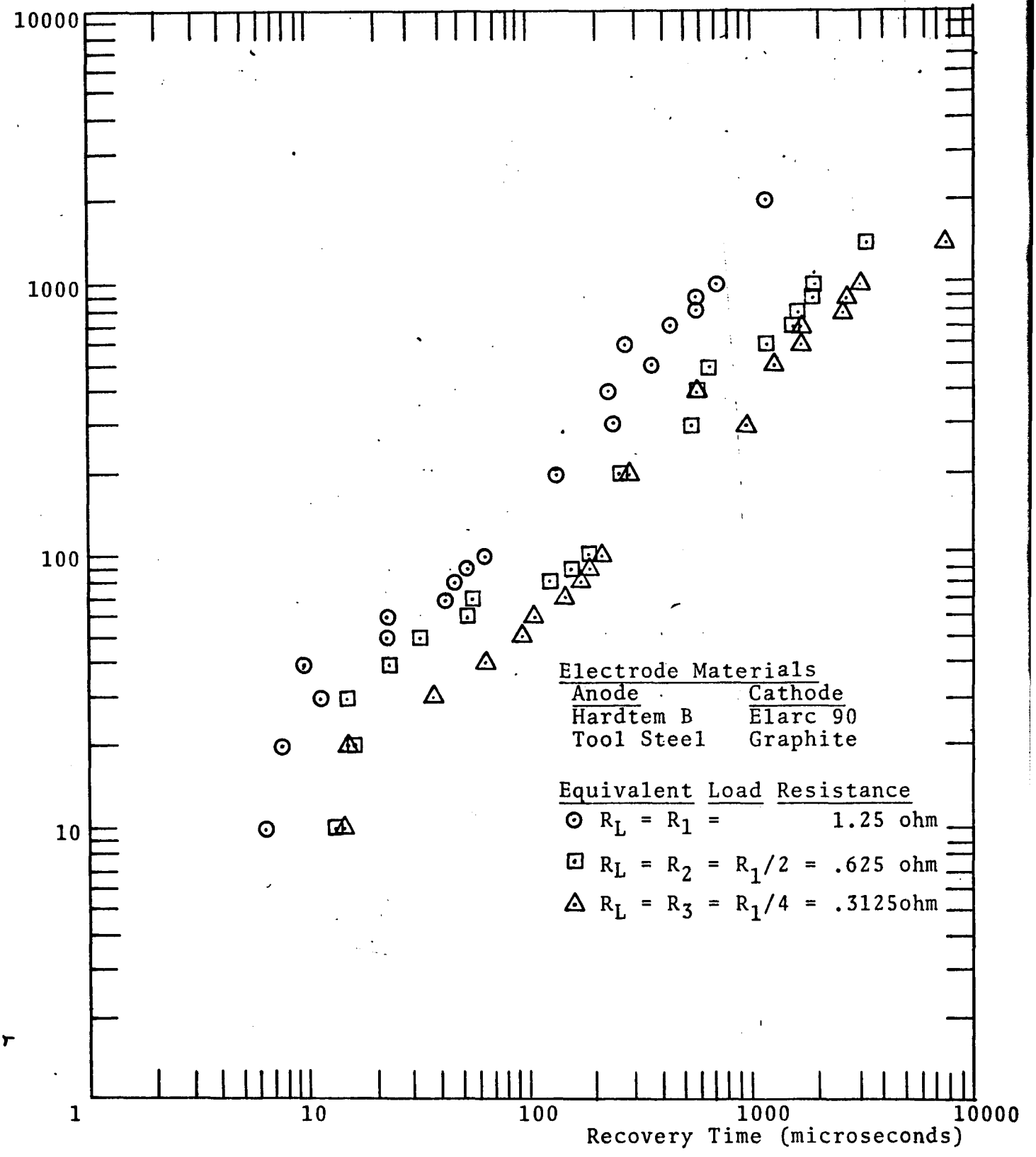

Figure 3.7 Recovery Times for Elarc 90 on Hardtem B Tool Steel in Normal Polarity with a Coking Condition and Texaco Code 499 EDM Fluid

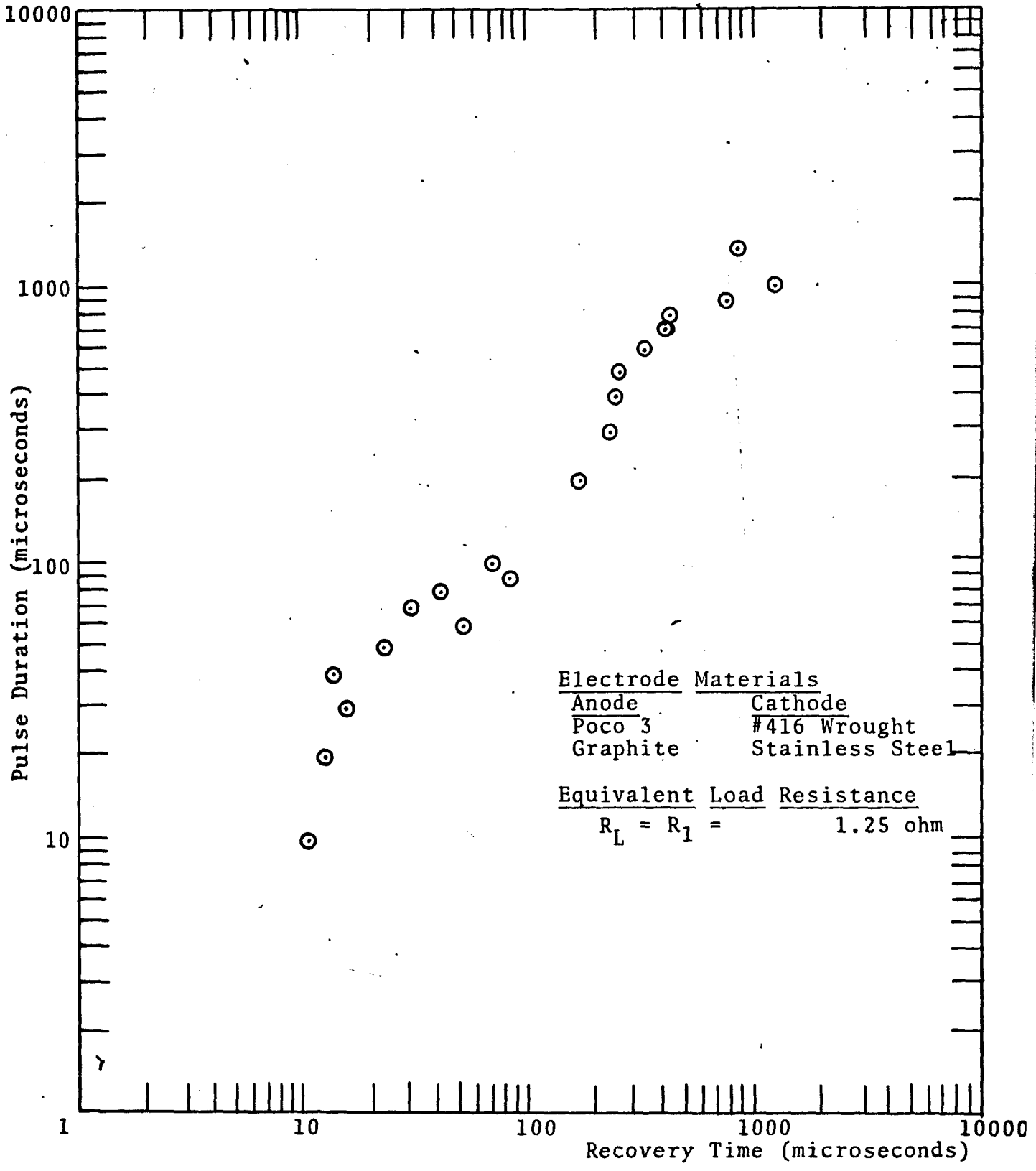

Figure 3.8 Recovery Times for Poco 3 on #416 Wrought Stainless Steel in Reverse Polarity with a Coking Condition and Texaco Code 499 EDM Fluid

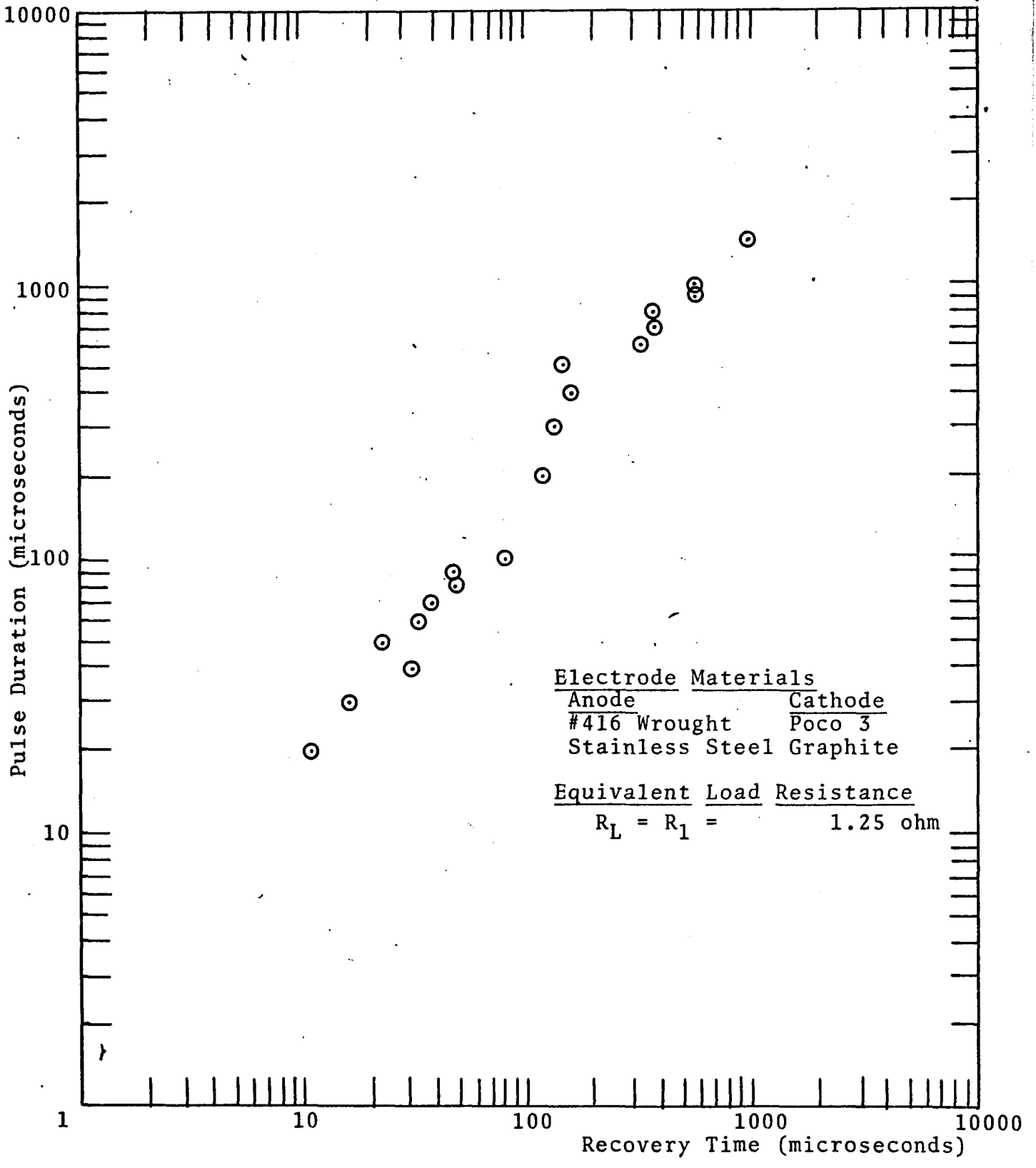

Figure 3.9 Recovery Times for Poco 3 on #416 Wrought Stainless Steel in Normal Polarity with a Coking Condition and Texaco Code 499 EDM Fluid

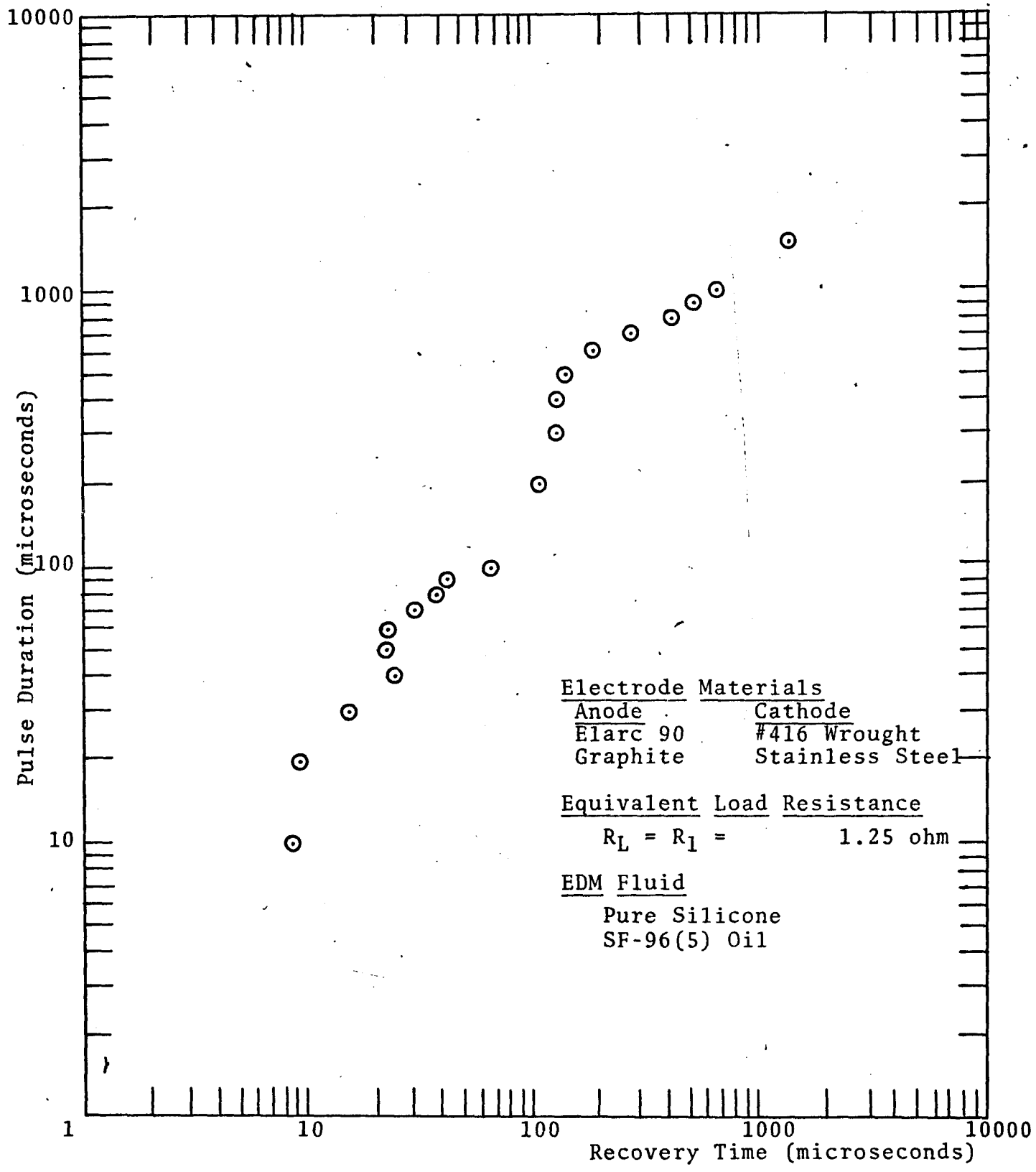

Figure 3.10 Recovery Times for Elarc 90 on #416 Wrought Stainless Steel in Reverse Polarity with a Coking Condition and Pure Silicone SF-96(5) Oil

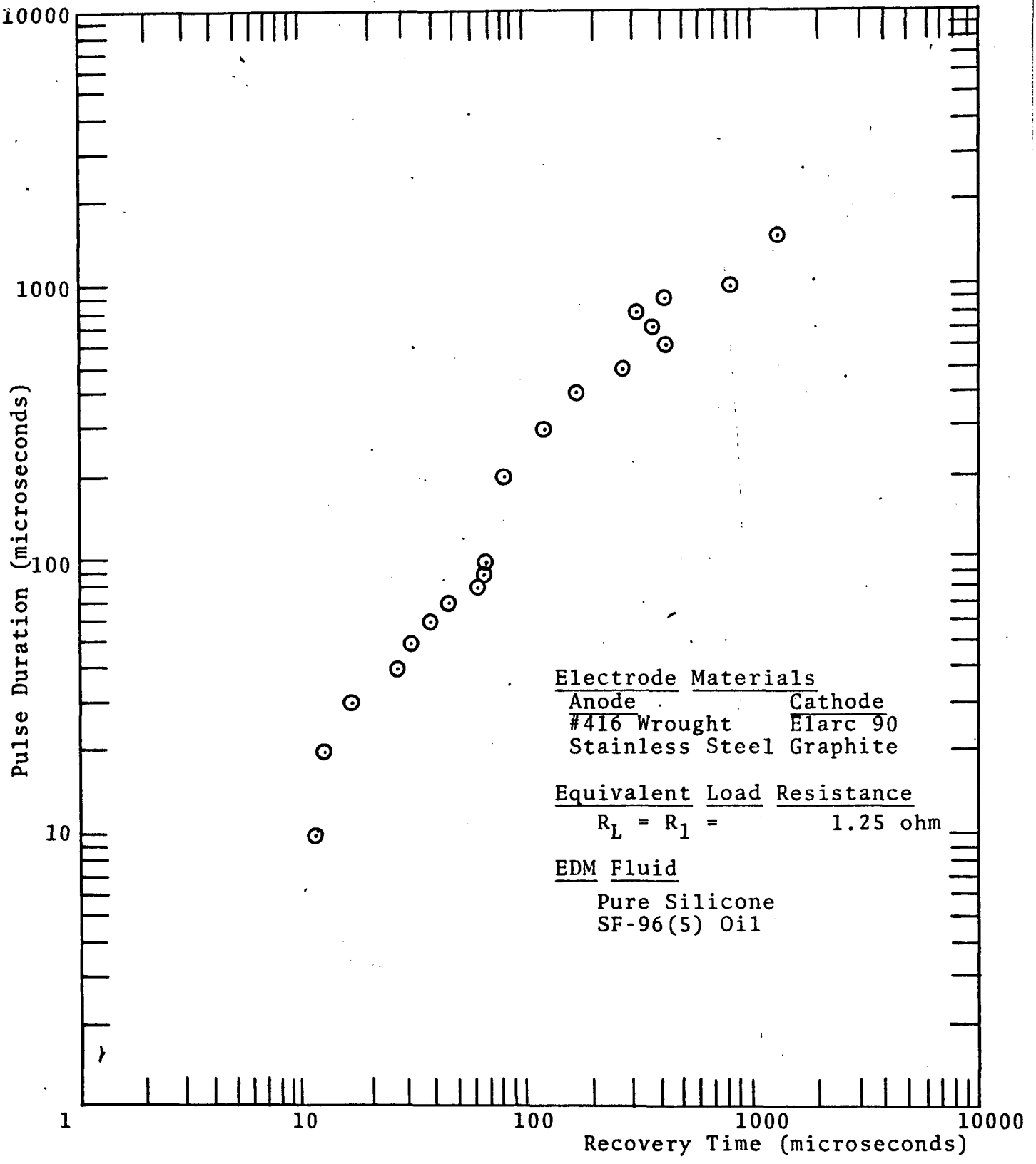

Figure 3.11 Recovery Times for Elarc 90 on #416 Wrought Stainless Steel in Normal Polarity with a Coking Condition and Pure Silicone SF-96(5) Oil

times required for an actual machining operation may be as much as 5 or 6 times longer than the recovery times found with the experimental apparatus because of the close succession of discharges in a machining condition. The rapid succession of discharges would produce a more cumulative heating effect than was observed in these tests. The results also indicate that the type of materials used initially does not affect the coking condition except that certain materials produce the condition more easily than others. Very little, if any, difference in recovery times occurred when the electrode materials were changed, when the fluid was varied, or when the gap polarity was reversed.

B. Formation of a Burr on the Workpiece Surface

Besides the coking phenomena there is another machining effect that has also proved detrimental to the EDM process. This other condition has, for want of a better name, been termed "burring". The name resulted from the nature of the workpiece damage that occurs. Figure 3.12 illustrates the damage. The

The Top Three Cavities Illustrate the Burring Damage as Compared to Burr Free Cavities Below Them

Figure 3.12: Photograph of the Workpiece Damage Done When Burring Occurs During a Machining Operation

top three machining impressions had a "burring" condition that occurred during the machining operation, while the lower four cavities did not. Burring seems to occur most frequently when normal polarity is used with graphite as the tool electrode material.

Prior to the accumulation of the recovery time data presented in the previous chapters, several tests sequences were run using the prototype EDM machine in an attempt to gain some insight into the "burring" phenomena. Figure 3.13 and Table 3.2 show the results of one of those test sets. The duty cycle was varied from about 20% to 80% to determine if the duty cycle affected the burring phenomena. The equivalent load resistance was .4166 ohms, which indicates that the peak current output was between that of the $R_L = R_2$ and $R_L = R_3$ used for the recovery time tests (60 - 70 amp pulse). From Figure 3.13, it can be seen that "burring" occurred on the fifth through the twelfth machined cavity, although the effects are minor on the eighth and tenth cavity for some unknown reason. The "burring" first occurred with a duty cycle of approximately 35%. If the "burring" is a result of the application of a second discharge before the recovery interval of the first is completed, as was expected, then the 35% duty cycle implies that the recovery time for the 8 microseond discharge, using R_L = .4166 ohms is about 14.5 microseconds. This implied recovery time is in close agreement with the recovery times given in Chapter II for Elarc 90 on #416 steel in normal polarity. Refer to Figure 2.11 which indicated the measured recovery time is approximately 13 microseconds or slightly higher.

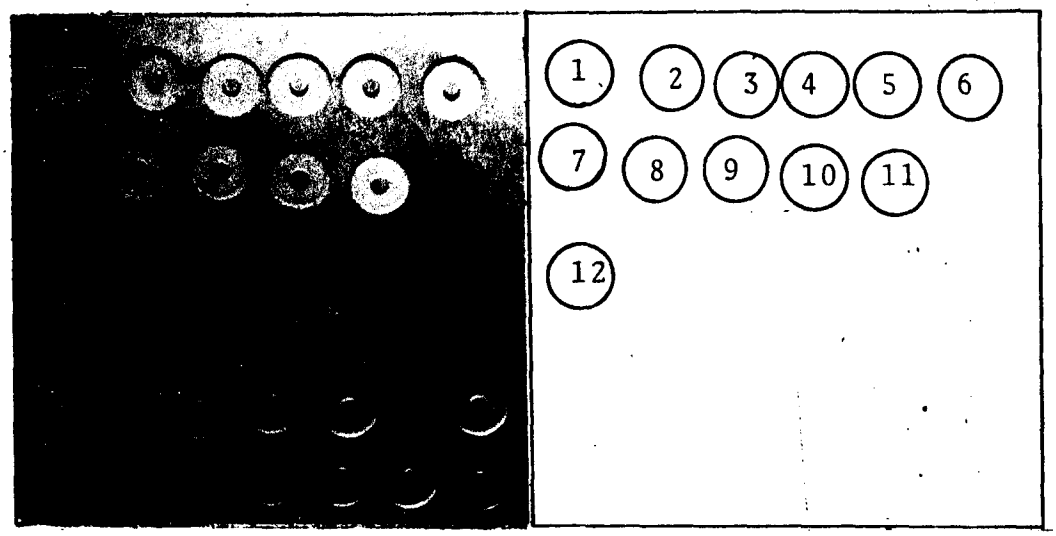

Figure 3.13: Test Cavities Produced by Changing the Duty Cycle from Low to Very High Values

Crater No.	Duty Cycle	Minimum Off Time microsec	Average Current Amps	Average Gap Voltage Volts	Machining Time Minutes
1	20%	32	1.0	90	10
2	25%	24	1.0	85	10
3	27%	21.6	1.5	85	5
4	30%	18.7	1.75	85	5
* 5	35%	14.5	2.0	85	5
6	40%	12	2.5	85	5
7	50%	8	4.0	85	5
8	60%	5.3	5.0	85	5
9	70%	3.4	6.0	85	2
10	75%	2.7	7.0	85	2
11	80%	2	8.0	90	1
12	50%	8	4.0	85	5

* Burring Observed and Low Machining Voltage Wave Forms Observed on Oscilloscope

Table 3.2: Machining Data Corresponding to the Machining Cavities Shown in Figure 3.13

Tests were also conducted to determine if the act of seating* the electrode surfaces influenced the "burring phenomena, since the majority of burring seemed to occur at the edge of the entrance hole in the workpiece. The results can be seen in Figure 3.14 and Table 3.3. Each machining cavity was first seated using a low duty cycle setting for about 5 minutes, then the test duty cycle was set and the test cavity completed. The burr is much less noticeable using this procedure, but it is still detectable from the fourth through the tenth cavity as before, which agrees closely with predicted recovery data again.

The limited testing described above indicates that the onset of burring corresponds to repeatedly interjecting a discharge into the recovering interval of the previous discharge. Additional correlation between the measured recovery times and the minimum 'off' times commonly used in the EDM utilization art was attempted. The minimum 'off' times were obtained by performing numerous machining tests at different duty cycles. Figures 3.15 and 3.16 show the minimum 'off' times required when the graphite-on-steel combination is used in reverse and normal polarity, with various current settings. The results with graphite are remarkably similar to the recovery time results with Elarc 90 (Figures 2.9 and 2.11). The data points show a very slight increase of minimum 'off' times for low

---

* Seating refers to the initial break into the workpiece material by the tool electrode, until the entire frontal surface of the tool has machined into the workpiece.

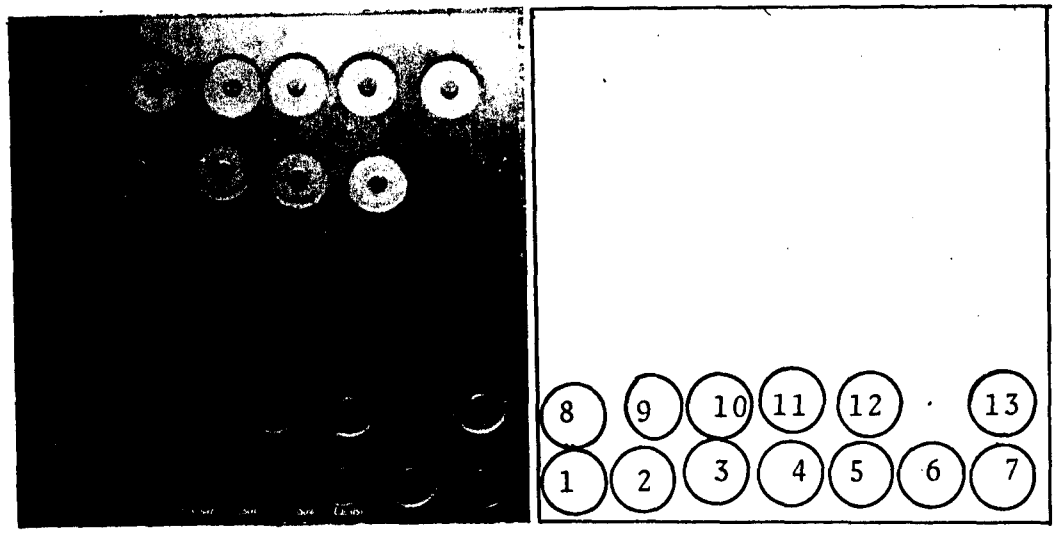

Figure 3.14: Test Cavities Produced by Changing the Duty Cycle from Low to Very High Values with a 5 Minute Seating Time at a Low Duty Cycle

Crater No.	Duty Cycle	Minimum Off Time microsec	Average Current Amps	Average Gap Voltage Volts	Machining Time Minutes
1	20%	32	.25	60	10
2	25%	24	.5	55	5
3	30%	18.7	1.0	50	5
* 4	38%	13.0	1.5	40	5
5	50%	8.0	2.0	45	5
6	55%	6.5	2.5	50	5
7					
8	60%	5.3	3.0	80	5
9					
10	70%	3.4	3.5	50	5
11	75%	2.7	4.0	55	5
12	80%	2.0	4.5	55	5
13					

* Burring Observed

Table 3.3: Machining Data Corresponding to the Machining Cavities Shown in Figure 3.14

pulse durations; followed by an increasing minimum 'off' time as the discharge duration is increased to higher pulse durations, which was the same graphic form found with the recovery time data. The rate of increase of the minimum 'off' time is also very similar to the rate of increase of the respective Elarc 90 recovery times. In the low pulse duration range, the minimum off-times are between 20% and 30% shorter than the measured recovery times. At longer durations, the minimum 'off' times were approximately where the current amplitudes indicated they would have been had the recovery times been measured at that amplitude.

The comparison of the recovery time results with the minimum 'off' times for the case of copper-on-steel (Figure 3.17 and 3.18) is not as encouraging as the comparison with graphite-on-steel. The rate of increase and the shape of the minimum 'off' time curve and recovery time curve are similar in reverse polarity. However, the minimum 'off' times results are consistently smaller than the recovery times.

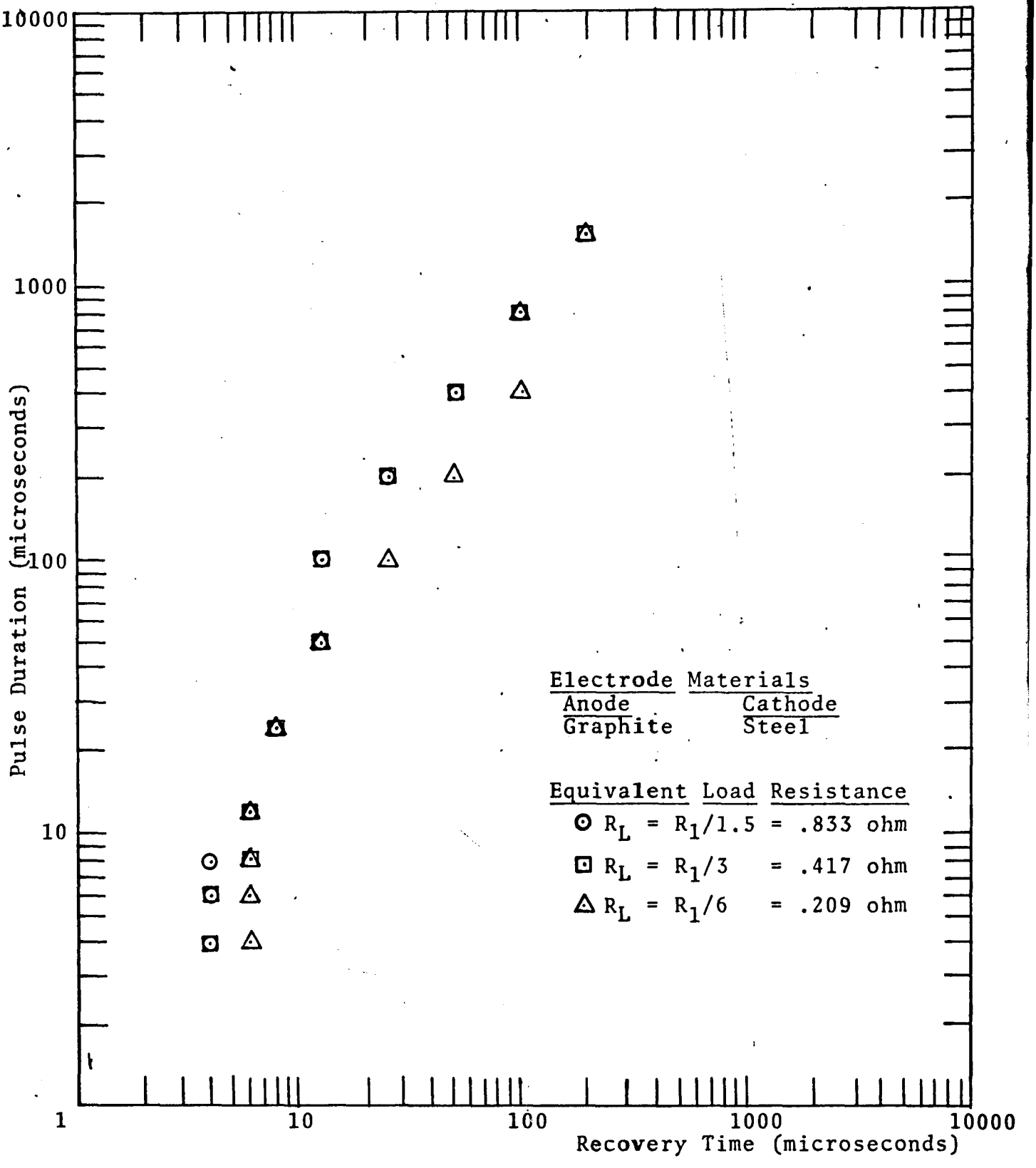

Figure 3.15 Minimum Off Times Indicated by Machining Test Results When Using a Graphite on Steel Electrode Combination in Reverse Polarity

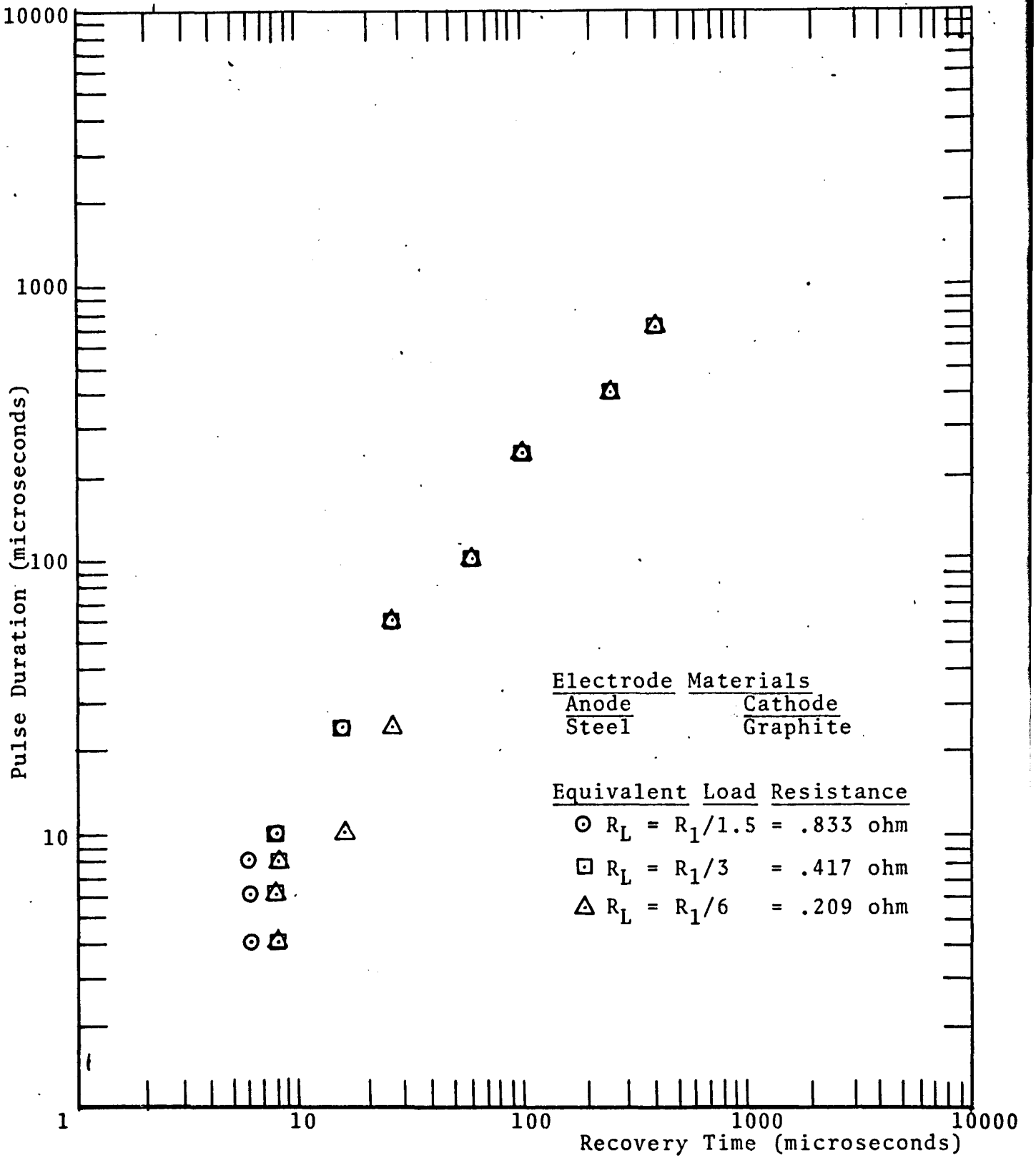

Figure 3.16 Minimum Off Times Indicated by Machining Test Results When Using a Graphite on Steel Electrode Combination in Normal Polarity

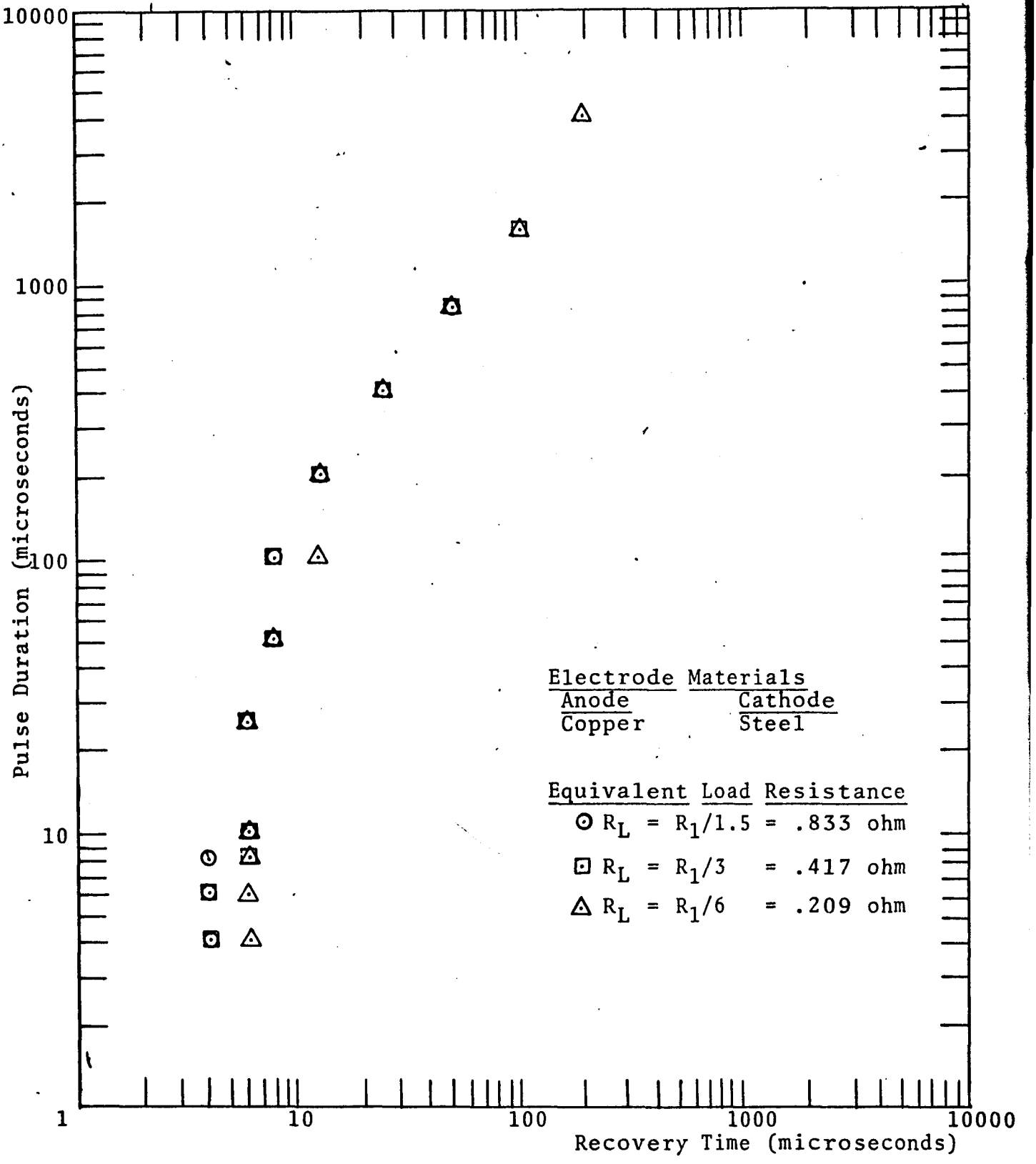

Figure 3.17 Minimum Off Times Indicated by Machining Test Results When Using a Copper on Steel Electrode Combination in Reverse Polarity

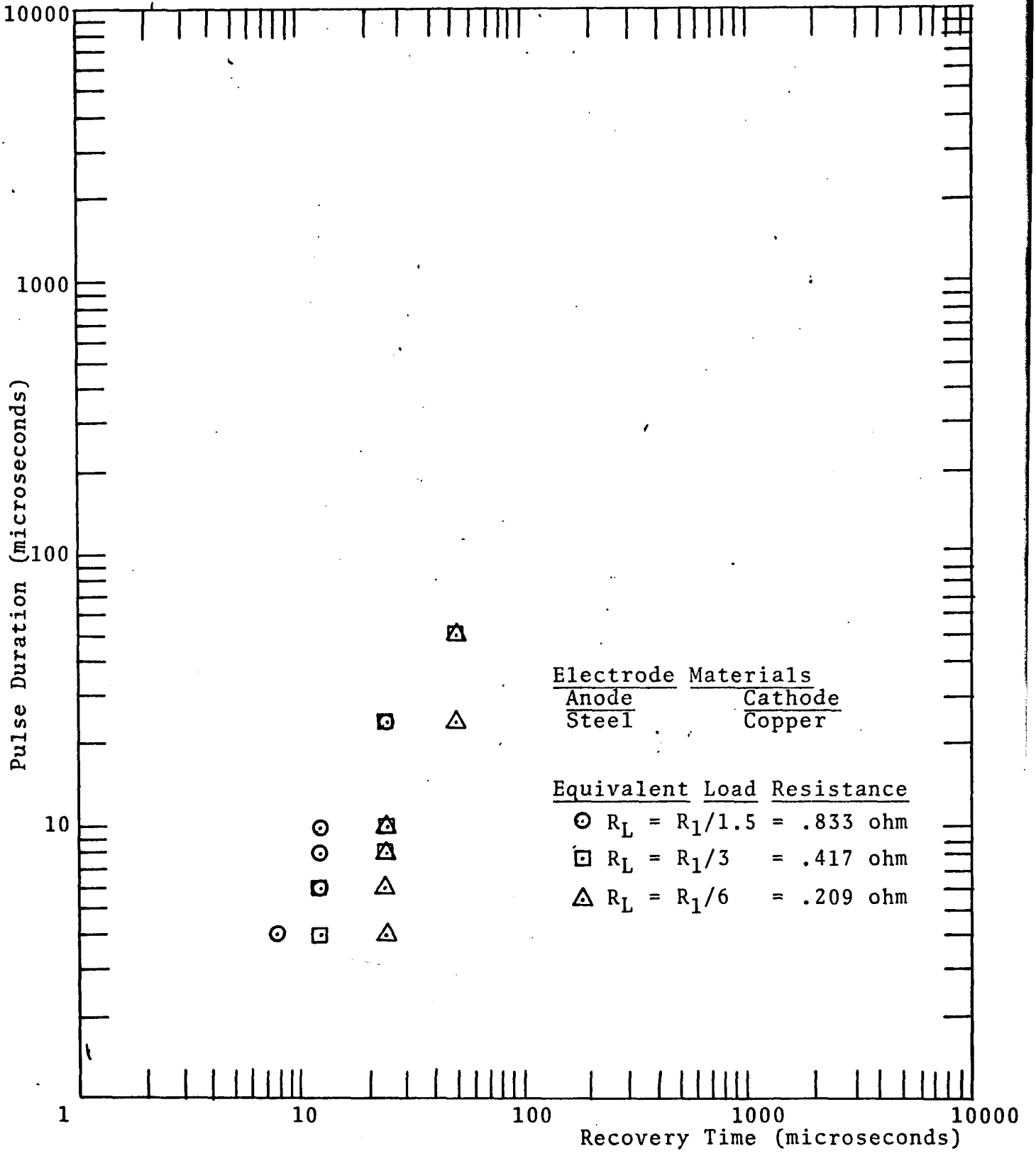

Figure 3.18 Minimum Off Times Indicated by Machining Test Results When Using a Copper on Steel Electrode Combination in Normal Polarity

CHAPTER IV

GENERAL CONCLUSIONS ABOUT THE INFLUENCE OF THE RECOVERY PROCESS AND SUGGESTIONS FOR FUTURE STUDY

A. Conclusions Relating to the EDM Machining Process and the Recovery Time Data

The conclusion indicated by the recovery times seems to be that there should be a minimum 'off' time between successive discharges in the EDM process, if damaging effects are to be avoided. This minimum 'off' time implies that there should be a maximum safe duty cycle for any particular pulse duration setting which would be governed by the recovery time required at that particular setting. The recovery times indicate that the maximum duty cycle is also electrode material dependent. Due to the large number of electrode material combinations possible, it seems best that any EDM machine should then have a great versatility. The more flexible machine would allow the operator to choose his own setting to best complete the job at hand. Also, large quantities of test data should be taken and made available in order to suggest possible settings to the operator for his particular electrode material combination. The older EDM machines, with a limited number of duty cycles and current settings are therefore, not versatile enough to meet all the possible current, pulse duration, and duty cycle settings that may be required, although, several of the newer machines do have these capabilities.

There were several conclusions reached regarding the effects of various parameters upon the recovery times during the course of this study. These general remarks and their relationship with the EDM process are:

(1) For any particular electrode material combination tested, the recovery interval increased as the pulse duration was made longer, and as the amplitude of the current discharge was increased. The increase in recovery times can be attributed to the increased energy available to heat the electrode at the higher pulse durations and current amplitudes. The more heat added to the electrode materials, the more that must be removed. The longer the time necessary to cool the electrodes, the longer the gases in the gap space will take to cool, expecially at the short gap spacings dealt with in EDM.

(2) For the materials tested here, the recovery times measured for normal polarity were always somewhat longer than the recovery times for reverse polarity. When carbon and graphite were used, this phenomena could be attributed to the higher discharge temperatures and longer thermal recovery associated with them, which cause the spark column gas temperatures to remain higher or ionized longer than with copper. When copper was used these differences were only slight and were probably caused by the increased current amplitudes found in normal polarity. (See Figure 1.8)

(3) Carbon and graphite electrode materials had associated with them longer recovery times than did metallic materials, such as copper, provided the pulse duration was long enough.

For pulse durations below 100 microseconds, the metallic and non-metallic materials had similar recovery times, but above that duration, the differences were very apparent.

(4) The recovery times associated with various different electrode material combinations were very similar for pulse durations below 100 microseconds, but above that duration the recovery data was noticeably different. The different recovery times found, with the various electrode combinations, could be attributed to the different electrical and thermal properties of each material. The specific heat, or heat capacity, of the materials seemed to be the dominant material property at the pulse duration used. These properties all affect the gap gas temperature which indicates the degree of ionization in the gap. The more or less constant recovery times found at lower pulse durations can possibly be attributed to lack of electrode involvement in the thermal recovery of the gap gas temperature.

(5) The various different brands of hydrocarbon fluid and silicone-hydrocarbon mixtures had no significant effect on the gap recovery time. The basic similarity of these fluids was attributed to the probable similarity of the gap gases generated when a discharge occurred in them. The pure silicone fluid, however, did cause the recovery times to be shorter than the reference data. This difference was probably caused by the difference in the gap gases produced by a discharge.

(6) There were definite differences in recovery times found when various graphite and carbon tool electrodes were

investigated. The physical properties of the various materials were not generally available for comparison purposes. Therefore, the only general conclusion that can be drawn from the materials tested is that some molded graphite materials tended to have a longer recovery time than other types of molded electrode materials.

(7) When the coking condition was present in the gap space, the recovery times indicated that it required the longest time interval for recovery of all the materials or conditions tested. The coking case was found to occur more easily when certain materials, graphite or carbon cathode electrode and gray cast iron as the anode electrode, were used, while the recovery times associated with coking appeared to be independent of the electrode materials used. The longer recovery times and the independence of the electrode materials can be attributed to the stalagmite and stalactite growths that occur with the coking condition. These carbonacious growths then dominate the thermal recovery of the gap.

(8) Pure silicone fluid appeared to act as a deterrent to the initiation of the coking condition, but once the condition was established in the fluid, the growth process continued as it had with the hydrocarbon fluids.

(9) There appeared to be an increase in the recovery time when the condition of the gap space was changed from clean uncontaminated EDM fluid to one that was highly contaminated with machining debris. This result can probably be attributed to the alteration of the thermal properties of the gap

space as a result of the large amount of contamination and changes in the surface properties of the electrode materials. (10) The condition referred to as 'burring' seems to be linked to the recovery interval and preliminary tests on an EDM machine seems to indicate this connection, but more extensive testing is needed before any conclusion can be reached. The burring appears to be the result of re-application of a potential power pulse prior to sufficient gap recovery time which results in the discharge occurring in almost the exact location as the previous pulse, causing a larger than desired crater.

B. Suggestions for Future Work

There are several interesting additions and continuations of the work discussed in this thesis which would be informative. They are:

(1) A series of corroborating tests should be performed on a conventional EDM machine, at varying pulse durations, current settings, electrode configurations and materials, and duty cycles. The machine should be fitted with an electrode combination used in the recovery time tests and allowed to machine a test cavity, using a certain pulse duration and current setting in the range investigated and a certain duty cycle. Then a series of tests should be conducted at different duty cycle settings that vary from extremely high values, (i.e., successive pulses will occur before the predicted gap recovery interval was completed) down to low values where the gap has more than ample time to recover, and all other parameters are held constant. Any

changes that occur from test to test should be noted: i.e., if burring occurred, if a coking condition occurred, machine stability, gap voltages, currents, surface finishes, etc. The duty cycle at which detrimental effects no longer occur would then indicate a minimum off time. It would also be interesting to determine the influence forced fluid flushing might have on these tests and the recovery time data.

(2) An extension of the recovery time data to very long and very short pulse durations would also be interesting. The long pulse data could be used to determine how closely resistive recovery data corresponds to the voltage recovery data investigated by many arc researchers.

(3) The effects of series inductance and shunt capacitance on recovery times might also prove interesting and could possibly explain why the minimum 'off time'data shown in Chapter III suggested shorter recovery times in certain instances than were found in this investigation.

(4) Another interesting project would be a computer simulation of the recovery interval to gain a more complete understanding of what is occurring in the gap spacing during the recovery interval.

APPENDIX A

CIRCUIT DETAILS FOR THE EXPERIMENTAL APPARATUS USED

This appendix presents a detailed description of the circuits used to obtain the recovery time data presented in this study. The schematics of the main circuit elements contained in the block diagram of Figure 1.5 will be shown in this section.

The pulse generator used to produce the single discharges and the repetitive discharges was a Burroughs Corporation wide range pulse generator. The delay units used were also made by the Burroughs Corporation. They were a coarse delay unit No. 1301 and a fine delay unit No. 1302.

The flip-flop circuitry and its accompanying buffering stages are shown in Figure A-1. It is designed to have two lines of input information. Input No. 1 is the main trigger input, but its function is dependent on the conditions at the gap, which are monitored according to Input No. 2. Input 2 prevents the flip-flop from changing state until the machining gap voltage indicates to the Schmitt trigger circuitry that the conditions are suitable for a discharge to occur.

The Monostable Multivibrator 1 and 2 shown in the block diagram have identical curcuitry, except No. 2 has a set 1-microsecond output pulse duration, that is used to trigger the checking circuit. No. 1 has a variable output duration that is used to trigger the checking circuit. No. 1 has a variable

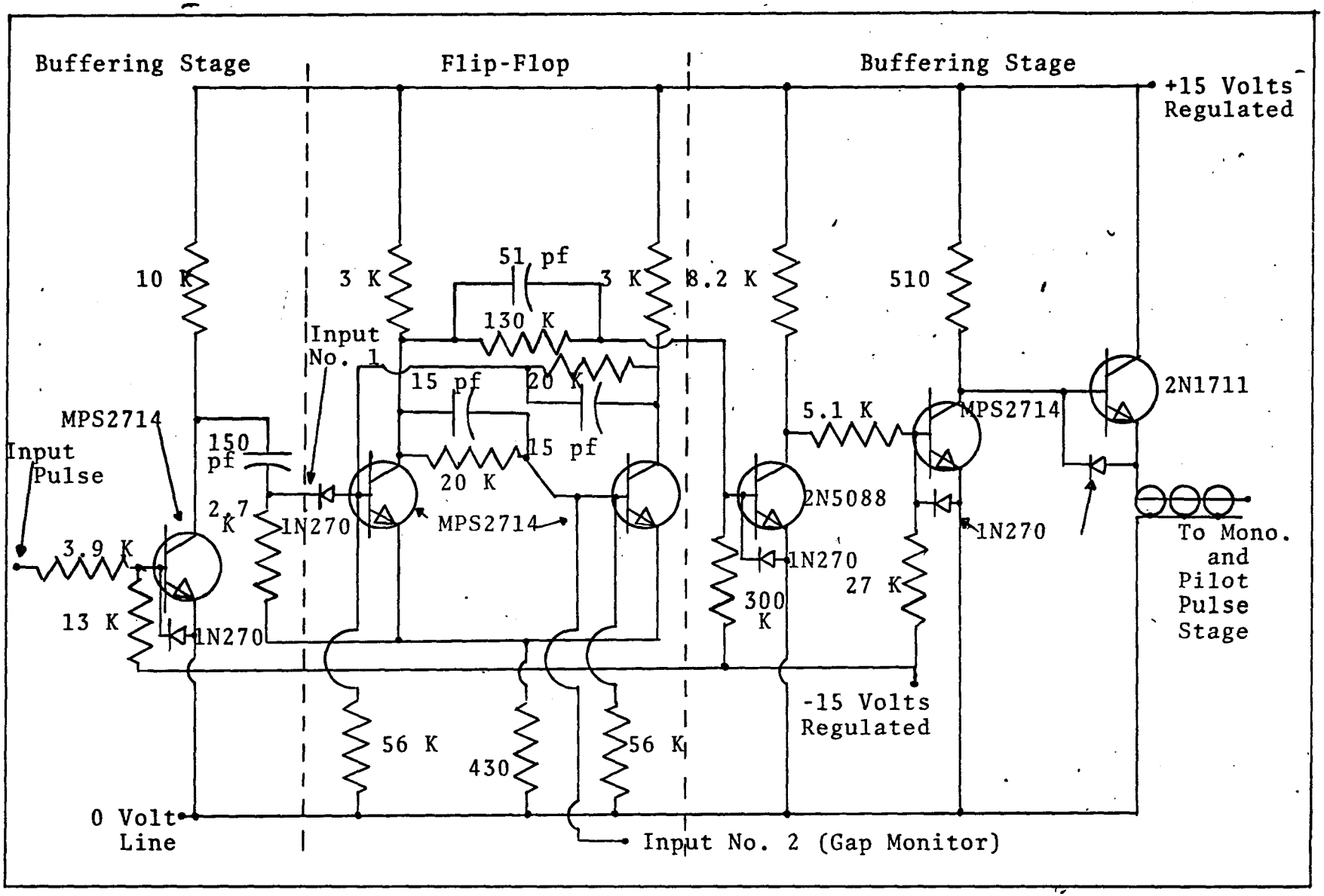

Figure A-1 Buffering Stage and Flip-Flop Stage Circuitry

output duration that is amplified and used to produce the power discharges at the machining gap. The circuitry is very similar to that shown in the General Electric Transistor Manual[91]

The pre-amp and power amp circuitry was constructed by using standard saturated switching design and high frequency transistors to provide fast switching. There were eight identical stages used in the power gap to provide the variable output current pulses.

The circuitry used to produce the breakdown pulse is shown in Figure A-2. The circuitry uses a supply voltage of 190 volts. The input signal is received from the buffered output of the flip-flop. Since the flip-flop changes state when the machining gap broke down, the pilot pulse will turn off almost immediately after breakdown and allow only the power discharge to commence.

The gap-sensing circuitry which consisted of an integrator and a Schmitt trigger, is shown in Figure A-3. The Schmitt trigger is designed to trigger between -9 and -20 volts, in order to determine when a discharge is taking place or when the gap is shorted. Only if the Schmitt trigger output is off, will the flip-flop be able to change states and thereby initiate another discharge. The integrator circuit is used to delay the trigger of the Schmitt to insure that the power pulse has actually started before the flip-flop and pilot pulse is turned off.

The previously discussed circuitry has associated with it a certain amount of leakage current which interfered with the measurement of recovery time. To eliminate the effects of this leakage, a gap shorting circuit was added across the machining

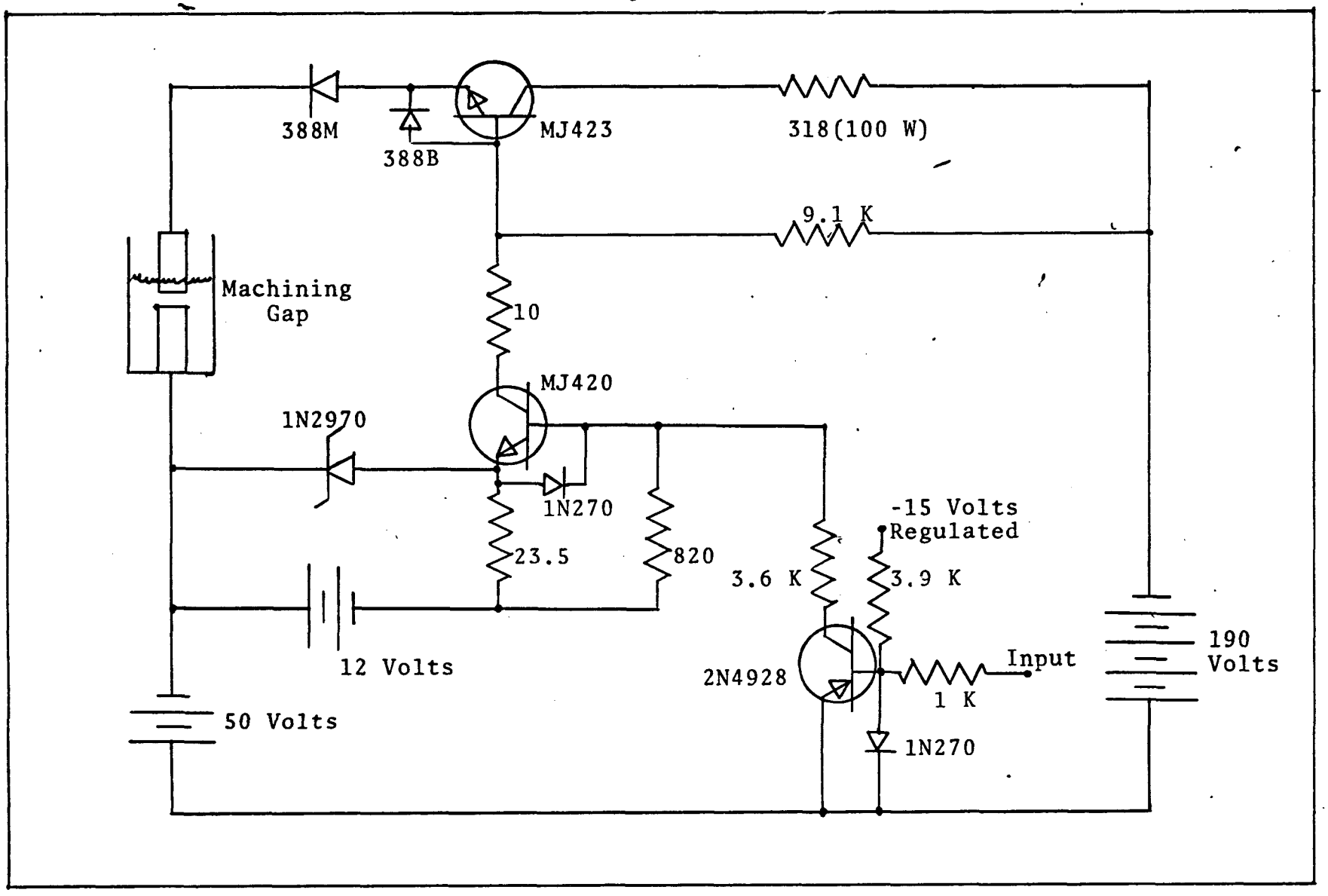

Figure A-2 Pilot Pulse Breakdown Circuitry

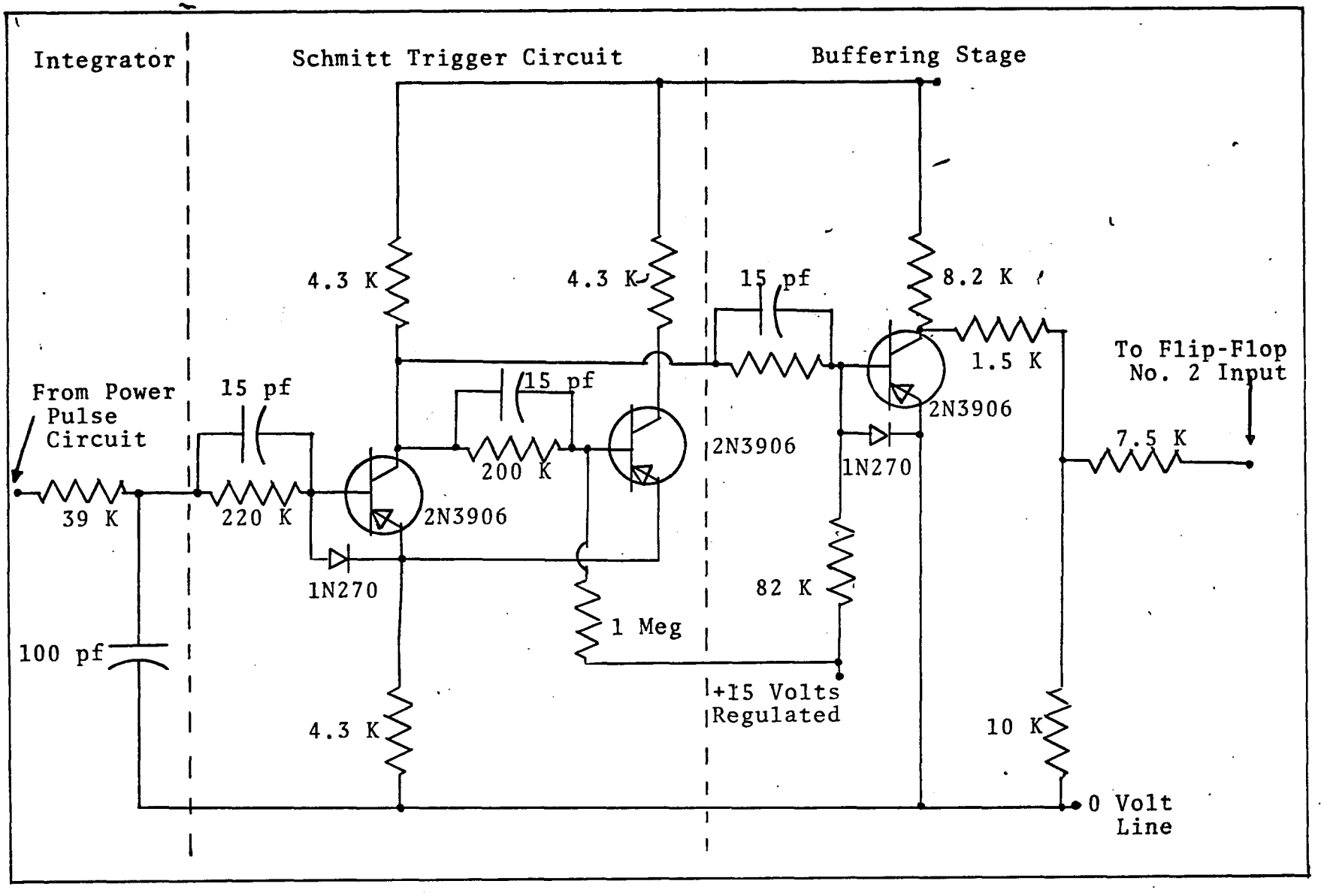

Figure A-3 Integrator, Schmitt Trigger, and Buffering Circuitry

and its circuitry is shown in Figure A-4. This circuitry consists of a one-shot timing circuit and a gap-shorting transistor. There are several problems that occur with this circuitry. Spurious triggering causes the shorting transistor to turn on in the middle of a power discharge, resulting in the loss of several transistors. Therefore, a current-limiting resistor was added to the collector of MJ421 to prevent the destruction of the device. The resistive value is low enough so that any voltage appearing across it caused by the leakage current will not interfere with the recovery time measurements. This circuitry is designed to shortout the leakage current for several milliseconds after the discharge pulse and allow for recovery tests. A blocking diode is used to enable the recovery checking pulse to test only the gap space and not the gap shorting circuitry.

The circuitry shown in Figure A-5 was used to detect when the power output pulse is completed. The output signal is then used to trigger the Burroughs' delay units, which, in turn, triggers the Monostable No. 2 and the gap-shorting circuitry.

The gap checking circuitry is shown in Figure A-6. This circuitry was placed as close to the machining gap as physical constraints would allow. It is designed to produce a low current, 10 volt pulse across the recovering gap space, which is used to determine the condition of the gap. The IN1893 diode is used to isolate the power pulse cables from the gap and to prevent the checking pulse from being effected by the short circuit caused by gap shorting circuitry. In this manner,

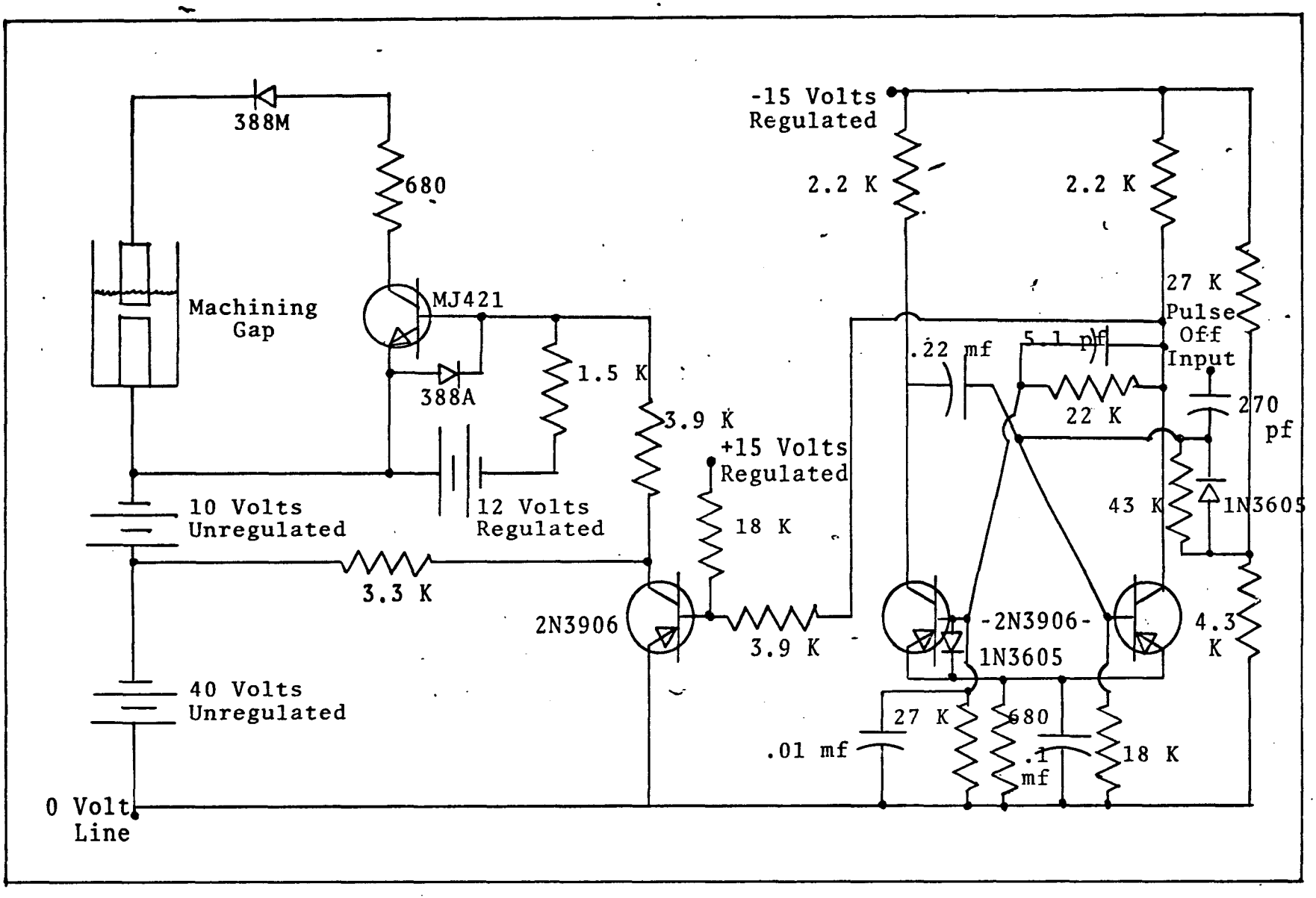

Figure A-4 The Gap Shorting and Supplemental Circuitry

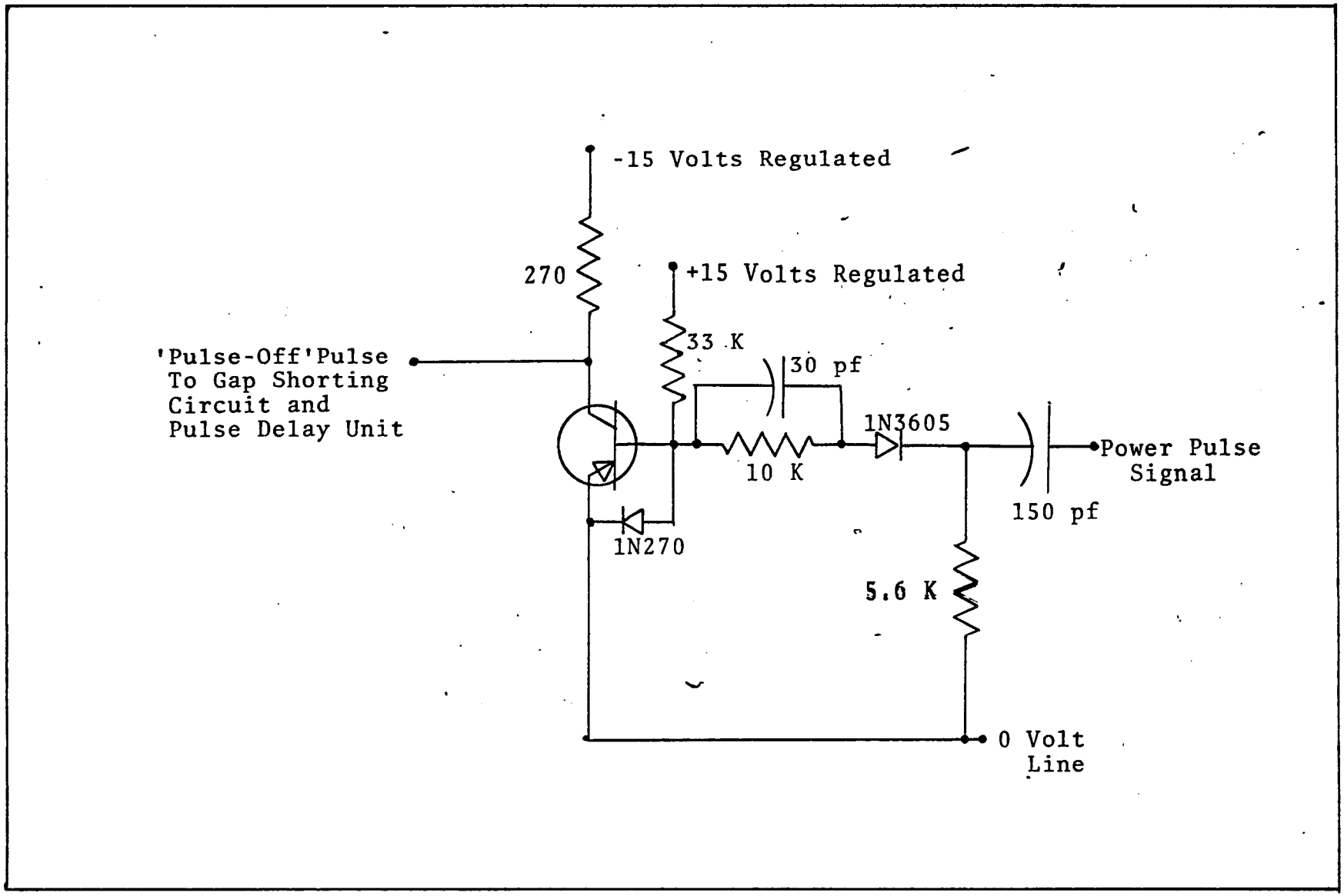

Figure A-5 The Circuitry Used to Indicate That the Power Pulse Has Terminated

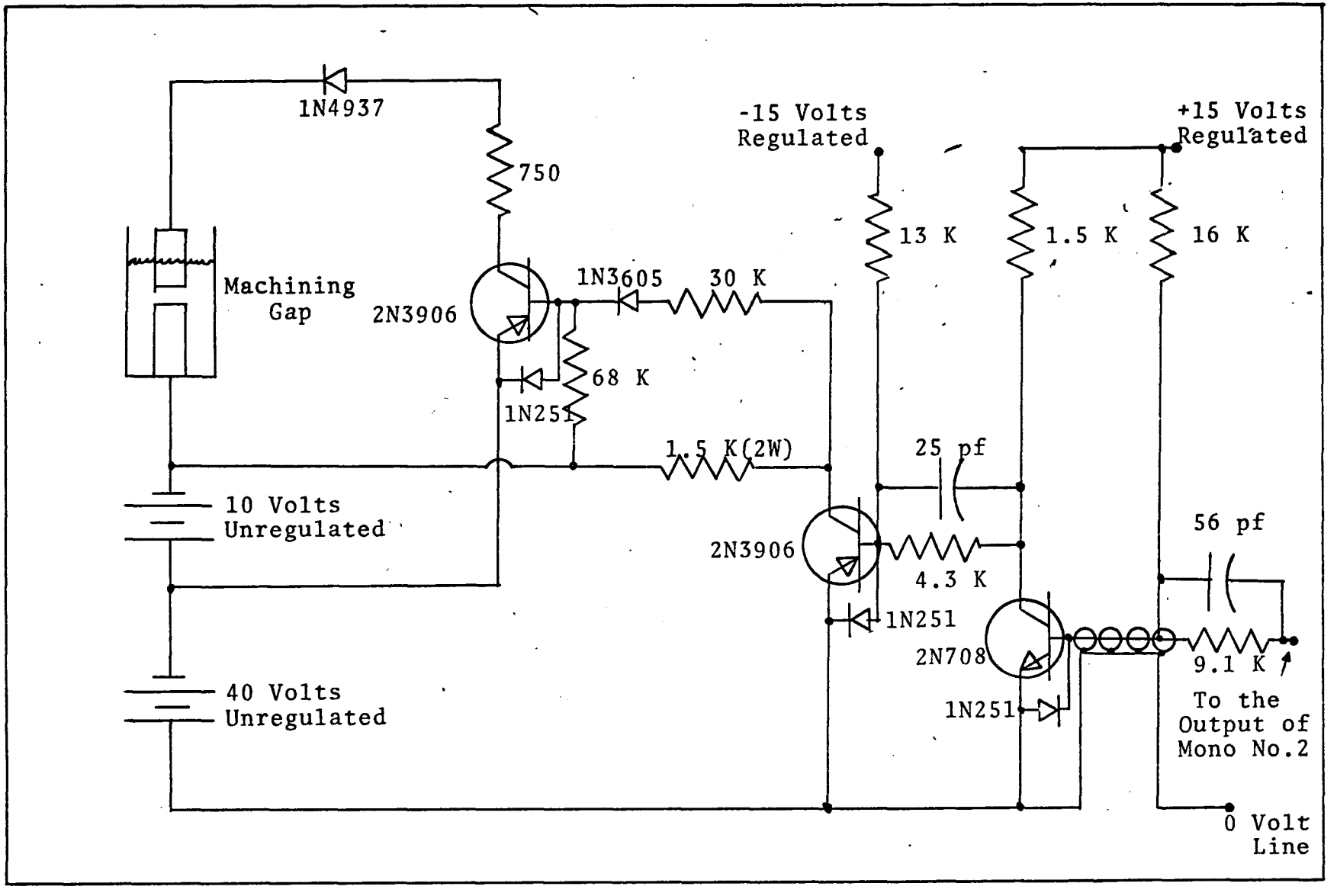

Figure A-6 The Gap Recovery Checking Circuitry

only the gap conditions can influence the checking pulse.

Some of the power supplies used with the previously discussed circuitry are unregulated, but they remain within 10% of the stated values during operation, unless otherwise specified. The lower power circuitry, especially the sensitive circuits, such as the flip-flop and monostable multivibrators, required regulated power supplies with output voltages regulated to 1%.

APPENDIX B

EXTRANEOUS TEST DATA REGARDING DIFFERENT EDM FLUIDS

Prior to the recovery time testing of the various EDM fluids mentioned in Table 2.2, a number of preliminary tests were conducted to determine if there were any major differences between the various fluids. This data was only intended to determine possible differences for later recovery time tests and is not meant to be a complete array of test information.

The apparatus used to gather this information was the same equipment that Haswell[27] used in his thesis work. The electrodes used were copper and Hardtem B Tool-Steel with copper as the cathode and Hardtem B as the anode, in normal polarity. The pulse current amplitude was set to 100 amps, initially, and the pulse duration was variable from 5 microseconds to 500 microseconds. The discharge machining voltage, and current magnitude were noted for each discharge and two machining results were determined. The two results were the average gas bubble volume liberated owing to a single discharge and the average diameter of the crater produced by a single discharge.

The volume measurement was accomplished by collecting the gas in an inverted, liquid filled, milliliter pipet. When a sufficient number of gas bubbles had been collected to cause a measurable change in the liquid level in the pipet, the vol-

ume change would be divided by the number of discharges used to produce the change and the average gas bubble volume per discharge would result.

The average crater diameter for a certain pulse duration was obtained by causing a single discharge to occur between the copper and the Hardtem B. The resultant crater was then observed under a microscope and the diameter measured in four directions. The crater was assumed to consist of the area damaged or changed by the discharge. The average of the four measured values was then termed the average crater diameter for that particular fluid at the set pulse width.

The results of the tests are given in Figures B-1 through B-13. As can be seen, there are no appreciable differences found between the fluids tested. Only the 3-M Company's Fluro Chemical FC-77 shows any significant difference, but this fluid causes the gap to become extremely sensitive to contamination. Because of this over-sensitivity, only one discharge could be produced in the gap spacing and then the gap had to be brushed clean before another discharge could be initiated. This problem prevented the accumulation of bubble data and the use of the fluid in the recovery time tests.

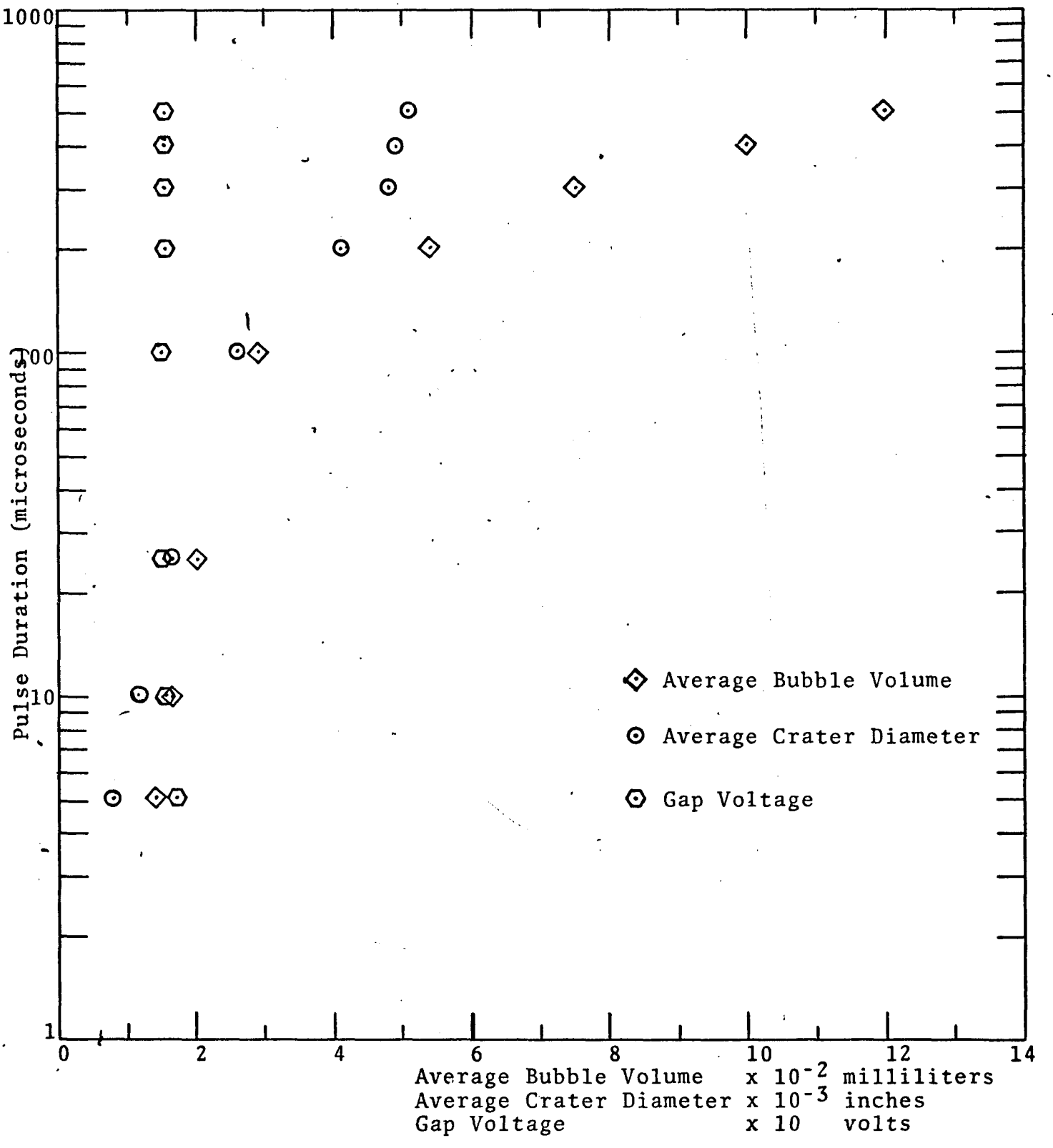

Figure B-1 Average Bubble Volume, Average Crater Diameter, and Gap Machining Pulse Voltage for Texaco Code 499 EDM Fluid

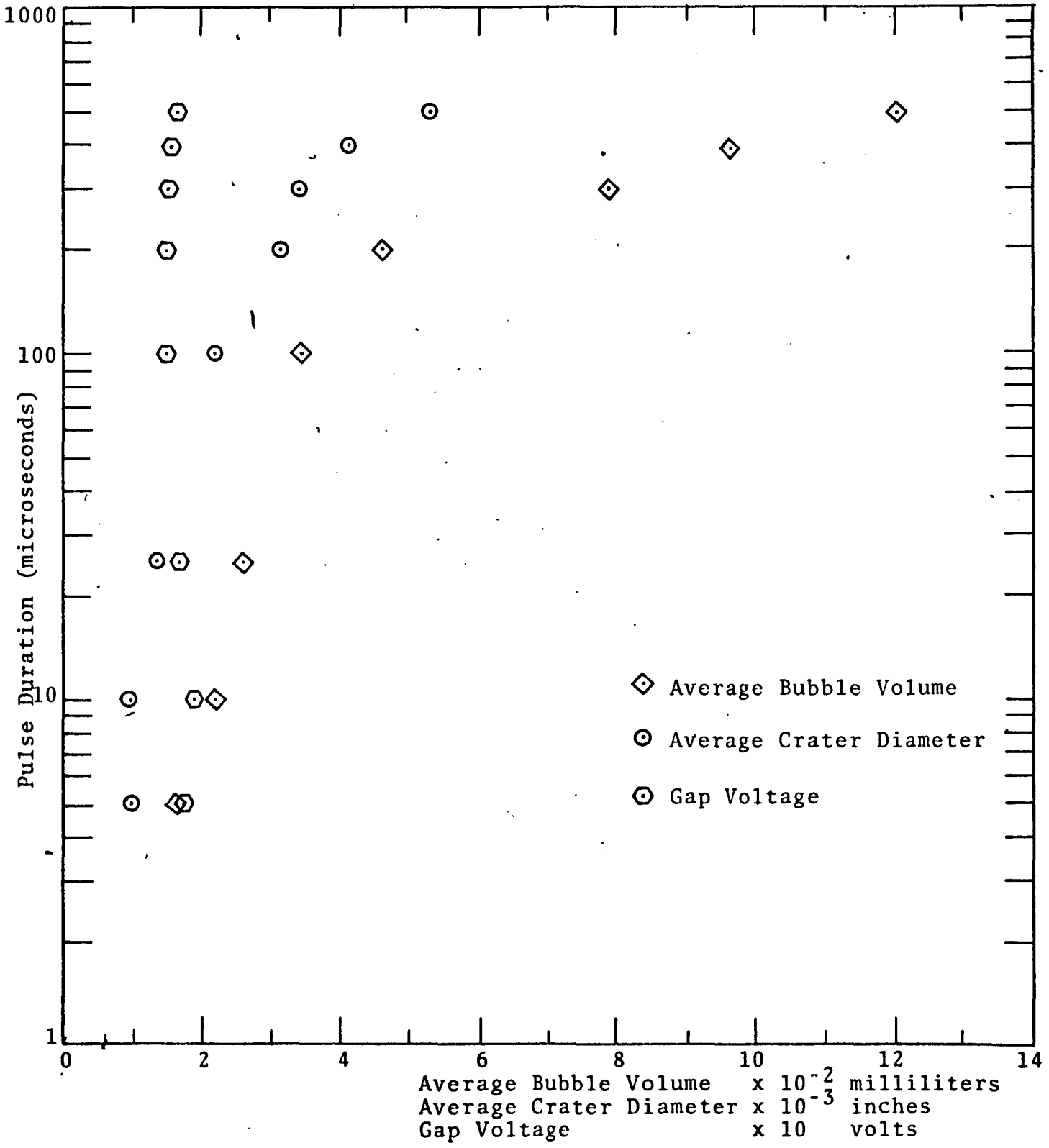

Figure B-2 Average Bubble Volume, Average Crater Diameter, and Gap Machining Pulse Voltage for Amoco MOS EDM Fluid

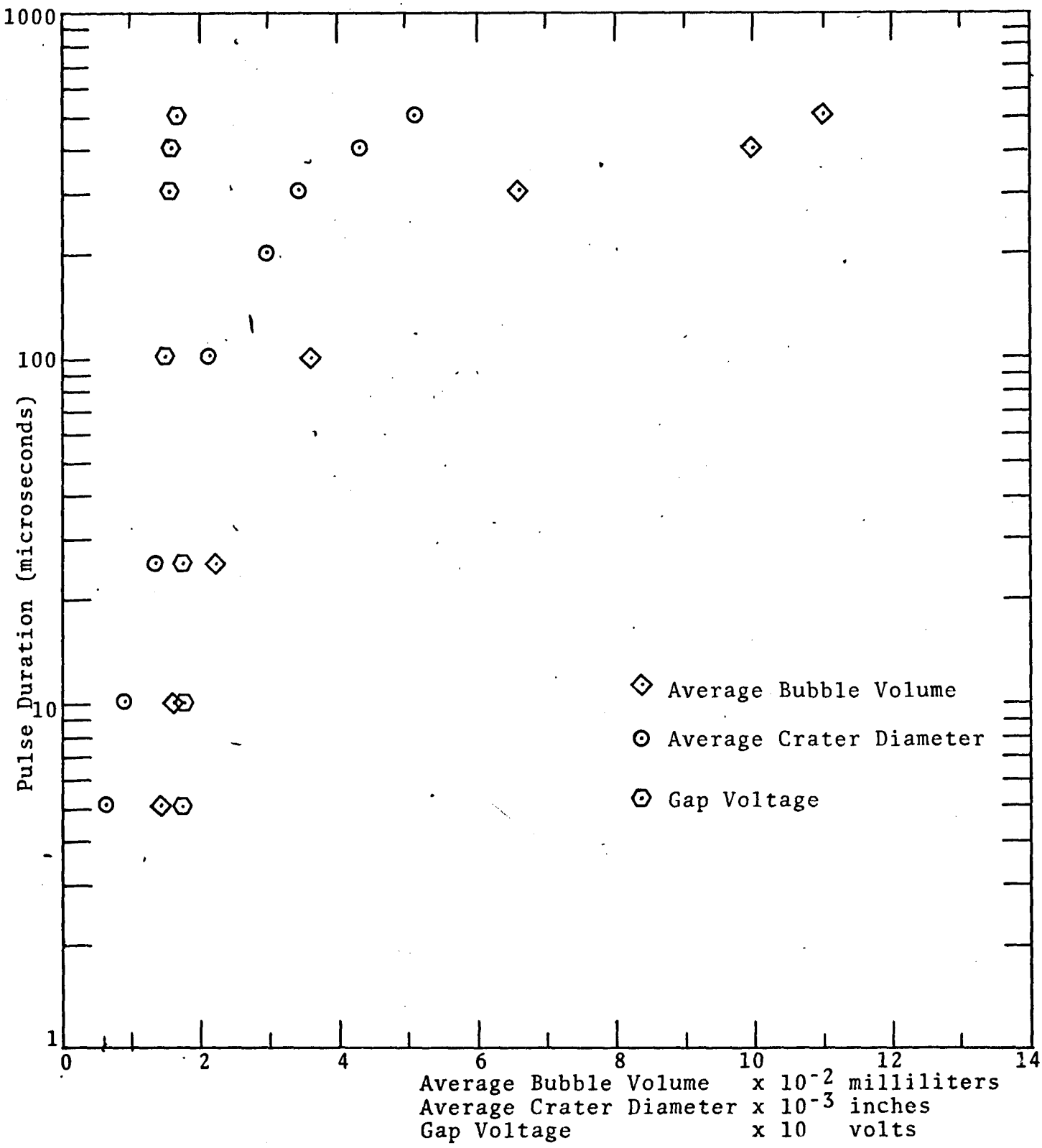

Figure B-3 Average Bubble Volume, Average Crater Diameter, and Gap Machining Pulse Voltage for Wolf's Head 510 EDM Fluid

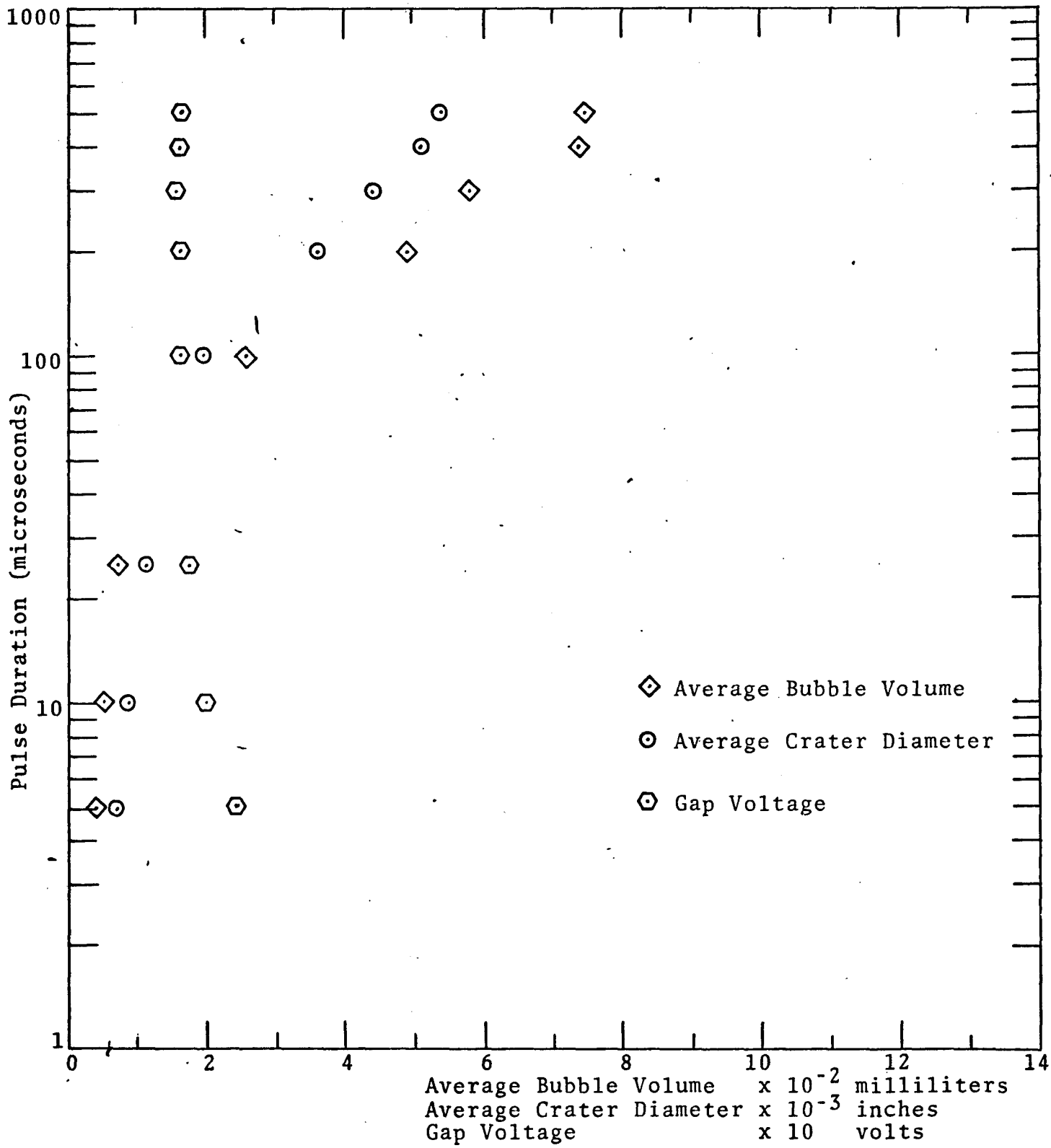

Figure B-4 Average Bubble Volume, Average Crater Diameter, and Gap Machining Pulse Voltage for Factopure EDM Fluid

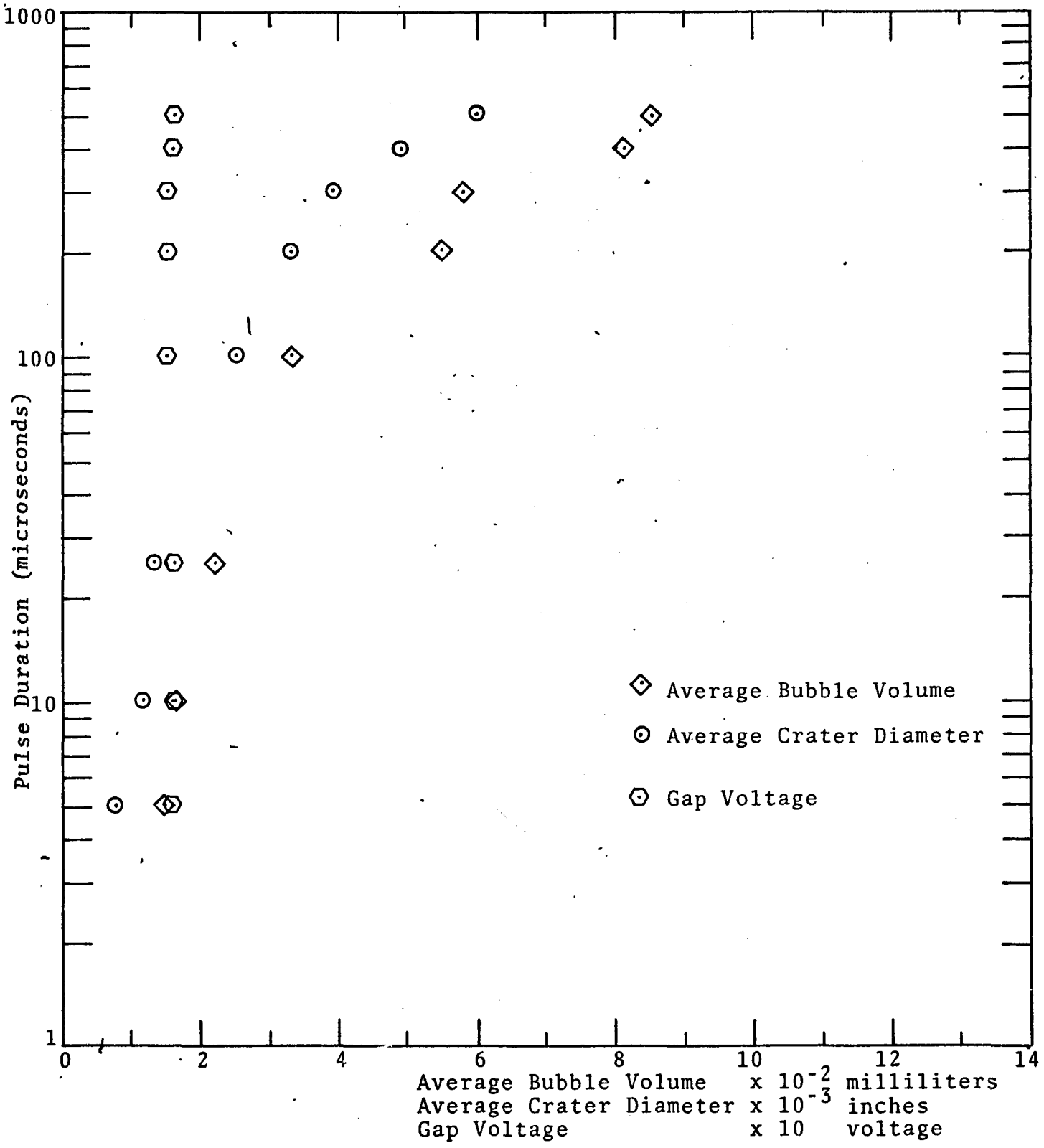

Figure B-5 Average Bubble Volume, Average Crater Diameter, and Gap Machining Pulse Voltage for Shell EDM Fluid

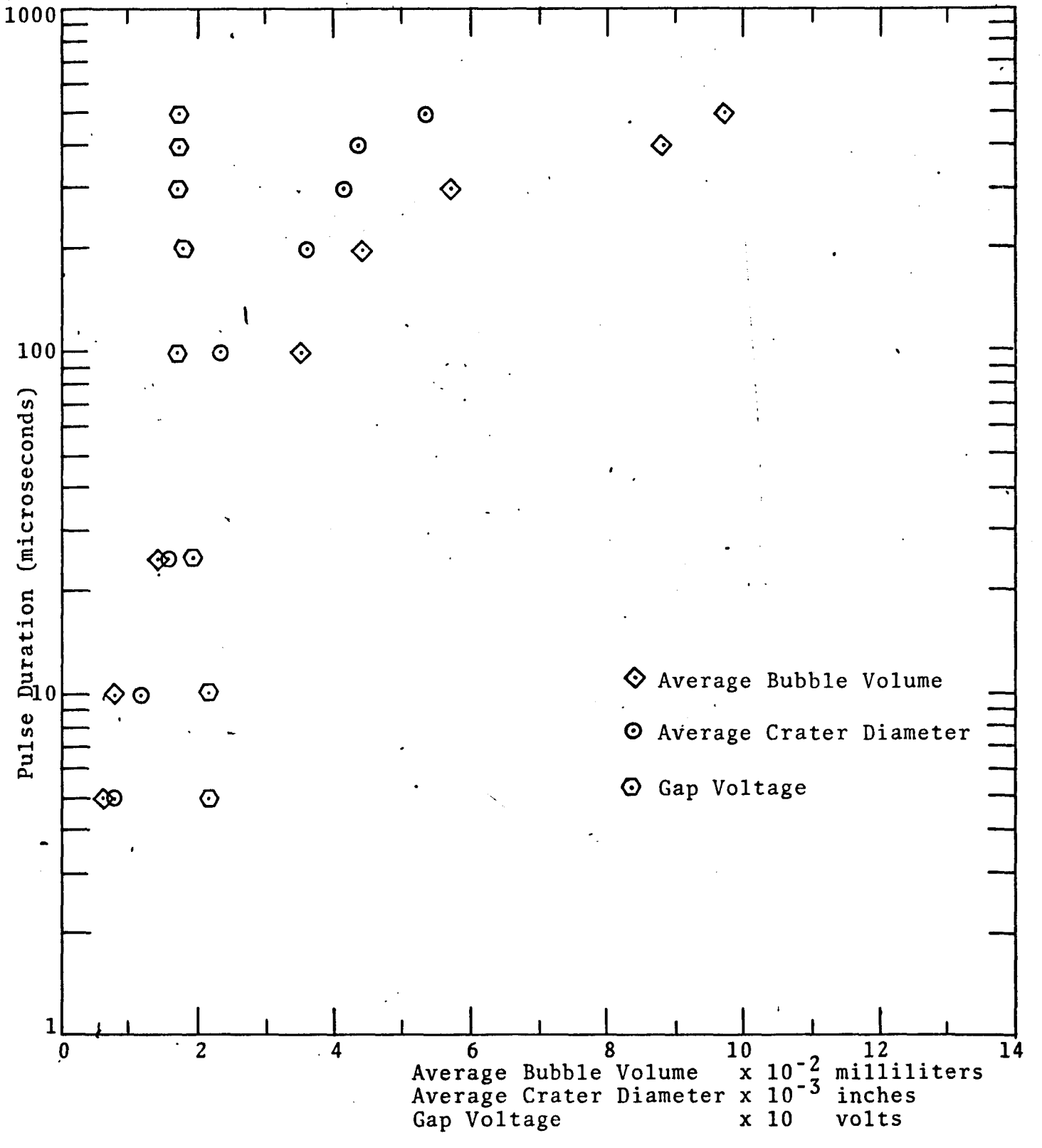

Figure B-6 Average Bubble Volume, Average Crater Diameter, and Gap Machining Pulse Voltage for Mineral Seal Oil

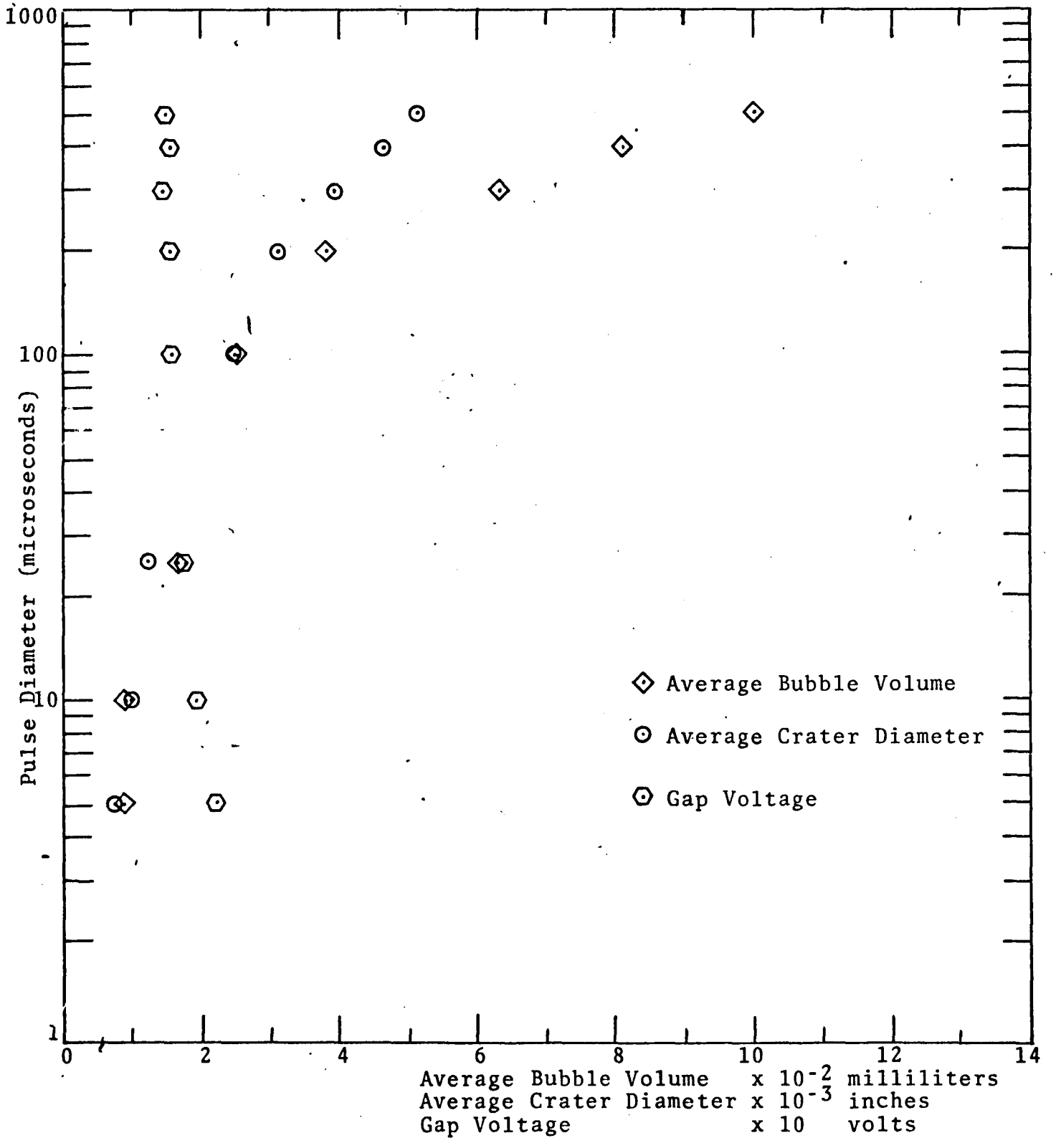

Figure B-7 Average Bubble Volume, Average Crater Diameter, and Gap Machining Pulse Voltage for Citgo No. 90109 EDM Fluid

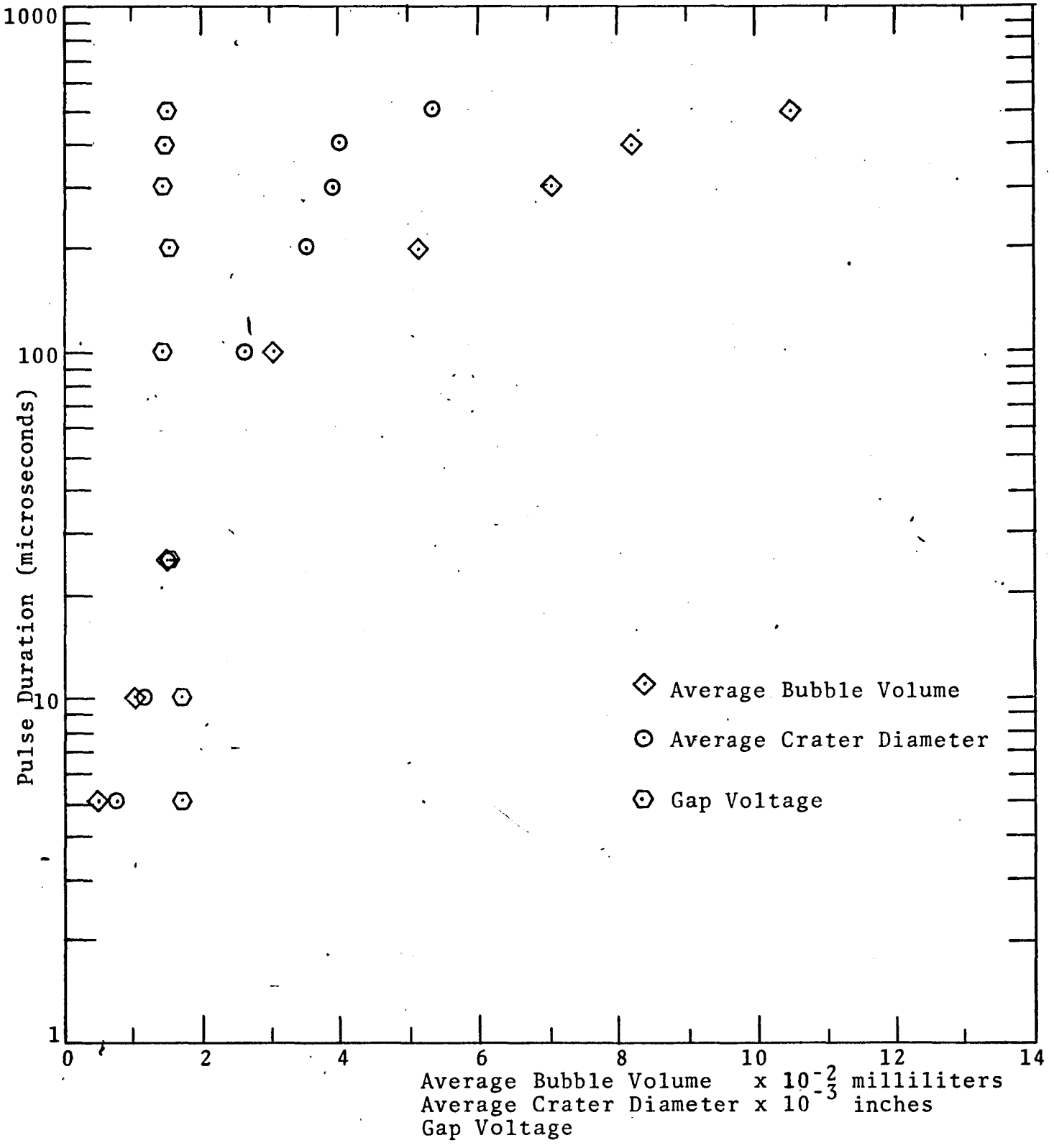

Figure B-8 Average Bubble Volume, Average Crater Diameter, and Gap Machining Pulse Voltage for Silicone 40 EDM Fluid

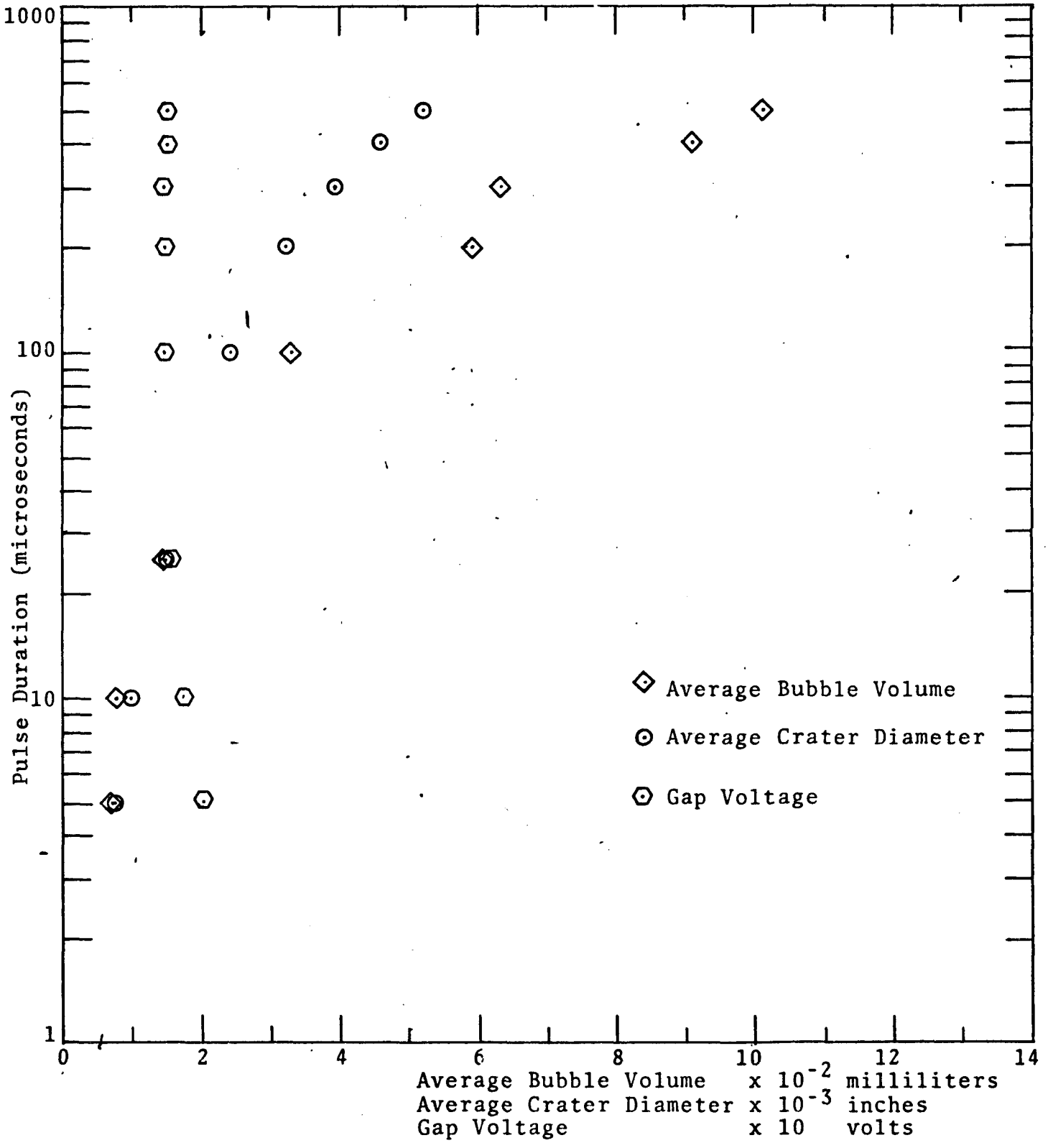

Figure B-8 Average Bubble Volume, Average Crater Diameter, and Gap Machining Pulse Voltage for Silicone 80 EDM Fluid

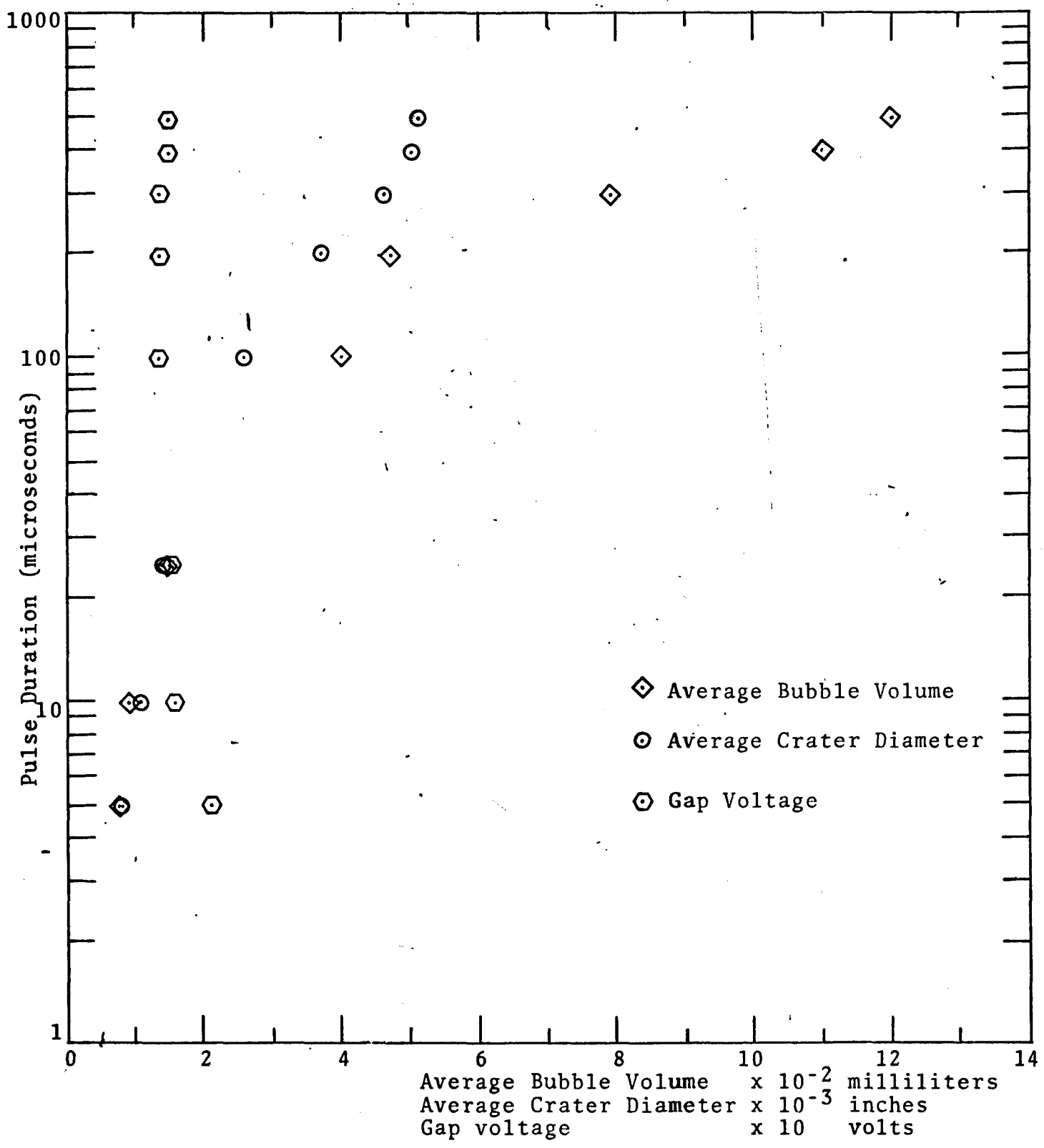

Figure B-10 Average Bubble Volume, Average Crater Diameter, and Gap Machining Pulse Voltage for Silicone 100 EDM Fluid

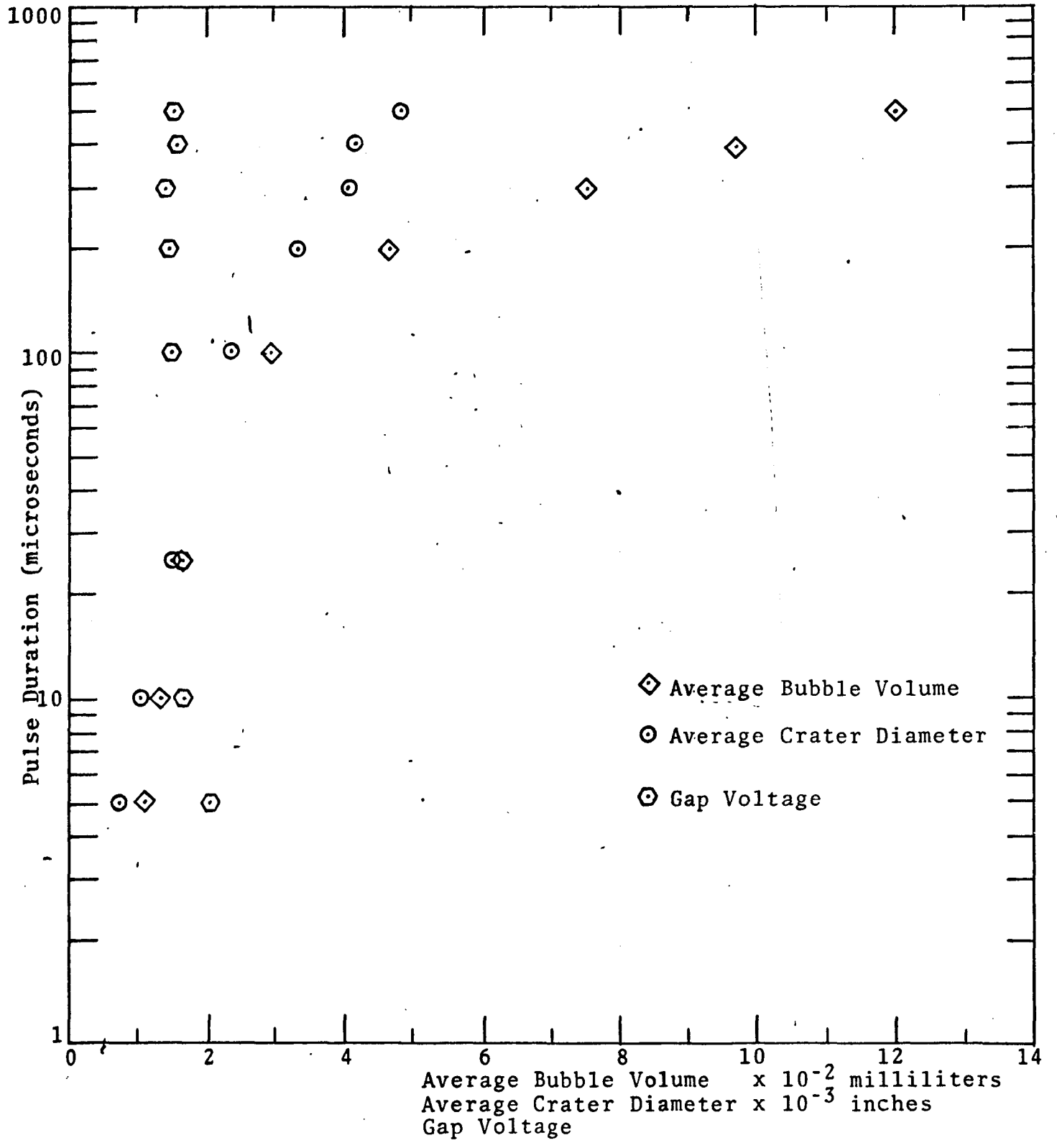

Figure B-11 Average Bubble Volume, Average Crater Diameter, and Gap Machining Pulse Voltage for Silicone 200 EDM Fluid

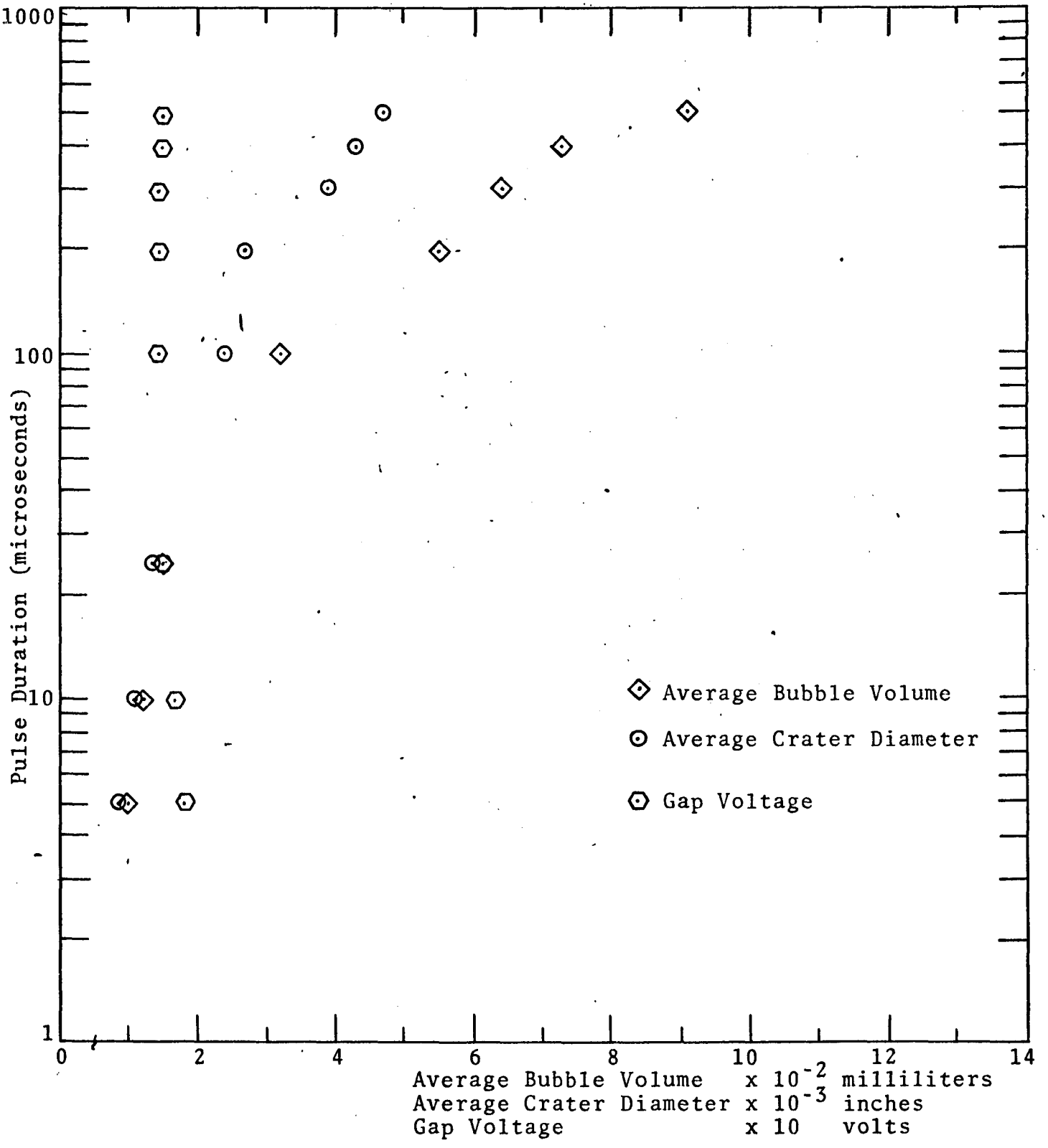

Figure B-12 Average Bubble Volume, Average Crater Diameter, and Gap Machining Pulse Voltage for Pure Silicone SF-96(5) Oil

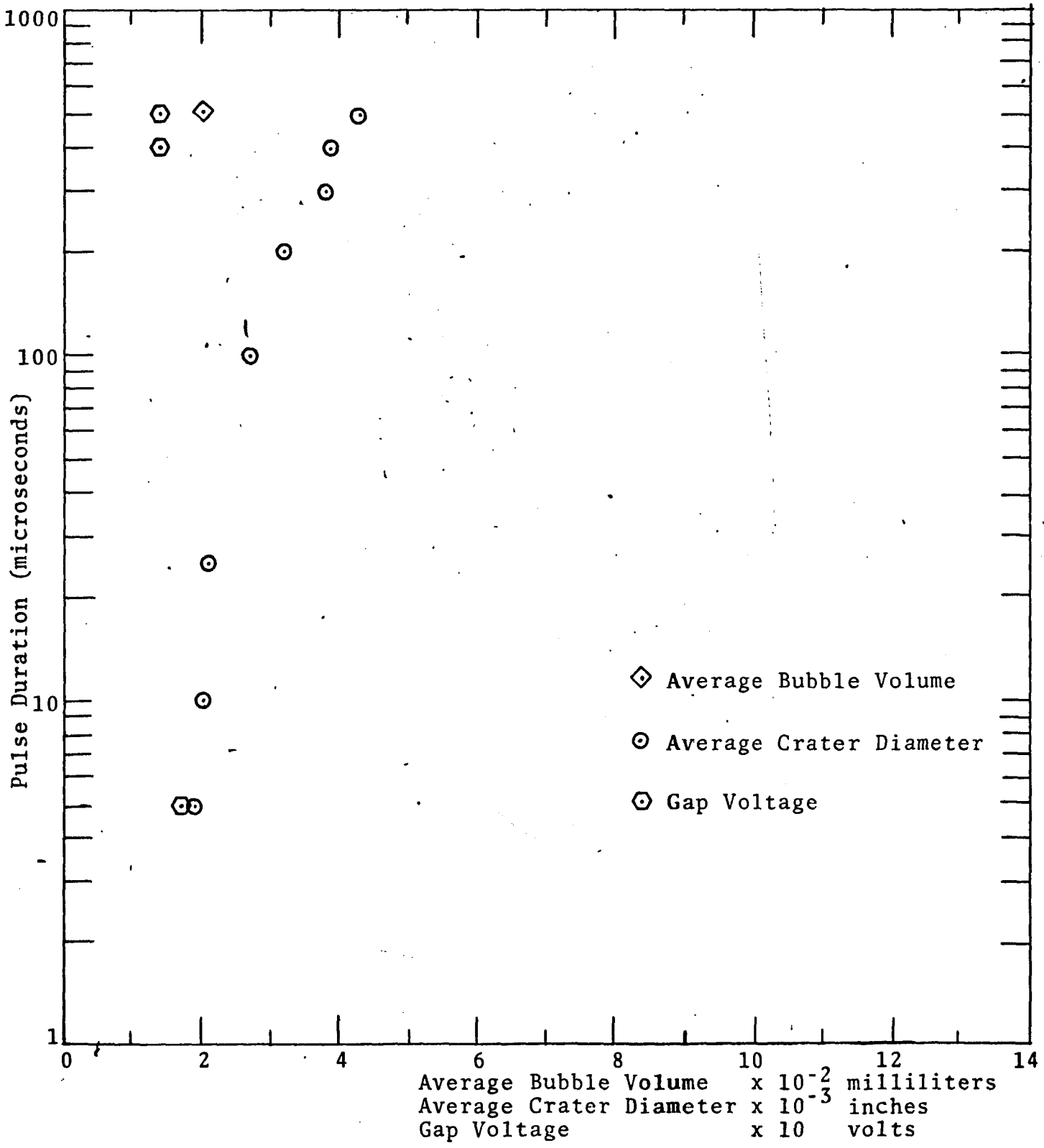

Figure B-13 Average Bubble Volume, Average Crater Diameter, and Gap Machining Pulse Voltage for Florochemical FC-77 Fluid

LIST OF REFERENCES

1. Lazarenko, B.R. and Lazarenko, N.I. : "Electric Spark Method for the Machining of Metals.", (in Russian), Stanki I Instruments, Vol. 17, No. 12, 1946, pp. 8-11 and Vol 18, No. 2, pp. 4-8.

2. Lazarenko, B.R. and Lazarenko, N.I. : "Machining by Erosion", American Machinist, Vol. 91, December 18, 1947, pp. 120-1.

3. Mote, Harry: "Boosting EDM Cutting Time", American Machinist, Vol. 112, April 8, 1968, pg. 93.

4. Hockenberry, T.O. : "The Influence of Hydrodynamic Effects on Electrode Erosion In Transient Arc Discharges in Liquids", Doctorial Dissertation, Carnegie Institute of Technology, 1964.

5. Berghausen, P.E., Brettschreider, H.D., Davis, M.F., et. al.,: "Electro-Discharge Machining Program", Interim Technical Documentary Program Report, USAF Materials Laboratory, Report No. ASD-TDR-7-545 (IR II), 15 November 1960 - 15 May 1961.

6. Haswell, W.T. III : "Electrode Phenomena and Thermal Analysis Associated with Low Voltage Transient Arcs Under Liquid Dielectrics at Short Interelectrode Gap Spacing", Doctorial Dissertation, Carnegie Mellon University, 1969.

7. Longfellow, J., Wood, J.D., and Palmer, R.B. : "Effects of Electrode Material Properties on Wear Ratio in Spark Machining", Institute of Metals Journal, Vol. 96, Part 2, February 1968, pp. 43-8.

8. Grachis, G.J. : "Steady-State Flow of the Liquid Dielectric and the Dynamics of the Machining By-Products in the Electrical Discharge Machining Process", Doctorial Dissertation, Carnegie Mellon University, 1969.

9. Churchill, R.J. : "Reignition of Freely Recovering Spark Channels in Hydrogen", Canadian Journal of Physics, Vol. 41, April 1963, pp. 610-24.

10. Edels, H., Whittaker, D., Evans, K.G., and Shaw, A.G.: "Experiments and Theory on Arc Reignition by Spark Breakdown", The Institution of Electrical Engineers - London Proceedings, Vol. 112, December 1965, pp. 2343-52.

11. Williams, E.M. : "Theory of Electric Spark Machining", Electrical Engineering, Vol. 71, March 1952, pp. 257-60.

12. Pittman, P.F. : "Voltage Recovery of the Over-Volted Liquid Dielectric Spark Gap", Doctorial Dissertation, Carnegie Institute of Technology, 1961.

13. Allen, J.W.S., Edels, H., and Whittaker, D. : "Post Arc Temperature Decay", Physical Society Proceedings, Vol. 78, November 15, 1961, pp. 948-57.

14. Edels, H. and Ettinger, Y. : "Arc Interruption and Thermal Reignition", Institution of Electrical Engineers - London Proceedings, Vol. 109A, 1962, pp. 89-98.

15. Reference 10, pg. 2345.

16. Rich, J.A. and Farrell, G.A. : "Vacuum Arc Recovery Phenomena", Institute of Electrical and Electronic Engineers - Proceedings, Vol. 52, November 1964, pp. 1293 - 1301.

17. Reference 14, pg. 95.

18. Edels, H. and Kimblin, C.W. : "Electrical Conductance Decay of Interrupted Arc Columns", British Journal of Applied Physics, Vol. 17, December 1966, pp. 1607 - 19.

19. Reference 12, pg. 22.1 - 22.5.

20. Reference 4, pg. 30.

21. Reference 5, pg. 5.

22. Reference 8, pg. 147.

23. Konnerth, K.L. : "A Systematic Experimental Study of Electrode Phenomena Accompanying Low-Voltage Arcs in Liquid Dielectrics",Doctorial Dissertation, Carnegie Institute of Technology, 1961.

24. Reference 4, pp. 32 - 34.

25. Cobine, J.D. : Gaseous Conductors, Dover Publications, Inc., New York, 1958.

26. Hoyaux, M.F. : Arc Physics, Springer-Verlog, Inc., New York, 1968.

27. Reference 6, pg. 3.

28. Great Lakes Carbon Co. Bulletin 16-001.

29. Lyman, T.,(Editor) : Metals Handbook, Vol. 1, American Society for Metals, Metals Park, Ohio, 1961.

30. Armco Iron, Lapham-Hickey Co., Chicago.

31. Alloy Digest, Engineering Alloy Digest, Inc., New Jersey, Vol. 5, File Code TS-134, June 1963.

32. Reference 31, Vol. 4, File Code SS 164, 1964

33. Goldsmith, A., Waterman, T.E., and Hirschhorn, H.J. : The Handbook of Thermophysical Properties of Solid Materials, Vol. 2,The MacMillan Co., New York, pg. 57.

34. Reference 31, Vol. 1, File Code CI 15, 1963.

35. Texaco Code 499 EDM Fluid Data Sheet.

36. Reference 4, pg. 9.

37. Noll, Walter: Chemistry and Technology of Silicones, Academic Press, New York, 1968.

38. Reference 10, pg. 2349.

39. Edels, H. and Holme, J.C. : "Measurement of the Decay of Arc Column Temperature Following Interruption", British Journal of Applied Physics, Vol. 17, December, 1966, pp. 1595 - 1606.

40. Reference 6, pg. 21.

41. Eckman, P.K. : "Radial Growth of Low Voltage Spark Discharge in Liquid Dielectrics", Doctorial Dissertation, Carnegie Institute of Technology, 1959.

42. Reference 9, pg. 615.

43. Reference 10, pg. 2352.

44. Churchill, R.J., Parker,A.B., and Graggs, W.D. : Measurement of the Reignition Voltage Characteristics of a High Current Spark Gap in Air", Journal of Electronics and Control, Vol. 11, 1961, pg. 32.

45. Reference 39, pg. 1603.

46. Reference 39, pg. 1598.

47. Gray, D.E. (Co-ordinating Editor): American Institute of Physics Handbook, McGray Hill Book Co.,Inc., New York, 1963, pp. 4 - 93.

48. Edels, H. and Crawford, F.W. : "Arc Interruption Part I", Journal of Institution of Electrical Engineers, Vol. 21, December 1956, pg. 715.

49. Reference 10, pg. 2344.

50. Reference 6, pg. 92.

51. Mantell, C.L. : Carbon and Graphite Handbook, Interscience Publications, Inc., New York, 1968 .

52. Reference 51, pg. 34.

53. Electro-Carb 'EC-3' Data Sheet, More-Wear Tools, Inc.

54. Condon, E.W. and Odishow, H. : Handbook of Physics, 2nd Edition, McGraw Hill Book Co., New York, 1962.

55. McGregor, R.R. : Silicones and Their Uses, McGraw Hill, New York, 1954.

56. Ponomareva, T.I., Krasouskaya, T.A., Sobolevskii, M.V., and Ponomakev, A.N. :"Radiation Chemical Investigation of Liquid Polyorganosiloxanes with Different Amounts of Aromatic Groups in Main Chain or as Side Chains", Kinetics and Catalysis, Vol. 7, November - December 1966, pp. 845 - 50.

57. Reference 4, pg. 29.1.

58. Reference 25, pp. 143 - 161.

59. Reference 48, pp. 712-16.

60. Reference 41, pg. 67.

61. Reference 4, pp. 10 - 25.

62. Reference 6, pp. 91 - 133.

63. Reference 25, pg. 90.

64. Reference 25, pg. 335.

65. Reference 44, pg. 17 - 33.

66. Curzon, F.L. and Gautam, M.S. : "The Influence of Electrode Heat Transport in Spark Recovery", British Journal of Applied Physics, Vol. 18, January 1967, pp. 79 - 87.

67. Reference 44, pp. 26 - 27.

68. Edels, H. and Crawford, F.W. : "Arc Interruption Part 2", Journal of Institution of Electrical Engineers, Vol. 3, February 1957, pp. 88 - 93.

69. Reference 14, pg. 89.

70. References 66, 39, and 72.

71. Reference 66, pp. 80 and 87.

72. Parker, A.B., Poole, D.E., and Perkins, J.e., : "Measurement of Electrode Surface Temperature and its Role in Recovery of High Current Spark Gaps", British Journal of Applied Physics, Vol. 16, June 1965, pp. 851 - 5.

73. Reference 72, pg. 854.

74. Reference 10, pg. 2352 and Reference 9, pg. 621.

75. Reference 5, pg. 87.

76. Kurafuji, Hisao, and Suda Ko : Study on Electrical Discharge Machining I, Journal of the Faculty of Engineering, University of Tokyo (B), Vol. XX, VIII, No. 1, 1965.

77. Reference 5, pg. 87 - 141.

78. Reference 5, pg. 137.

79. Reference 4, pp. 27 - 30.

80. Smith, R.E.: "Phenomena Accompanying Low Voltage Discharge in Liquid Dielectrics", Doctorial Dissertation, Carnegie Institute of Technology, 1954.

81 Poole, D.E., Parker, A.B., and Churchill, R.J. : Measurement of the Temperature of a high current Spark Channel in Air", Journal of Electronics and Control, Vol. 15, 1963, pp. 131 - 144.

82. Reference 8, pg. 27.

83. Bacon, R. : "Growth, Structure and Properties of Graphite Whiskers, Journal of Applied Physics, Vol. 31, February 1960, pp. 283 - 90.

84. Reference 83, pg. 284.

85. Davis, W.R., Slawson, R.J., and Rigby, G.R.: "An Unusual Form of Carbon", Nature, Vol. 171, 1953, pg 756.

86. Grisdale, R.O., Pfister, A.C., and Van Roosbroeck, W.: "Pyrolytic Film Resistors, Carbon and Borocarbon", Bell System Technical Journal, Vol. 30, 1951, pp. 271 - 314.

87. Reference 5, pg. 46.

88. Pechuro, N.S. and Merkur'ev, A.N.: "Electrical Arc Craking of Liquid Organic Feedstock", Applied Electrical Phenomena, Vol. 2, 1965, pg. 125.

89. Grodzinskii, E.Ya., Pechuro, N.S., and Pesin, O.Yu. : "Effect of the Circulation of the Raw Material and the Electrical Parameters on the Process of Decomposition of Hydrocarbons in a High Voltage Arc Discharge", Electrospark Machining of Metals, Vol. 3, B.A. Krasyuk Editor, Consultants Bureau (translation), New York, 1965.

90. Chepikov, A.T. and Ryabchikov, S.Ya. : "Gas Production in High Voltage Pulsed Discharges in Liquid", Applied Electrical Phenomena, Vol. 6, 1967, pg. 391.

91. Cleary, J.F. (editor) : General Electric Transistor Manual, General Electric Company, pg. 201.

92. Reference 4, pg. 29.2.